SEARCH FOR PHYSICS BEYOND THE STANDARD MODEL WITH ADDITIONAL NON-STANDARD PARTICLES AT FUTURE COLLIDERS

by

ABDULKADİR ŞENOL

THESIS SUBMITTED TO

THE GRADUATE SCHOOL OF NATURAL AND APPLIED SCIENCES

OF

THE ABANT İZZET BAYSAL UNIVERSITY

IN PARTIAL FULFILLMENT OF THE REQUIREMENTS FOR THE

DEGREE OF

DOCTOR OF PHILOSOPHY

IN

THE DEPARTMENT OF PHYSICS

FEBRUARY 2008

Approval of the Graduate School of Natural Sciences

Prof. Dr. Nihat ÇELEBİ

Director

I certify that this thesis satisfies all the requirements as a thesis for the degree of Doctor of Philosophy.

Prof. Dr. Ahmet Turan ALAN

Head of Physics Department

This is to certify that we have read this thesis and that in our opinion it is fully adequate, in scope and quality as a thesis for the degree of Doctor of Philosophy.

Prof. Dr. Ahmet Turan ALAN

Supervisor

Examining Committee Members

1. Prof. Dr. Namık Kemal PAK .....
2. Prof. Dr. Takhmasib M. ALİEV .....
3. Prof. Dr. Ahmet Turan ALAN .....
4. Assoc. Prof. Dr. Resul ERYİĞİT .....
5. Assoc. Prof. Dr. Nurettin KARAGÖZ .....

ABSTRACT

SEARCH FOR PHYSICS BEYOND THE STANDARD MODEL WITH ADDITIONAL NON-STANDARD PARTICLES AT FUTURE COLLIDERS

Şenol, Abdulkadir

Ph.D. Thesis, Department of Physics

Supervisor: Prof. Dr. Ahmet Turan ALAN

February 2008, 104 pages

This thesis is based on work done in three different problems related with additional non-standard particles in framework of physics beyond the standard model:

In the first problem, we investigate the production of fourth family up-type quarks using effective Lagrangian approach at future lepton-hadron colliders and study the kinematical characteristics of the signal with an optimal set of cuts. We obtain the upper mass limits 500 GeV at THERA and one TeV at Linac $\otimes$ LHC.

In the second problem, we investigate the single production and decay of charge -1/3 ,weak isosinglet vectorlike exotic D quarks in string inspired E_6 theories at future ep colliders; THERA with $\sqrt{s}$=1 TeV, $L = 40\ pb^{-1}$ and CERN

Large Hadron Electron Collider (LHeC) with $\sqrt{s}$=1.4 TeV, $L = 10^4\ pb^{-1}$. We found that an analysis of the decay modes of D should probe the mass ranges of 100-450 GeV and 100-1200 GeV at the center of mass energies, 1 and 1.4 TeV , respectively.

In the last problem, we examine the possible single and pair production of a heavy neutrino (ν_4) in ep, $pp(p\bar{p})$ and e^-e^+ collisions in the context of a new $e\nu_4 W$ and $\nu_4\bar{\nu}_4 Z$ anomalous magnetic dipole moment type interactions and analyze the background using optimal cuts. We have obtained the mass limits of 700 GeV for THERA ($\sqrt{s}$=1 TeV), 2.8 TeV for LC$\otimes$ LHC ($\sqrt{s}$=3.74 TeV) and 2 TeV at Large Hadron Collider (LHC). At ILC options $\sqrt{s} = 0.5$ and 1 TeV these limits are 450 and 950 GeV, respectively.

Keywords: Fourth generation, Exotic quark, Models beyond the standard model, String inspired E_6 model.

ÖZET

STANDART OLMAYAN EK PARÇACIKLARLA STANDART MODEL ÖTESİ FİZİĞİN GELECEK ÇARPIŞTIRICILARDA ARAŞTIRILMASI

Şenol, Abdulkadir

Doktora Tezi, Fizik Bölümü

Tez Danışmanı: Prof. Dr. Ahmet Turan ALAN

Şubat 2008, 104 sayfa

Bu tez, standart model ötesi fizik çerçevesinde standart olmayan ek parçacıklar ile ilişkili üç farklı problem üzerindeki çalışmalara dayanmaktadır.

Birinci problemde, gelecek lepton-hadron çarpıştırıcılarında efektif Lagranjiyen yaklaşımı kullanarak üst tipi dördüncü aile kuarkların üretimini inceledik ve optimal sınırlandırmlar ile sinyalin kinematik karakteristiğini çalıştık. Kütle üst limitini THERA ($\sqrt{s}$= 1 TeV) da 500 GeV ve Linac $\otimes$ LHC ($\sqrt{s}$= 5.3 TeV) de 1 TeV bulduk.

İkinci problemde, gelecek *ep* çarpıştırıcılarından, kütle merkezi enerjisi 1 TeV ve ışınlığı 40 pb^{-1} olan THERA ve kütle merkezi 1.4 TeV, ışınlığı 10^4 pb^{-1} olan CERN Büyük Hadron electron Çarpıştırıcısı (LHeC)' nda, yükü -1/3 olan zayıf

eştekli vektörbenzer egzotik D quarkların üretimini ve bozunumunu sicim esinli E_6 modeli çerçevesinde inceledik. D nin bozunum modlarının analizinden kütle aralığının kütle merkezi enerjisi 1 TeV iken 100-450 GeV ve kütle merkezi enerjisi 1.4 TeV iken 100-1200 GeV araştırılması gerektiğini bulduk.

Son problemde ise, ep, pp ($p\bar{p}$) ve e^-e^+ çarpıştırıcılarında ağır nötrinoların (ν_4) yeni $e\nu_4 W$ ve $\nu_4\nu_4 Z$ anormal manyetik moment tipi etkileşmelerini içeren tek ve çift üretimini inceledik ve optimal sınırlandırmalar kullanarak fonu analiz ettik. Kütle sınırlarını THERA için 700 GeV, $LC \otimes LHC$ için 2.8 TeV ve Büyük Hadron Çarpıştırıcısı (LHC) için 2 TeV bulduk. Bu kütle sınırları Uluslararası Doğrusal Çarpıştırıcısı (ILC)'nın iki seçeneği $\sqrt{s}$= 0.5 TeV ve $\sqrt{s}$= 1 TeV için sırayla 450 ve 950 GeV dir.

Anahtar kelimeler: Dördüncü aile, Egzotik kuark, Standart model ötesi modeller, String inspired E_6 model.

To my loving wife, Sevim...

ACKNOWLEDGEMENTS

There are several people who I would like to thank. Foremost is my wife, Sevim, who has always been especially supportive and encouraged when I have had to work into the late hours. I would also like to thank my thesis advisor Professor A.T. Alan, who has shared with me many of his ideas on which to pursue research, and encouraged me to learn interesting and invaluable ideas, techniques and skills. He has put forward the problems which make up to main subject of this thesis and during days in school and even till midnight in house he helped me solved this problems.

Many thanks go to teachers from whom I have learned during my graduate years. Especially I would like to thank to Dr. Resul Eryiğit who has help me with the technical problems in computing.

Thanks to my parents, who have always encourage and supported me.

Finally, I thank all my friends especially my officemate, A.T. Taşçı, for his friendship over the past years.

This thesis was supported in part by Abant Izzet Baysal University Research Fund (Grant No.2005.03.02.216)

TABLE OF CONTENTS

LIST OF TABLES

LIST OF FIGURES

CHAPTER 1

INTRODUCTION

The main purpose of elementary particle physics is to expose the inmost building blocks of matter and fundamental forces acting between them. The physics of elementary particles is also important to understand the evolution of the Universe from the Bing Bang to its present appearance. The development of elementary particle physics have two important sides: one is setting up physical models and calculating the observables with the appropriate mathematical methods. The other one is discovering new particles with the particle accelerators and detectors and measuring them with high precision.

1.1 Standard Model

The Standard Model (SM) describes matter-constituting and force-carrying particles and the interaction between them, except gravity. The matter-constituting particles are divided into two kind of fermions (which obey the Pauli exclusion principle); quarks and leptons. Each of leptons have two groups; one carries an electric charge which includes electron (e), muon (μ), tau (τ) and an another is electrically neutral which is electron neutrino (ν_e), muon neutrino (ν_μ) and tau neutrino (ν_τ). The quarks, have fractional charges, include up (u) and down (d) which are bound in protons and also other massive quarks, charm (c), strange (s), top (t) and bottom (b). The matter-constituting particles are summarized in Table 1.1. The matter constituting particles interact with each other through the exchange of integer spin gauge boson. These bosons are the mediators of

Table 1.1: The fundamental matter constituting particles of SM.

	1st generation	2nd generation	3rd generation
Quarks	up (u) mass : $1.5 - 3.0$ MeV charge $= 2/3$	charm (c) mass : 1.25 GeV charge $= 2/3$	top (t) mass : 174.2 GeV charge $= 2/3$
	down (d) mass : $3 - 7$ MeV charge $= -1/3$	strange (s) mass : 95 MeV charge $= -1/3$	bottom (b) mass : $4.20 - 4.70$ GeV charge $= -1/3$
Leptons	electron (e) mass : 0.511 MeV charge $= -1$	muon (μ) mass : 105.6 MeV charge $= -1$	tau (τ) mass : 1.776 GeV charge $= -1$
	electron neutrino (ν_e)	muon neutrino (ν_μ)	tau neutrino (ν_τ)

the three fundamental forces; the electromagnetic, weak and strong. These force carrier particles are summarized in Table (1.2). Among the forces the gravity can be ignored in high energy physics because it is too weak compared to the other forces acting between elementary particles.

The strong force binds the quarks together into the hadrons such as protons and neutrons which are described by Quantum Chromo Dynamic (QCD). Its exchange particles are called gluons (g). They act on everything that has color charge, which is carried by quarks and by the gluons themselves. QCD is a non-abelian $SU(3)$ gauge symmetry (if the group elements commute with each other in a group, this group is an Abelian group) which includes quarks come in three color (red, blue and green) and gluons come in eight colors. The theory predicts, the effective coupling strength (α_s) decreases with the increase of energy, therefore quarks are confined in hadrons but behave like free particles at high energy (short distance or asymptotic freedom). The electromagnetic interaction is described by the Quantum Electrodynamics gauge theory (QED). This theory based on the Abelian $U(1)$ symmetry which yields the conservation of the electromagnetic charge and the appearance of massless gauge boson called photon (γ). The weak interactions are mediated by $W^{\pm}$ and Z^0 bosons which affect on all

Table 1.2: The force carrier particles in the Standard Model.

Carrier Particle	Force	Mass (GeV)	Range(m)
Gluon (g)	Strong	0	10^{-15}
Photon (γ)	Electromagnetic	0	∞
$W^{\pm}$ Z^0	Weak	80.403 91.1876	10^{-18}

fermions. In 1967, the electromagnetic and the weak interactions are combined by Glashow-Weinberg-Salam (GWS) [1, 2] as called electroweak interactions. The unification is based on the theory that both quarks and leptons carry internal quantum numbers which transform under the $SU(2)_L \times U(1)_Y$ symmetry group. Here $SU(2)$ is non-Abelian electroweak isospin group and $U(1)$ is the Abelian hypercharge group.

In the SM, particle masses are generated by spontaneous breaking of the $SU(2)_L \times U(1)_Y$ symmetry of vacuum which is generally called Higgs mechanism [3, 4, 5]. In this mechanism, we consider an $SU(2)$ doublet of complex scalar as

$$\phi(x) = \begin{pmatrix} \phi^+ \\ \phi^0 \end{pmatrix} = \frac{1}{\sqrt{2}} \begin{pmatrix} \phi_1 + i\phi_2 \\ \phi_3 + i\phi_4 \end{pmatrix} \tag{1.1}$$

A convenient selection of the neutral direction is $\phi_1 = \phi_2 = \phi_4$=0 to preserve electric charge conservation. Therefore, the non-zero vacuum expectation value of ϕ is

$$\phi(x) = \frac{1}{\sqrt{2}} \begin{pmatrix} 0 \\ v + h(x) \end{pmatrix} \quad \text{with} \quad v = (-\frac{\mu}{\lambda})^{1/2} \tag{1.2}$$

an explicit renormalizable Lagrangian (Renormalizable theory is a theory in which all physical infinite contributions can be consistently eliminated through a can-

celation procedure)that leads to a vacuum expectation value

$$\mathcal{L} = |D_\mu \phi|^2 - \mu^2 \phi^\dagger \phi - \lambda(\phi^\dagger \phi)^2 \tag{1.3}$$

where $D_\mu = \partial_\mu - (1/2)ig\sigma^a W_\mu^a - (1/2)ig' B_\mu$, $B_\mu = \partial_\mu B_\nu - \partial_\nu B_\mu$ and $W_\mu = \partial_\mu W_\nu - \partial_\nu W_\mu - gW_\mu \times W_\nu$ are respectively, the gauge fields of $SU(2)_L$ and $U(1)_Y$ symmetries, with g and g' the corresponding gauge couplings and $\sigma^a (a = 1, 2, 3)$ are the Pauli matrices. The gauge boson mass term comes from the square of the covariant of the ϕ

$$\begin{aligned} |D_\mu \phi|^2 &= |(\partial_\mu - \frac{i}{2} g\sigma^a W_\mu^a - \frac{i}{2} g' B_\mu)\phi|^2 \\ &= \frac{g^2 v^2}{8}(W_1^\mu + iW_2^\mu)(W_\mu^1 - iW_\mu^2) + \frac{v^2}{8}(gW_3^\mu - g'B^\mu)^2 + \frac{1}{2}(\partial^\mu h)^2 + .. \end{aligned} \tag{1.4}$$

the mass term of the charged gauge boson field and neutral components of the gauge fields W_3^μ and B^μ in Eq. (1.4) are given by

$$\begin{aligned} W^\pm &= \tfrac{1}{\sqrt{2}}(W_\mu^1 \pm iW_\mu^2) \quad \text{with} \quad M_W = g\tfrac{v}{2} \\ Z_\mu^0 &= \tfrac{1}{\sqrt{g^2+g'^2}}(gW_\mu^3 - g'B_\mu) \quad \text{with} \quad M_Z = \sqrt{g^2+g'^2}\tfrac{v}{2} \\ A_\mu &= \tfrac{1}{\sqrt{g^2+g'^2}}(gW_\mu^3 + g'B_\mu) \quad \text{with} \quad M_A = 0 \end{aligned} \tag{1.5}$$

If the arrangement of scalar Higgs fields ϕ allows one to construct $SU(2)_L \times U(1)_Y$ invariant interaction of the Higgs fields with fermions, the fermion masses are obtained. Finally, The pure SM Higgs Lagrangian which includes kinetic part of Higgs field, the last term in Eq. (1.4), and Higgs mass and self interaction parts come from the scalar potential $V(\phi) = \mu^2 \phi^\dagger \phi + \lambda(\phi^\dagger \phi)^2$ are given by

$$\mathcal{L}_h = \quad = \frac{1}{2}(\partial^\mu h)^2 - \frac{\mu^2}{2}(h+v)^2 - \frac{\lambda}{4}\lambda(h+v)^4 \tag{1.6}$$

$$= \frac{1}{2}(\partial^\mu h)^2 - \lambda^2 v^2 h^2 - \lambda v h^3 - \frac{\lambda}{4}h^4 + \frac{\lambda v^4}{4}.$$

From this Lagrangian, the Higgs boson mass is

$$m_h = \sqrt{2}\mu^2 = \sqrt{\frac{\lambda}{2}}v.$$

This particle is known as the Higgs boson which is the agent of electroweak symmetry breaking. Therefore, the search for Higgs boson with the Large Hadron Collider (LHC) is the highest priority steps to understand the origins of electroweak symmetry breaking.

1.1.1 Standard Model Lagrangian

The SM Lagrangian is constructed to be locally invariant under the $U(1)_Y$ of weak hypercharge, the $SU(2)_L$ of weak isospin and $SU(3)_c$ of color. These components are given by

$$\begin{aligned}
\mathcal{L} \;=\; & -\frac{1}{4}W_{\mu\nu}\cdot W^{\mu\nu} - \frac{1}{4}B_{\mu\nu}\cdot B^{\mu\nu} - \frac{1}{4}G_{\mu\nu}\cdot G^{\mu\nu} \\
& + \bar{L}\gamma^\mu(i\partial_\mu - \frac{1}{2}g\tau\cdot W_\mu - \frac{1}{2}g'YB_\mu)L + \bar{R}\gamma^\mu(i\partial_\mu - \frac{1}{2}g'YB_\mu)R \\
& + |(i\partial_\mu - \frac{1}{2}g\tau\cdot W_\mu - \frac{1}{2}g'YB_\mu)\varphi|^2 - V(\varphi) \\
& - (g_1\bar{L}\varphi R + g_2\bar{L}\tilde{\varphi}R + h.c.) \\
& + \frac{1}{2}g_s(\bar{\psi}_q^j\gamma^\mu\lambda_{jk}^a\psi_q^k)G_\mu^a.
\end{aligned} \tag{1.7}$$

where $G_{\mu\nu} = \partial_\mu G_\nu^a - \partial_\nu G_\mu^a - g_s f_{abc}G_\mu^b G_\nu^c$ are gluon fields with $a = 1, 2, ..., 8$ runing over gluon indices, L and R represents a left handed fermion doublet and right handed singlet, respectively, $\varphi(\tilde{\varphi})$ the Higgs doublet and its conjugate and ψ_q^j a quark color field. First line of this Lagrangian describes kinetic energies and self

interactions of gauge bosons ($W^{\pm}$, Z^0, γ and gluon), second line is fermion kinetic energies and their electroweak interactions, third line is masses and couplings of the $W^{\pm}$, Z^0, γ and Higgs boson, last line is interaction between quark-gluon couplings.

To summarize, the SM defines the behaviour of strong and electroweak interactions between 25 particles as six quarks and leptons, twelve gauge bosons and Higgs boson. These interactions are described by 19 parameters: three gauge couplings (g, g' and g_s), the self-coupling (λ) and vacuum expectation (v) of Higgs field, the mixing angle ($\sin\theta_w$), the nine fermion masses and four elements of the CKM matrix. The SM assumes that there are no right handed neutrinos and thus they are expected to be massless. However, the recent observation of neutrino oscillations gives evidence that the neutrino mass is non-zero [6, 7, 8, 9]. If we include mass of these neutrinos, three more mass parameters and additional mixing matrix elements like CKM type must be added to the SM Lagrangian.

1.2 Neutrino Physics

The history of the neutrino begins in 1930. On 4 December 1930 Wolfgang Pauli postulated the existence of massless, chargeless and non interacting new particle [10]. These particles are emitted together with electrons in nuclear β-decay ($n \rightarrow p + e^- + \bar{\nu}_e$) as the carrier of missing energy. He called this new particle "neutron", but it was later renamed the "neutrino" by Enrico Fermi in 1934 [11]. The first experimental evidence of W. Pauli's postulate was directly observed by Reines and Cowan in a nuclear reactor experiment, inverse β decay ($\nu + p \rightarrow n + e^+$), in 1953 [12]. The second neutrino from pion decay, muon neutrino (ν_μ), was detected by Lederman et.al. in 1962 [13] and third neutrino is tau neutrino which was observed in 2001 at FermiLab [14].

Neutrinos have played a special role in the SM in that they are the only particles that have zero mass and only interact via the weak interaction. All neutrinos have only been observed in left handed states (spin parallel to their momentum), while anti-neutrinos have only been observed in right-handed (spin and momentum are anti-parallel). This is a consequence of the Vector-Axial $(V - A)$ structure of the weak interaction. In this theory the spinor of the fermions or anti fermions produced in $W^{\pm}$ vertex are projected with $(1 \pm \gamma_5)$. So, particles are produced in weak interaction vertices with a well defined chirality. Neutrino interactions occur through two types of boson exchange; the two gauge bosons which carry the weak force are the W and the Z. Exchange of Z is called a neutral current interaction, and exchange of a W^+ or W^- is called a Charged Current (CC) interaction.

However, recent experimental evidence of neutrino oscillation indicate that neutrinos have a mass [6, 7, 8, 9]. One of the fundamental principle (Neutrino mass is zero in the SM) of the Standard Model of particle interaction is destroyed by these experimental results. Therefore, the discovery that the neutrinos have mass paved the path to extension of the SM.

1.2.1 Neutrino Masses

In the SM, neutrinos only appear in the doublets of the group $SU(2)_L$ which do not allow any Yukawa coupling. Therefore, neutrinos have no mass with particle content of the SM. The nature of neutrino mass and character of neutrino mixing is determined in Lagrangian by the explicit neutrino mass terms. There are two possible types of mass terms

$$-L_M = \sum M_{il}^D \bar{\nu}_{iR} \nu_{lL} + \frac{1}{2} M_{ij}^M (\nu_{iR})(\nu_{jR})^c + h.c. \tag{1.8}$$

The first term is a Dirac mass term which allows a conserved lepton number but might violate the individual lepton flavor numbers, because it has a neutrino and antineutrino field. M_{il}^{D} is a complex $3 \times m$ matrix.

The second term in Eq. (1.8) is a Majorana mass term. It is a singlet of the SM gauge group and involves two neutrino fields. Therefore, this term breaks lepton number conservation by two units and it is allowed only if the neutrinos have no additive conserved charges. The M_{ij}^{M} is a symmetric matrix of dimension $m \times m$.

If three light left-handed neutrinos ν_{lL} and heavy (sterile) ν_{jR} neutrinos are both present, both Dirac and Majorana mass terms exist simultaneously. The Lagrangian has the form

$$-L_M = \frac{1}{2}\bar{\nu^c} M_\nu \nu + h.c., \tag{1.9}$$

here

$$\nu = \begin{pmatrix} \nu_{lL} \\ (\nu_{jR})^c \end{pmatrix} \quad \text{and} \quad M_\nu = \begin{pmatrix} 0 & M^D \\ (M^D)^T & M^M \end{pmatrix}.$$

The matrix M_ν is complex and symmetric. It can be diagonalized by a unitary matrix of dimension $(3 + m)$ which yields two Majorana mass eigenvalues and eigenstates. There are several interesting cases, in the hierarchy of scales between M^M and M^D.

i) If the scale of the M^M is very large, this case called the seesaw mechanism. In this case, there are three light active Majorana neutrinos.

ii) If the scale of some eigenvalues of M^M is not higher than the scale of electroweak symmetry breaking, there are more than three light Majorana neutrinos and mixture of active and sterile neutrinos.

iii) Finally, if $M^M = 0$, there are six massive Majorana neutrinos that combine

to form three massive Dirac neutrinos. This result is a pure Dirac netrino field.

1.2.2 Neutrino Oscillation

The neutrino oscillation phenomena hinges on the assumption that neutrinos have mass and that the mass eigenstates are not the same as the flavor eigenstates. The idea of the possible existence of neutrino oscillations was first introduced by Pontecorvo [15] and independently by Maki et.al. [16]. According to this theory the three neutrino flavors ν_e, ν_μ and ν_τ are not mass eigenstates but quantum mechanical superposition of three mass eigenstates ν_1, ν_2 and ν_3 with mass eigenvalues m_1, m_2 and m_3, respectively

$$\mid \nu_\alpha\rangle = \sum_j U^*_{\alpha j} \mid \nu_j\rangle \tag{1.10}$$

where $\mid \nu_\alpha\rangle$ represents a flavor eigenstate, $\mid \nu_j\rangle$ represents a mass eigenstate and $U^*_{\alpha j}$ represents a matrix known Pontecorvo-Maki-Nakayawa-Sakata (PMNPS) leptonic mixing matrix, which can be parametrised as:

$$\begin{aligned} U &= \begin{pmatrix} 1 & 0 & 0 \\ 0 & c_{23} & s_{23} \\ 0 & -s_{23} & c_{23} \end{pmatrix} \begin{pmatrix} c_{13} & 0 & s_{13}e^{-i\delta} \\ 0 & 1 & 0 \\ -s_{13}e^{-i\delta} & 0 & c_{13} \end{pmatrix} \begin{pmatrix} c_{12} & s_{12} & 0 \\ -s_{12} & c_{12} & 0 \\ 0 & 0 & 1 \end{pmatrix} \\ &= \begin{pmatrix} c_{12}c_{13} & s_{12}c_{13} & s_{13}e^{-i\delta} \\ -s_{12}c_{23} - c_{12}s_{13}s_{23}e^{i\delta} & c_{12}c_{23} - s_{12}s_{13}s_{23}e^{i\delta} & c_{13}s_{23} \\ s_{12}s_{23} - c_{12}s_{13}c_{23}e^{i\delta} & -c_{12}s_{23} - s12s_{13}c_{23}e^{i\delta} & c_{13}c_{23} \end{pmatrix} \end{aligned} \tag{1.11}$$

where $c_{ij} = \cos\theta_{ij}$ and $s_{ij} = \sin\theta_{ij}$, $(i, j = 1, 2, 3)$. The three angles θ_{12}, θ_{23} and θ_{13} represent the mixing angles and δ is the CP violating phase.

1.2.3 Two neutrinos oscillation

The neutrino oscillations are clearly demonstrated for simplified case of two generation mixing. In this case the mixing matrix U is described by only one real parameter θ. Considering the two neutrino flavors (for example ν_e, ν_μ) as mixtures of two mass eigenstates ν_1 and ν_2 with masses m_1 and m_2. The relation between flavor and mass eigenstates can then be written in matrix form as:

$$\begin{pmatrix} \mid \nu_e\rangle \\ \mid \nu_\mu\rangle \end{pmatrix} = \begin{pmatrix} \cos\theta & \sin\theta \\ -\sin\theta & \cos\theta \end{pmatrix} \begin{pmatrix} \mid \nu_1\rangle \\ \mid \nu_2\rangle \end{pmatrix} \tag{1.12}$$

We assumed that an electron neutrino is created at time $t = 0$ with momentum p. This corresponds to the initial states:

$$\mid \nu(t=0)\rangle = \mid \nu_e\rangle = \cos\theta \mid \nu_1\rangle + \sin\theta \mid \nu_2\rangle \tag{1.13}$$

Applying the time evolution operator, e^{-iHt}, a time t the neutrino state will be:

$$\mid \nu(t)\rangle = \cos\theta e^{-iE_1 t} \mid \nu_1\rangle + \sin\theta e^{-iE_2 t} \mid \nu_2\rangle \tag{1.14}$$

here E_1 and E_2 are energies of two different neutrino states. Then, the probability that a neutrino originally of the ν_e flavor will at a time t be detected as a ν_μ is

$$\begin{aligned} P(\nu_e \to \nu_\mu; t) &= \mid \langle \nu_\mu \mid \nu(t)\rangle \mid^2 \\ &= \mid \{-\sin\theta\langle \nu_1 \mid + \cos\theta\langle \nu_2 \mid\} \mid \nu(t)\rangle \mid^2 \\ &= \cos^2\theta \sin^2\theta \mid e^{-iE_2 t} - e^{-iE_1 t} \mid^2 \qquad (1.15) \\ &= 2\cos^2\theta \sin^2\theta\{1 - \cos[(E_2 - E_1)t]\} \\ &= \sin^2 2\theta \sin^2[\frac{(E_2 - E_1)t}{2}] \qquad (1.16) \end{aligned}$$

where we have used the approximation, valid for $m \ll p$,

$$E_i = \sqrt{p^2 + m_i^2} \approx p(1 + \frac{m_i^2}{2p}) \tag{1.17}$$

then,

$$\begin{aligned} E_2 - E_1 &= \sqrt{p^2 + m_2^2} - \sqrt{p^2 + m_2^2} \\ &\approx \frac{m_2^2 - m_1^2}{2p} \qquad (1.18) \\ &\approx \frac{\triangle m^2}{2E} \qquad (1.19) \end{aligned}$$

If L is the distance the particle travels in time t, Eq. (1.15) becomes

$$P(\nu_e \to \nu_\mu; L) = \sin^2(2\theta) \sin^2(1.27 \frac{\triangle m^2 L}{E}) \tag{1.20}$$

where L is measured in km, $\triangle m^2$ is measured in eV, E is measured in GeV and the factor of 1.27 arises from the unit conversion. Eq. (1.20) describes an appearance oscillation formula with amplitude equal to $\sin^2 2\theta$ and oscillation length L given by

$$\lambda = 2.48 \frac{E}{\triangle m^2} \tag{1.21}$$

We note that, if the oscillation length L is much shorter than the size of the neutrino source or of the detector (or of both), the periodic term in Eq. (1.20) averages to 1/2 and the oscillation probability becomes independent of L :

$$P = \frac{1}{2} \sin^2 2\theta \tag{1.22}$$

1.2.4 Neutrino Oscillation experiments

There are two types of oscillation searches:

1. Appearance experiments, in which one looks for the appearance of a new flavor, e.g., of ν_e or ν_τ (i.e. of e or τ) in an initially pure ν_μ beam.

2. Disappearance experiments, in which one looks for a change in, e.g., the ν_μ flux as a function of L and E.

The three main experiments provide evidence of neutrino oscillation: firstly SuperKamiokande, which investigates the interactions of both solar and atmospheric neutrinos, secondly Sudbury Neutrino Observatory (SNO), which investigates the interactions of solar neutrinos, and finally KamLAND and LSND, which study the interactions of reactor neutrinos. These experiments are briefly discussed here

Super Kamiokande

Super Kamiokande uses a 50 kiloton water Cherenkov detector where constructed under Mt. Ikenoyama located at the central part of Japan to detect neutrinos produced by cosmic ray interactions in the atmosphere as well as the properties of neutrinos produced in the sun [6]. Atmospheric neutrino production is dominated by the process $\pi^\pm \rightarrow \mu^\pm + \nu_\mu(\bar{\nu}_\mu)$. The $\mu^\pm$ then decays via the reaction $\pi^\pm \rightarrow e^\pm + \nu_e(\bar{\nu}_e)$. Both the ν_μ and the ν_e are detected in the Cherenkov detector, and the number of each neutrino type observed is compared to the expected value. The Super Kamiokande detector used in cooperation with another measurement of oscillations done by the KEK (High Energy Accelerator Research Organization) to Kamioka (K2K) neutrino oscillation experiment [17]. The neutrino beam is produced by a 12 GeV proton beam from the KEK proton synchrotron. After the production of the neutrinos at KEK they are sent to the SK detector in Kamioka mine 250 km away.

SNO

SNO is a water Cherenkov detector located at a depth of 6010 m of water equivalent in the INCO, Ltd. Creighton mine near Sudbury, Ontario, Canada [7]. Three neutrino interactions are detected by SNO ; First, the charged current (CC) reaction $\nu_e + d \rightarrow p + p + e^-$ is sensitive exclusively to electron-type neutrinos. Second, neutral current reaction $\nu_x + d \rightarrow p + n + \nu_x$ $(x = e, \mu, \tau)$ is equally sensitive to all active neutrino flavors and finally, the elastic scattering reaction $\nu_x + e^- \rightarrow \nu_x + e^-$ is sensitive to all flavors as well, but with reduced sensitivity to ν_μ and ν_τ. SNO clearly demonstrates that the flavor of solar neutrinos changes during the journey from the sun to the earth.

KamLAND

The evidence for the oscillations of solar neutrinos has been recently dramatically confirmed by the Kamioka Liquid Scintillator Anti-Neutrino Detector (KamLAND) experiment [8] with a measurement of the flux of reactor neutrinos for long (L $\sim$ 180 Km) distance. The sensitive volume of the KamLand detector is a sphere of 6.5 meters radius that contains 1000 tons of liquid scintillator, instrumented with photomultipliers. Electron anti-neutrinos can be detected with the usual reaction: $\nu_e + p \rightarrow e^+ + n$, measuring the positron in the liquid scintillator, the photon emitted in the neutron capture is also observable. The ν_e flux is provided by an ensemble of approximately 70 reactor cores located at a distance between 150 and 210 Km from the detector in several commercial nuclear plants.

LSND

The Liquid Scintillator Neutrino Detector (LSND) [9] is one other experiment that claims to observe neutrino oscillations at Los Alamos. This collaboration has also reported evidence for neutrino flavor transitions of type $\bar{\nu_\mu} \rightarrow \bar{\nu_e}$. The

LSND neutrino source is obtained from an accelerated 800 MeV proton beam, the detector is a tank filled with 167 tons of liquid scintillator at a distance of 30 meters from neutrino source. The large number of charged pions was created and stopped in target region and decay with usual sequence $\pi^+ \rightarrow \nu_\mu + \mu^+$ followed by $\mu^+ \rightarrow \bar{\nu_\mu} + \nu_e + e^-$. The contribution of π^- is much suppressed because they are capture on nuclei with very high probability and thus, the beam contains $\nu_\mu, \bar{\nu_\mu}$ and ν_e. These neutrinos all have very well defined energy spectra and note that there are no $\bar{\nu_e}$ produced in this process.

1.3 Beyond the Standard Model

Despite the impressive success of the SM in explaining available experimental observation to very high degree of precision, it contains theoretical problems which cannot be solved without an introduction of some new physics. As a result, further test of the SM and the search for the signature of new physics are highly needed. The more common complaints about the SM can be summarized as follows;

The number of fermion generations and their mass spectrum are not explained by the SM. Up to date, there is no experimental evidence for extra generations of fermions, but there is no experimental or theoretical result disregarding such a possibility.

The neutrino is massless in the SM. However, there is by now quite solid evidence supporting the existence of non-zero neutrino mass, coming from the explanation of the neutrino oscillation experiment [6, 7, 8]. However, the SM with just left-handed neutrinos and a Higgs doublet is unable to provide a non-zero mass. Simply adding neutrino mass terms to the SM Lagrangian would introduce the right-handed states ν_R.

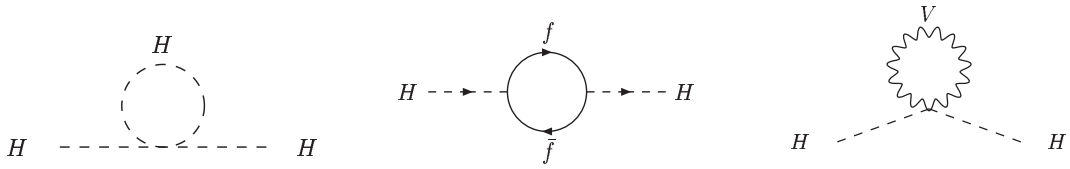

Figure 1.1: Divergent loop contributions to the Higgs boson mass.

The origin of baryon asymmetry, the excess of matter over antimatter in the universe, is explicitly ruled out by the SM. In order to generate the observed baryon asymmetry, the non conservation of baryon number, CP violation and existence of non-equilibrium processes are needed.

One of the most common issue for physics beyond the SM is the hierarchy problem. This theoretical problem is related to the fact that loop corrections to the scalar (Higgs) masses are quadratically divergent as shown in Fig.1.1, a cut off Λ must be introduced in the loop integral to regulate the divergence. Hierarchy problems are related to fine-tuning problems. Although the large quantum contributions (quadratically divergent) to the square of the Higgs boson mass would inevitably make the mass huge at the Planck scale, the Higgs mass must remain smaller than 900 GeV to maintain unitarity in longitudinal gauge boson scattering. This constraint requires fine-tuning cancelation between the quadratic radiative corrections and bare mass. This is called fine-tuning problem.

The SM fails to describe any details of gravitational force and their interactions, while the other forces and interactions between the particles are defined. Therefore, the unification all fundamental forces is not achieved.

The three interaction coupling strengths of the SM are energy dependent. These coupling constants would not meet a single point at high energies as one would expect in Grand Unified Theories (GUT). GUT combines the SM group $SU(3) \times SU(2) \times U(1)$ in a larger group with the aim of relating the different

gauge couplings.

Measurements of matter energy density of the universe from WMAP(Wilkinson Microwave Anisotropy Probe) experiment find that SM particles contributes only a small fraction of matter density of Universe. So, the SM is not a good candidate for the dark matter. Until now there is no description for dark matter and dark energy.

Finally, the SM has unrelated 19 parameters. These parameters are three coupling constants, three charged lepton masses, six quark masses, three CKM mixing angles, one CP violating phase, Higgs quartic coupling and Higgs vacuum expectation value in the Higgs sector and QCD parameter. If the neutrino masses and leptonic mixings are taken into account, this number is further increased. This large number of parameters can itself be seen as a disadvantage of the SM.

The unsolved theoretical problems of the SM motivated the development of some other theories beyond the SM. Two methods can be used to investigate the physics beyond the SM. For the first method, a specific model is used for the calculation while in the second method parametrization of any given high energy model by the coefficients of the series of the effective operators without any specific theory. Thus, there are many different theories for new physics beyond the SM in recent years e.g., supersymmetry [18, 19], technicolor [20] extra dimensions [21, 22, 23, 24], two Higgs doublet model [25], String inspired E_6 model [26, 27, 28] , left-right symmetric model [29, 30, 31], Zee Model [32, 33], Randall-Sundrum model [34] and others. There are also reasons to believe that the SM will be inadequate at higher energies than those available today. Therefore, the future colliders might discover new physics which could hold the answer to these questions. Especially, the Large Hadron Collider (LHC) will begin taking data in a few months and it is widely believed that new physics beyond the SM will

be discovered in the coming years.

As a result, the search for the signatures of new physics are highly needed. This thesis describes searches for new physics using additional non-standard particles at future colliders. The outline of this thesis is as follows: in chapter 2, the anomalous production and decay of fourth generation up quarks at lepton hadron colliders are discussed. Chapter 3, deals with the single production and decay of charge -1/3, weak isosinglet vectorlike exotic quarks in string inspired E_6 theories at future ep colliders and we also discussed the background processes of this quark. In chapter 4, the fourth generation neutrino production in the context of a new $e\nu_4 W$ and $\nu_4\bar{\nu}_4 Z$ magnetic dipole moment type interaction is investigated and the background is analyzed using optimal cuts. This chapter is divided into three section; in section 4.1, the possible single production of fourth generation neutrino in ep collisions are discussed, in section 4.2 the single and pair production of fourth generation neutrino using pp colliders is studied and in section 4.3, we present the single and pair production of fourth generation neutrino at future e^+e^- colliders options. Chapter 5 contains summary and conclusions. In the appendix, we display some properties of Pauli and Dirac matrices and useful formulae of the trace theorems.

CHAPTER 2

ANOMALOUS PRODUCTION OF FOURTH GENERATION UP QUARKS AT FUTURE LEPTON HADRON COLLIDERS

As is well known, the Standard Model (SM) with three families is in excellent agreement with experimental data available today [35]. But it leaves some open questions. At the most fundamental level, the number of fermion generations and the origin of their mass hierarchy are not explained by the SM. For these reasons, and others, several models extending SM have been proposed [36, 37, 38, 39, 40, 41]. Except the minimal SU(5) GUT all these models accommodate extra fermion generations [42, 43, 44].

In the context of the search programs of future colliders, many analyses have been done for the production of fourth generation quarks at the linear [45, 46, 47, 48, 49] and at hadron colliders [50, 51, 52, 53, 54]. The potentials of the future lepton-hadron colliders in the new physics searches are comparable to those of the linear and hadron colliders [55, 56]. Thus, in this chapter, we investigate the possibility of a single production of a fourth-generation up quark (u_4) suggested by the effective Lagrangian approach. In this approach the most general effective Lagrangian, which describes the Flavour Changing Neutral Current (FCNC) interactions between u_4 and ordinary quarks, involving electroweak boson and gluon is given as follow [57, 58, 59]:

$$\mathcal{L}_{eff} = \sum_{U=u,c} i\frac{ee_U}{\Lambda}\kappa_{\gamma,u_4}\bar{u}_4\sigma_{\mu\nu}q^\nu U A^\mu$$

$$+ \quad \frac{g}{2\cos\theta_W}\bar{u}_4[\gamma_\mu(v_{Z,U}-a_{Z,U}\gamma^5)+i\frac{\kappa_{Z,u_4}}{\Lambda}\sigma_{\mu\nu}q^\nu]UZ^\mu$$
$$+i\frac{g_s}{\Lambda}\kappa_{g,u_4}\bar{u}_4\sigma_{\mu\nu}q^\nu\frac{\lambda^i}{2}UG^{i\mu}+h.c., \tag{2.1}$$

where $\sigma_{\mu\nu}$=(i/2)[γ^μ , γ^ν], θ_W is the Weinberg angle, q is the four-momentum of the exchanged boson; e, g and g_s denote the gauge couplings relative to U(1), SU(2) and SU(3) symmetries, respectively; e_U is the electric charge of up-type quarks, A^μ, Z^μ and $G^{i\mu}$ the fields of the photon, Z boson and gluon, respectively; and Λ denotes the scale up to which the effective theory is assumed to hold. By convention, we set Λ=m$_4$, mass of the fourth family quark in following.

2.1 The Anomalous Decays of Fourth Family Up Quark

For calculation of the eqV (here $q = u, c, t$ and V= γ, Z, g) cross section including fourth generation up-quark contributions, the total width Γ_{u_4} is needed. In this section, all of the tree level two-body decay widths for u_4 are computed. Therefore, the generic two-body decay formula is given by [60]

$$\Gamma = \frac{S|\mathcal{M}_{12}|}{16\pi m_1}\beta_{123} \tag{2.2}$$

where $m_i, i = 1, 2, 3$ are the masses of the particles, p_i, in the decay process $p_1 \rightarrow p_2 p_3$,

$$\beta_{123} = \sqrt{1-\frac{2(m_2^2+m_3^2)}{m_1^2}+\frac{(m_2^2-m_3^2)^2}{m_1^4}} \tag{2.3}$$

S is a symmetry factor for the outgoing particles, p_2 and p_3, $\mathcal{M}_{12}$ is the amplitude for the process.

From Eq. (2.1), the amplitude of the $u_4(1) \rightarrow q(2)\gamma(3)$ decay process can be written as

$$\mathcal{M} = \bar{u}(p_2)[\frac{ee_U}{\Lambda}\kappa_\gamma\sigma_{\mu\nu}(p_1-p_2)^\nu]\epsilon_\mu^* u(p_1) \tag{2.4}$$

f	$Charge$	a^f	v^f
ν_e, ν_μ, ν_τ	0	$\frac{1}{2}$	$\frac{1}{2}$
e^-, μ^-, τ^-	-1	$-\frac{1}{2}$	$-\frac{1}{2}+2\sin^2\theta_W$
u, c, t	$\frac{2}{3}$	$\frac{1}{2}$	$-\frac{1}{2}-\frac{4}{3}\sin^2\theta_W$
d, s, b	$-\frac{1}{3}$	$-\frac{1}{2}$	$-\frac{1}{2}-\frac{4}{3}\sin^2\theta_W$

Table 2.1: Neutral Vector and Axial Vector Couplings

and then matrix element squared is:

$$|\mathcal{M}|^2 = \frac{4e^2e_U^2\kappa_\gamma^2}{\Lambda^2}[-4(3m_1^2+4m_1m_2+3m_2^2-2p_1.p_2)(m_1m_2-p_1.p_2)] \tag{2.5}$$

with $p_1.p_2 = (m_1^2+m_2^2)/2$ and plugging into Eq. (2.2) gives

$$\Gamma(u_4 \to q\gamma) = \alpha e_U^2\kappa_\gamma^2 m_1(1-\frac{m_2^2}{m_1^2})^3 \tag{2.6}$$

here α is fine structure constant, m_1 is mass of the u_4 and m_2 is mass of the ordinary quarks.

In order to obtain the decay width $\Gamma(u_4 \to qZ)$, we write the decay amplitude again from Eq. (2.1);

$$\mathcal{M} = \frac{g_Z}{2}\bar{u}(p_2)[\gamma^\mu(v_q-a_q\gamma^5)+\frac{i\kappa_Z}{\Lambda}\sigma^{\mu\rho}(p_1-p_2)_\rho]u(p_1)\epsilon_\mu^* \tag{2.7}$$

where $g_Z = g/\cos\theta_W$, v_q and a_q neutral vector and axial vector couplings of quarks are given in Table 2.1. We compute the matrix element squared are:

$$|\mathcal{M}|^2 \;=\; g_Z^2[\frac{(a_q^2+v_q^2)}{m_3^2}(p_1.p_2(m_1^2+m_2^2+2m_3^2)-2m_1^2m_2^2)-6v_q\kappa_Z(p_1.p_2-m_2^2)$$

Table 2.2: Branching ratios (%) and total decay widths of u_4 quark depending on its mass ($\kappa_\gamma = \kappa_Z = \kappa_g = 0.1$, $\Lambda = m_{u_4}$)

Mass (GeV)	$gu(c)$	gt	$Zu(c)$	Zt	$\gamma u(c)$	γt	Γ(GeV)
300	3.1	0.9	70.5	25.2	0.1	0.04	7.15
400	1.4	0.8	61.1	36.6	0.07	0.04	20.12
500	0.8	0.6	57.3	41.2	0.04	0.03	42.31
600	0.5	0.4	55.2	43.8	0.03	0.02	76.29
700	0.4	0.3	53.9	45.4	0.02	0.02	124.45

$$- \quad \frac{\kappa_Z}{m_1^2}(2(p_1.p_2)^2 + 4m_1^2 m_2^2 - 3(m_1^2 + m_2^2)p_1.p_2)] \tag{2.8}$$

with $p_1.p_2 = (m_1^2 - m_2^2)/2$ and $m_2 = 0$ which yields, via Eq. (2.2),

$$\begin{aligned} \Gamma(u_4 \to qZ) &= \frac{\alpha m_1}{4 s_W^2 c_W^2}(1 - \frac{m_3^2}{m_1^2})^2[\kappa_Z^2(1 + \frac{m_3^2}{2m_1^2}) \\ &- 3v_q\kappa_Z + (a_q^2 + v_q^2)(1 + \frac{m_1^2}{m_3^2})] \end{aligned} \tag{2.9}$$

The other decay mode of u_4 is $\Gamma(u_4 \to qg)$. This decay is obtained by following steps similar to Eqs. (2.2)-(2.5). Accordingly the corresponding decay width is obtained from Eq. (2.5) via replacements $\alpha e_0^2 \to 3\alpha_s e_0^2$;

$$\Gamma(u_4 \to qg) = 3\alpha_s e_U^2 \kappa_g^2 m_1 (1 - \frac{m_2^2}{m_1^2})^3 \tag{2.10}$$

Using Eqs. (2.5), (2.8), (2.9), we have presented Table 2.2 the branching ratios and total decay widths of u_4 with $\kappa_\gamma = \kappa_Z = \kappa_g = 0.1$.

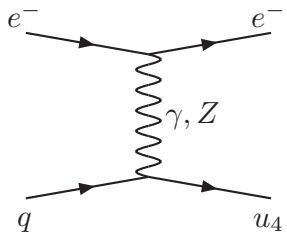

Figure 2.1: The Feynman diagram at parton level for single fourth generation up quark production in ep collisions via FCNC interaction.

2.2 The Anomalous Production of Fourth Generation Up Quark

Following (2.1), the vertices of the FCNC transitions $u_4 \to q\gamma$ and $u_4 \to qZ$ can be written as follows;

$$\begin{aligned} \Gamma^{\gamma}_{\mu} &= \frac{iee_U}{\Lambda}\kappa_{\gamma}\sigma^{\mu\nu}q_{\nu} \\ \Gamma^{Z}_{\mu} &= \frac{g_Z}{2}[\gamma^{\mu}(v_q - a_q\gamma^5) + i\kappa_Z\sigma^{\mu\nu}q_{\nu}]. \end{aligned} \tag{2.11}$$

and the propagator for massless and massive spin-1 particles are defined

$$-i\frac{g_{\mu\nu}}{q^2} \quad \text{for massless} \tag{2.12}$$

$$-i\frac{g_{\mu\nu}-q_\mu q_\nu/M^2}{q^2-M^2+i\Gamma M} \quad \text{for massive} \tag{2.13}$$

here Γ and M decay width and mass of the massive spin-1 particles, respectively.

The u_4 are produced via $e(p_1)+q(p_2) \to e(p_3)+u_4(p_4)$. The Feynman diagram for this process is given in Fig. 2.1. Contributions from Photon exchange, Z-

boson exchange, and their interference are included. The complete matrix element squared has the form;

$$< |\mathcal{M}|^2 >=< |\mathcal{M}_\gamma|^2 > + < |\mathcal{M}_Z|^2 > + < \mathcal{M}_\gamma \bar{\mathcal{M}}_Z > + < \bar{\mathcal{M}}_\gamma \mathcal{M}_Z > \quad (2.14)$$

Using the effective vertices Γ^γ_μ and Γ^Z_μ given by Eq. (2.11), the amplitudes of subprocess $eq \to eu_4$ are written as

$$\begin{aligned}
\mathcal{M}_\gamma &= \bar{u}(p_3)(ie\gamma^\mu)u(p_1)[\frac{g_{\mu\nu}}{(p_1+p_2)^2}]\bar{u}(p_4)(\Gamma^\gamma_\nu)u(p_2) && (2.15)\\
\mathcal{M}_Z &= \bar{u}(p_3)(-i\frac{g_Z}{2}\gamma^\mu(v_e - a_e\gamma^5))u(p_1)[\frac{g_{\mu\nu} - q_\mu q_\nu/M_Z^2}{[q^2 - M_Z^2 + i\Gamma_Z M_Z]}] \\
&\times \bar{u}(p_4)(\Gamma^Z_\nu)u(p_2) && (2.16)
\end{aligned}$$

$$\begin{aligned}
\mathcal{M}_\gamma\bar{\mathcal{M}}_Z &= \bar{u}(p_1)(-i\frac{g_Z}{2}\gamma^\alpha(v_e - a_e\gamma^5))u(p_3)[\frac{g_{\alpha\beta} - q_\alpha q_\beta/M_Z^2}{[q^2 - M_Z^2 - i\Gamma_Z M_Z]}] \\
&\times \bar{u}(p_2)(\Gamma^Z_\beta)u(p_4)\bar{u}(p_3)(ie\gamma^\mu u(p_1)(-i\frac{g_{\mu\nu}}{q^2})\bar{u}(p_4)(\Gamma^\gamma_\nu u(p_2) && (2.17)
\end{aligned}$$

$$\begin{aligned}
\bar{\mathcal{M}}_\gamma\mathcal{M}_Z &= \bar{u}(p_2)(\Gamma^\gamma_\rho)u(p_4)(-i\frac{g_{\rho\sigma}}{q^2})\bar{u}(p_1)(ie\gamma^\sigma)u(p_3) \\
&\times \bar{u}(p_3)(i\frac{g_Z}{2}\gamma^\alpha(v_e - a_e\gamma^5))u(p_1)[\frac{g_{\mu\nu} - q_\mu q_\nu/M_Z^2}{[q^2 - M_Z^2 + i\Gamma_Z M_Z]}]\bar{u}(p_4)(\Gamma^Z_\nu u(p_2) \\
& && (2.18)
\end{aligned}$$

and the trace form of the amplitude squared are

$$\begin{aligned}
< |\mathcal{M}_\gamma|^2 > &= \frac{e_U^2 e^4 \kappa_\gamma^2}{4\Lambda^2 q^4} Tr[(\not{p}_1 + m_1)\gamma^\mu(\not{p}_3 + m_3)\gamma^\rho] \\
&\times Tr[(\not{p}_4 + m_4)\sigma_{\mu\alpha}q^\alpha(\not{p}_2 + m_2)\sigma_{\rho\beta}q^\beta]. && (2.19)\\
< |\mathcal{M}_Z|^2 > &= \frac{g_Z^4}{64[(\hat{t} - M_Z^2)^2 + \Gamma_Z^2 M_Z^2]}[g_{\mu\nu} - q_\mu q_\nu/M_Z^2][g_{\alpha\beta} - q_\alpha q_\beta/M_Z^2] \\
&\times \{Tr[(\not{p}_3 + m_3)\gamma^\mu(v_e - a_e\gamma^5)(\not{p}_1 + m_1)\gamma^\alpha(v_e - a_e\gamma^5)]
\end{aligned}$$

$$
\begin{aligned}
&\times \quad Tr[(\not{p}_4 + m_4)[\gamma^\nu(v_q - a_q\gamma^5) + i\frac{\kappa_Z}{\Lambda}\sigma^{\nu\rho}q_\rho](\not{p}_2 + m_2)[\gamma^\beta(v_q - a_q\gamma^5) \\
&\quad -i\frac{\kappa_Z}{\Lambda}\sigma^{\beta\delta}q_\delta]]\} \qquad (2.20)
\end{aligned}
$$

$$
\begin{aligned}
< \mathcal{M}_\gamma\bar{\mathcal{M}}_Z > \quad &= \quad -\frac{ie_U e^2 g_Z^2\kappa_\gamma[(\hat{t} - M_Z^2) + i\Gamma_Z M_Z]}{16\Lambda q^2[(\hat{t} - M_Z^2)^2 + \Gamma_Z^2 M_Z^2]}[g_{\alpha\beta} - q_\alpha q_\beta/M_Z^2] \\
&\times \quad Tr\{(\not{p}_1 + m_1)[\gamma^\alpha(v_e - a_e\gamma^5)](\not{p}_3 + m_3)\gamma^\mu\} \qquad (2.21) \\
&\times \quad Tr\{(\not{p}_2 + m_2)[\gamma^\beta(v_q - a_q\gamma^5) - i\frac{\kappa_Z}{\Lambda}\sigma^{\beta\delta}q_\delta](\not{p}_4 + m_4)\sigma^{\beta\rho}q_\rho\}. \\
< \bar{\mathcal{M}}_\gamma\mathcal{M}_Z > \quad &= \quad \frac{ie_0 e^2 g_Z^2\kappa_\gamma[(\hat{t} - M_Z^2) - i\Gamma_Z M_Z]}{16\Lambda q^2[(\hat{t} - M_Z^2)^2 + \Gamma_Z^2 M_Z^2]}[g_{\mu\nu} - q_\mu q_\nu/M_Z^2] \\
&\times \quad Tr\{(\not{p}_2 + m_2)\sigma^{\rho\beta}q_\beta(\not{p}_4 + m_4)[\gamma^\nu(v_q - a_q\gamma^5) + i\frac{\kappa_Z}{\Lambda}\sigma^{\nu\delta}q_\delta]\} \\
&\times \quad Tr\{(\not{p}_1 + m_1)\gamma_\rho(\not{p}_3 + m_3)[\gamma^\mu(v_e - a_e\gamma^5)]\} \qquad (2.22)
\end{aligned}
$$

Using the usual Mandelstam invariants $\hat{s} = (p_1 + p_2)^2, \hat{t} = (p_1 - p_3)^2$ and $\hat{u} = (p_1 - p_4)^2$, which yields total differential production cross sections are

$$
\begin{aligned}
\frac{d\hat{\sigma}}{d\hat{t}} \quad &= \quad \frac{1}{16\pi\hat{s}^2} < |\mathcal{M}|^2 > \\
&= \quad \frac{2\pi e_U^2\alpha\kappa_\gamma^2}{\hat{s}^2\hat{t}}[(2\hat{s} + \hat{t}) - \frac{2\hat{s}(\hat{s} + \hat{t})}{m_4^2} - m_4^2] \\
&+ \quad \frac{\pi\alpha^2}{8\sin^4\theta_W\cos^4\theta_W\hat{s}^2 m_4^2[(\hat{t} - M_Z^2)^2 + \Gamma_Z^2 M_Z^2]} \\
&\times \quad \{(a_e^2 + v_e^2)\kappa_Z^2[(2\hat{s} + \hat{t})m_4^2 - 2\hat{s}(\hat{s} + \hat{t}) - m_4^4]\hat{t} \\
&+ \quad 2\kappa_Z m_4^2[v_q(a_e^2 + v_e^2)(\hat{t} - m_4^2) - 2a_e v_e a_q(2\hat{s} + \hat{t} - m_4^2)]\hat{t} \qquad (2.23) \\
&+ \quad [(a_q^2 + v_q^2)(a_e^2 + v_e^2)[2\hat{s}^2 + 2\hat{s}\hat{t} - (2\hat{s} + \hat{t})m_4^2 + \hat{t}^2] \\
&- \quad 4a_e v_e a_q v_q(2\hat{s} + \hat{t} - m_4^2)]m_4^2\} \\
&+ \quad \frac{\pi e_U\alpha^2\kappa_\gamma(\hat{t} - M_Z^2)}{\sin^2\theta_W\cos^2\theta_W\hat{s}^2 m_t^2[(t - M_Z^2)^2 + \Gamma_Z^2 M_Z^2]} \\
&\quad \{a_e a_q(2\hat{s} + \hat{t} - m_4^2)m_4^2 + v_e[2\hat{s}^2\kappa_Z - (\hat{t} - m_4^2)(m_4^2(v_q + \kappa_Z) - 2\hat{s}\kappa_Z)]\}.
\end{aligned}
$$

2.3 Numerical Results and Discussion

The total cross section is obtained by the integral:

$$\sigma_{tot} = \int_{x_{min}}^{1} f_q(x)dx \int_{t_-}^{t_+} \frac{d\hat{\sigma}}{d\hat{t}} d\hat{t} \tag{2.24}$$

where $t_- = -(\hat{s} - m_4^2)$, $t_+ = -0.01$ and $x_{min} = m_4^2/s$. $f_q(x)$ is the quark distribution functions. In obtaining the mentioned behavior of the cross sections we have taken into account of both up and charm quark distributions [61, 62]. The charm quark is present inside the proton as part of the quark-antiquark sea and gives considerable contribution to the cross section. In order to enrich the statistics for the experimental observations of the signal, we also take into account $\bar{u}_4$ production through the subprocess $e\bar{q} \to e\bar{u}_4$. The contribution of this process is relatively small when compared with the u_4 production due to the sea quark distribution in the proton.

We present the total production cross sections as functions of u_4 mass in Fig. 2.2 and Fig. 2.3. In Fig. 2.2, we display the cross sections as functions of the mass of u_4, at future lepton-hadron collider THERA with the center of mass energy $\sqrt{s}$= 1 TeV and with the luminosity of $\mathcal{L} = 4.10^{30}$ cm^{-2}s^{-1} [55]. The new electron proton collider, THERA, can be built at DESY which is based on the linear accelerators TESLA and proton ring HERA (in the west Hall) with electron energies 250 GeV and proton energies 1 TeV.

Fig. 2.3 shows the behaviour of the cross section as a function of m_4 at Linac $\otimes$ LHC with $\sqrt{s}$= 5.3 TeV and with the luminosity of $\mathcal{L} = 10^{33}$ cm^{-2}s^{-1} [56]. This collider has been proposed to collide 1 TeV electron beams tagentially to proton beams at the LHC. In these figures the lower lines correspond to the photonic channel only and the upper lines correspond to the sum of γ and Z exchange

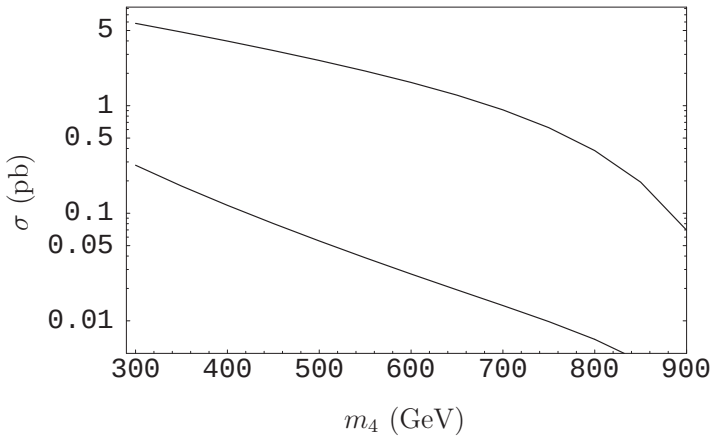

Figure 2.2: Photonic (lower line) and total (upper line) production cross section for the FCNC single u_4 at$\sqrt{s}$=1 TeV as a function of m$_4$ with $\kappa_\gamma = 0.1$ and $\kappa_\gamma = \kappa_Z = 0.1$, respectively.

diagrams. Graphs in Fig. 2.2 and 2.3 were computed by taking the illustrative anomalous coupling values $\kappa_\gamma = \kappa_Z = 0.1$. In Figures 2.4 and 2.5, the total production cross sections are shown also as a function of coupling κ_γ and κ_Z for center of mass energies 1 TeV and 5.3 TeV, respectively. The total production cross section for FCNC single u_4 with $\kappa_\gamma = \kappa_Z = 0.1$ as a function of center of mass energies and m_4 is plotted in Fig. 2.6.

We assume the anomalous decays of u_4 quark to be dominant, which is different from the case of top-quark decays where the SM decay mode is dominant. In Table 2.2, we present the branching ratios and the total decay widths of u_4 quark via anomalous interactions. SM decay modes are negligible for $\kappa/\Lambda > 0.01$ TeV^{-1} due to the small magnitude of the extended CKM matrix elements $V_{u_4 b}$ [63, 64].

Tables 2.3 and 2.4 present the total production cross sections of u_4 and $\bar{u}_4$ in addition to the number of signal and background events in various decay channels of u_4 at THERA and Linac⊗LHC, respectively.

When the fourth family u_4 (or $\bar{u}_4$) quarks are produced, they will decay via

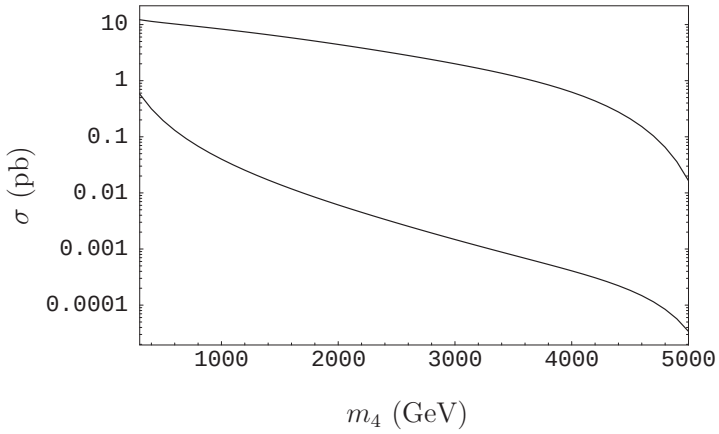

Figure 2.3: Photonic (lower line) and total (upper line) production cross section for the FCNC single u_4 at $\sqrt{s}$=5.3 TeV as a function of m_4 with $\kappa_\gamma = 0.1$ and $\kappa_\gamma = \kappa_Z = 0.1$, respectively.

FCNC interactions giving rise to the signal $e^- qV$, where $q = u, c, t$ (or $\bar{u}, \bar{c}, \bar{t}$) and V denotes the neutral gauge bosons γ, Z, g.

We consider the relevant backgrounds from the following subprocesses:

$$eq \to eq\gamma$$

$$eq \to eqZ$$

$$eq \to eqg$$

where $q = u, c$ (or $\bar{u}, \bar{c}$). The cross sections for these backgrounds are shown in table 2.3 (at THERA) and table 2.4 (at Linac $\otimes$ LHC) for the minimal cuts $p_T^{e,\gamma,j} > 10$ GeV and optimal cuts $p_T^{e,\gamma,j} > 20$ GeV and $M_{qV} > 250$ GeV on the final state particles. From Table 2.3, we conclude that the number of signal events for $u_4 \to gq$ and $u_4 \to Zq$ (q=u,c) channels is promising, which makes it possible to observe a u_4 production signal at the THERA, especially for low lying u_4-quark mass values (300-500 GeV). As can be seen from Table 2.4, it will be possible to observe the anomalous production of u_4 quark in all decay channels

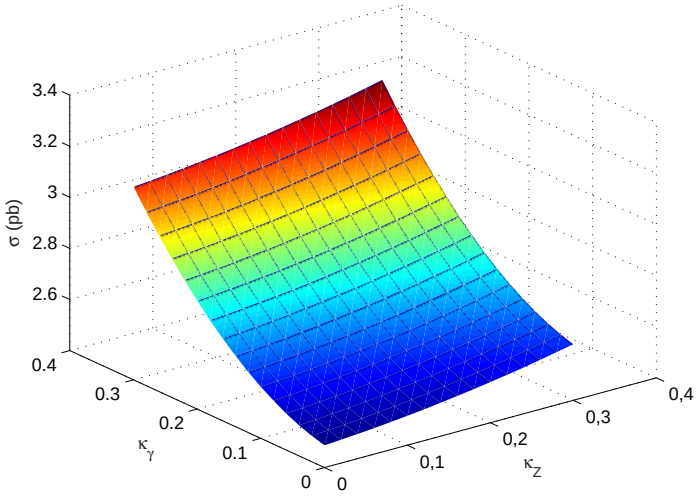

Figure 2.4: Total production cross section for the FCNC single u_4 at as a function of κ_γ and κ_Z with m_4=500 GeV and $\sqrt{s}$=1 TeV.

if the corresponding backgrounds is kept at a low level at Linac $\otimes$ LHC collider. We found that u_4 production signal at this machine is observable down to the anomalous coupling $\kappa_{V,u_4} = 0.01$ at the mass of u_4-quark about 700 GeV. For the channels including top quark in the final state ($e^- Vt$) we obtain very low number of background events, therefore we have not shown them in Tables 2.3 and 2.4.

Assuming Poisson statistics, we use the significance formula $S/\sqrt{B} \geq 3$ for signal observation at the 95% C.L., where the number of signal and background events S and B are calculated by multiplying the cross section with corresponding branching ratios depending on the decay channels and the integrated luminosities of the colliders considered.

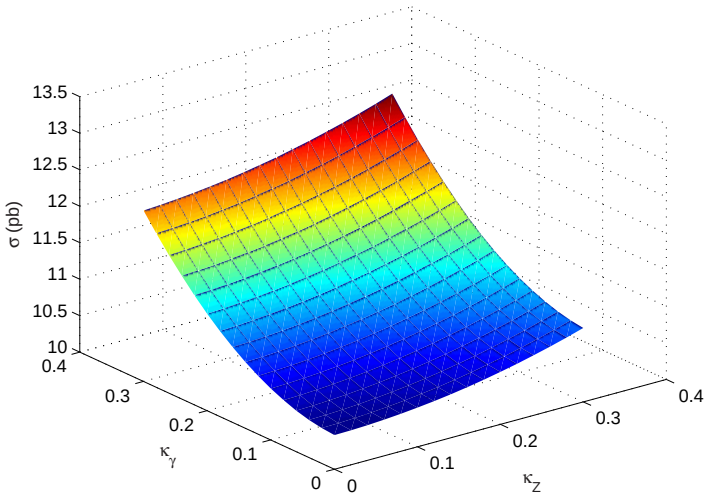

Figure 2.5: Total production cross section for the FCNC single u_4 at as a function of, κ_γ and κ_Z with m_4=500 GeV and $\sqrt{s}$=5.3 TeV.

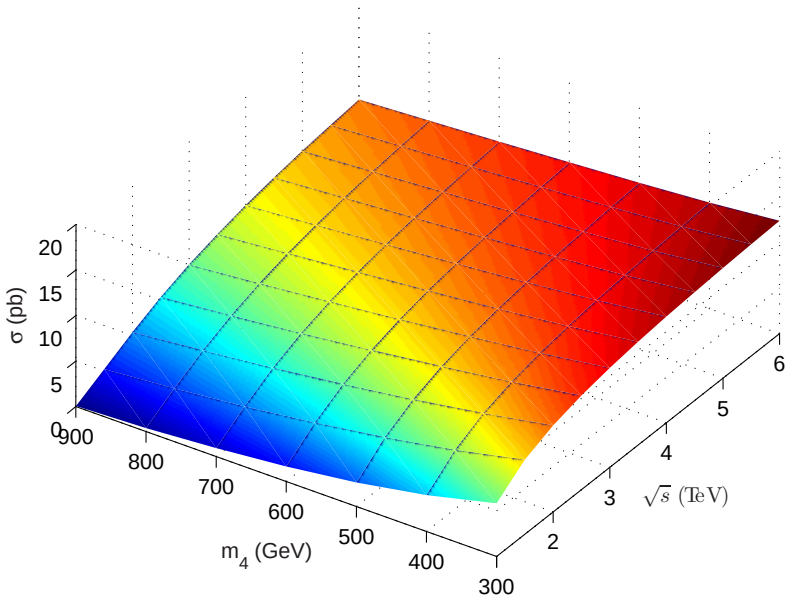

Figure 2.6: Total production cross section for the FCNC single u_4 as a function of m_4 and center of mass energy with $\kappa_\gamma = \kappa_Z = 0.1$.

Table 2.3: Number of signal and background events in various decay channels of u_4 quark at THERA with $\sqrt{s} = 1$ TeV and $L = 40$ pb^{-1} with corresponding total cross section ($\sigma_{tot} \equiv \sigma_{tot}(eu(c) \to eu_4)$ and $\bar{\sigma}_{tot} \equiv \sigma_{tot}(e\bar{u}(\bar{c}) \to e\bar{u}_4)$) in pb. B_1 and B_2 denote the number of background events with the cuts ($p_T^{e,\gamma,j} > 10$ GeV) and ($p_T^{e,\gamma,j} > 20$ GeV, $M_{Vq} > 250$ GeV), respectively.

Mass (GeV)	$gu(c)$	gt	$Zu(c)$	Zt	$\gamma u(c)$	γt	σ_{tot}	$\bar{\sigma}_{tot}$
300	12.4	3.6	280.1	100.3	0.56	0.17	6.67	3.26
400	4.1	2.2	176.6	105.8	0.20	0.10	4.57	2.66
500	1.7	1.2	117.8	84.6	0.08	0.06	3.02	2.12
600	0.7	0.6	75.9	60.1	0.04	0.03	1.88	1.55
700	0.3	0.3	43.3	36.4	0.02	0.01	1.05	0.96
B_1	17440	-	6.7	-	1152	-		
B_2	20.3	-	1.3	-	41.2	-		

Table 2.4: Number of signal and background events in various decay channels of u_4 quark at Linac⊗LHC with $\sqrt{s} = 5.3$ TeV and $L = 10^4$ pb^{-1} with corresponding total cross section ($\sigma_{tot} \equiv \sigma_{tot}(eu(c) \to eu_4)$ and $\bar{\sigma}_{tot} \equiv \sigma_{tot}(e\bar{u}(\bar{c}) \to e\bar{u}_4)$) in pb. B_1 and B_2 denote the number of background events with the cuts ($p_T^{e,\gamma,j} > 10$ GeV) and ($p_T^{e,\gamma,j} > 20$ GeV, $M_{Vq} > 250$ GeV), respectively.

Mass (GeV)	$gu(c)$	gt	$Zu(c)$	Zt	$\gamma u(c)$	γt	σ_{tot}	$\bar{\sigma}_{tot}$
300	6423.1	1835.2	144692.4	51786.5	286.7	86.0	13.97	6.54
400	2696.1	1423.3	115137.5	68945.8	131.1	65.5	13.06	5.78
500	1459.8	984.3	101194.3	72720.7	70.9	50.0	12.36	5.29
600	890.8	681.2	91990.9	72926.4	45.8	34.9	11.74	4.92
700	592.3	488.3	85088.9	71614.7	30.4	25.4	11.15	4.63
B_1	1.9×10^7	-	1.2×10^4	-	1.4×10^6	-		
B_2	6.5×10^4	-	3.3×10^3	-	5.1×10^4	-		

CHAPTER 3

EXOTIC QUARK PRODUCTION IN EP COLLISIONS

String inspired E_6 theories predict the existence of exotic particles. In E_6, each generation of fermions is assigned to the 27-dimensional representation [26, 27, 28]. The fermion content of a single E_6 27 representation containes fifteen standard fermions and right handed neutrino as follows

$$\begin{pmatrix} \nu_e \\ e \end{pmatrix}_L, \begin{pmatrix} u \\ d \end{pmatrix}_L, e_R,\ u_R,\ d_R \text{ and } N_R$$

and eleven new exotic fermion fields

$$\begin{pmatrix} \nu_E \\ E \end{pmatrix}_L, \begin{pmatrix} N_E \\ E \end{pmatrix}_R, D_L,\ D_R,\ \nu''_L$$

The fermion assignments in 27 representation are given Table 3.1 where Q,I_{3L} are the usual charge and weak isospin and $\tilde{Q}$, I_{3R} are proportional to the hypercharges of two additional $U(1)$ groups. The presence of additional fermions causes Flavor Changing Neutral Current (FCNC) interactions and possible deviations from weak universality in Charged Current (CC) [65]. In this study we consider exotic down quark (D), a charge -1/3, quark which is a weak isosinglet particle. As well as, the exotic quarks are vectorlike because their left-handed and right-handed chiralities have the same weak isospin, unlike the usual chiral quarks which are left-handed doublets and right-handed singlets.

Table 3.1: Decomposition of 27 and fermion quantum numbers.

		Left-handed					
$SO(10)$	$SU(5)$	state	$SU(3)$	Q	I_{3L}	$\tilde{Q}$	I_{3R}
16	5^*	d^c	3^*	1/3	0	-1/6	1/2
		e^-	1	-1	-1/2	-1/6	0
		ν_e	1	0	1/2	-1/6	0
	10	e^{-c}	1	1	0	1/3	1/2
		d	3	-1/3	-1/2	1/3	0
		u	3	2/3	1/2	1/3	0
		u^c	3^*	-2/3	0	1/3	-1/2
	1	N^c	1	0	0	5/6	-1/2
10	5^*	D^c	3^*	1/3	0	-1/6	0
		E^-	1	-1	-1/2	-1/6	-1/2
		ν_E	1	0	1/2	-1/6	-1/2
	5	D	3	-1/3	0	-2/3	0
		E^{-c}	1	1	1/2	-2/3	1/2
		N_E^c	1	0	-1/2	-2/3	1/2
1	1	ν''	1	0	0	5/6	0

Production of exotic quarks have been studied at HERA [66, 67], LEP [68, 69] and hadron colliders [70, 71, 72] as CC and FCNC reactions. We analyze the possible production of these quarks and some of their indirect signatures including the contributions of boson-gluon fusions [73] at two future high energy ep collider options; THERA with $\sqrt{s}$=1 TeV and $L = 40\ pb^{-1}$ [55] and CERN Large Hadron Electron Collider (LHeC) with $\sqrt{s}$=1.4 TeV and $L = 10^4\ pb^{-1}$ at which 7 TeV LHC protons collide with 70 GeV ring electron or positron beam [74]. These colliders complement the hadron collider programmes and provide new discovery potential to them. A relatively high integrated luminosity of 10 fb^{-1} at the LHeC makes an essential facility to resolve possible puzzles of the LHC data.

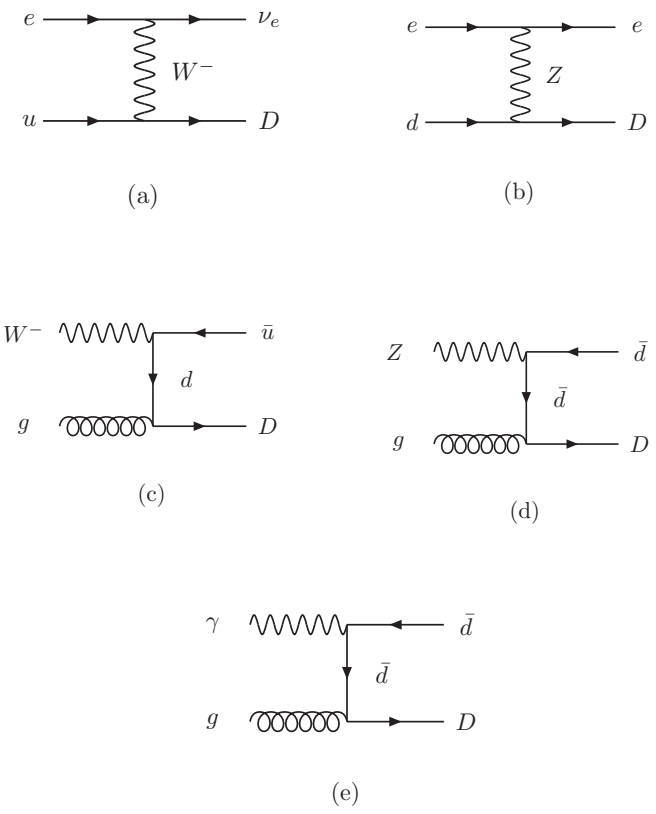

Figure 3.1: The Feynman diagram at parton level for single exotic down quark production in ep collisions via (a) charged current interaction (b) neutral current interaction (c) W-gluon fusion (d) Z-gluon fusion (e) γ-gluon fusion

3.1 Production and decays of Exotic Down Quark

3.1.1 Production of Exotic Down Quark

The single production of exotic down quarks occur via the following t-channel subprocesses in ep collisions as shown in Fig. 3.1;

i) Charged Current reaction; $eu \rightarrow \nu_e D$

ii) FCNC reaction; $ed \rightarrow eD$

iii) Boson-Gluon Fusions; $Wg \rightarrow \bar{u}D$, $Zg \rightarrow \bar{d}D$ and $\gamma g \rightarrow \bar{d}D$.

The CC and FCNC interactions for the exotic D quarks mixed with standard

fermions and standard bosons W, Z are given by

$$\begin{aligned}\mathcal{L}_{CC} &= \frac{g}{2\sqrt{2}}\bar{u}\gamma_\mu(1-\gamma_5)(d\cos\theta - D\sin\theta)W^\mu + h.c. \\ \mathcal{L}_{NC} &= \frac{g}{4c_W}\sin\theta\cos\theta\bar{d}\gamma_\mu(1-\gamma_5)DZ^\mu \end{aligned} \tag{3.1}$$

where θ are the mixing angels between the ordinary quarks and the exotic down quarks, g denotes the gauge coupling relative to SU(2) symmetries.

i) The single production of exotic down quarks occurs via charged current reaction $e(p_1) + u(p_2) \to \nu_e(p_3) + D(p_4)$, involving the exchange of a W boson in t-channel as shown in Fig. 3.1.(a). We can write the amplitude according to the expression of charged current vertices in Eq. (3.1)

$$\begin{aligned}\mathcal{M} &= \bar{u}(3)[-i\frac{g}{2\sqrt{2}}\gamma_\mu(1-\gamma_5)]u(1)[\frac{g_{\mu\nu} - q_\mu q_\nu/M_W^2}{t - M_W^2 + i\Gamma_W M_W}] \\ &\times \bar{u}(4)[-i\frac{g}{2\sqrt{2}}\sin\theta\gamma^\nu(1-\gamma_5)]u(2) \end{aligned} \tag{3.2}$$

after squaring this amplitude, we find

$$\begin{aligned}< |\mathcal{M}|^2 >= \frac{1}{4}\frac{g^4\sin^2\theta}{64[(t-M_W^2)^2 + \Gamma_W^2 M_W^2]}Tr[\not{p}_3\gamma^\mu(1-\gamma^5)\ \not{p}_1\gamma^\rho(1-\gamma^5)] \\ \times Tr[(\not{p}_4 + m)\gamma^\nu(1-\gamma^5)\ \not{p}_2\gamma^\sigma(1-\gamma^5)](g_{\mu\nu} - q_\mu q_\nu/M_W^2)(g_{\rho\sigma} - q_\rho q_\sigma/M_W^2) \end{aligned} \tag{3.3}$$

These trace of gamma matrices were evaluated by the algebraic computer program "FeynCalc". The usual Mandelstam variables for the all subprocess are defined as $\hat{s} = (p_1 + p_2)^2$, $\hat{t} = (p_1 - p_3)^2$, $\hat{u} = (p_1 - p_4)^2$, $\hat{s} + \hat{t} + \hat{u} = m^2$ is defined and electron, electron neutrino and light quark masses are neglected. The spin averaged matrix element squared can be written

$$< |\mathcal{M}|^2 >= \frac{g^4\sin^2\theta}{4[(t-M_W^2)^2 + \Gamma_W^2 M_W^2]}s(s-m^2) \tag{3.4}$$

We obtained differential cross section for the subprocess as

$$\frac{d\hat{\sigma}}{d\hat{t}}(eu \to \nu_e D) = \frac{\pi\alpha^2 \sin^2\theta}{4\sin^4\theta_W \hat{s}} \frac{(\hat{s}-m^2)}{[(\hat{t}-M_W^2)^2+\Gamma_W^2 M_W^2]} \tag{3.5}$$

ii) The FCNC reaction of the single D production is $e(p_1)+d(p_2) \to e(p_3)+D(p_4)$ as shown in Fig. 3.1.(b). Using the interaction vertices in Eq. (3.1), the amplitude of this reaction is written as

$$\begin{aligned} \mathcal{M} &= \bar{u}(3)[-i\frac{g_Z}{2\sqrt{2}}\gamma_\mu(v_e - a_e\gamma_5)]u(1)[\frac{g_{\mu\nu}-q_\mu q_\nu/M_W^2}{t-M_W^2+i\Gamma_W M_W}] \\ &\times \bar{u}(4)[-\frac{g_z}{4}\sin\theta\cos\theta\gamma^\nu(1-\gamma_5)]u(2) \end{aligned} \tag{3.6}$$

We compute square of this amplitude and differential cross section as follows

$$\begin{aligned} <|\mathcal{M}|^2> &= \frac{1}{4}\frac{g_z^4 \sin^2\theta\cos^2\theta}{64[(t-M_Z^2)^2+\Gamma_Z^2 M_Z^2]} Tr[\not{p}_3\gamma^\mu(v_e-a_e\gamma^5)\ \not{p}_1\gamma^\rho(v_e-a_e\gamma^5)] \\ &\times Tr[(\not{p}_4+m)\gamma^\nu(1-\gamma^5)\ \not{p}_2\gamma^\sigma(1-\gamma^5)](g_{\mu\nu}-q_\mu q_\nu/M_Z^2)(g_{\rho\sigma}-q_\rho q_\sigma/M_Z^2) \end{aligned} \tag{3.7}$$

and

$$\frac{d\hat{\sigma}}{d\hat{t}}(ed \to eD) = \frac{\pi\alpha^2\sin^2 2\theta[\hat{t}(\hat{t}+2\hat{s}-m^2)(a_e-v_e)^2+2\hat{s}(\hat{s}-m^2)(a_e^2+v_e^2)]}{4\hat{s}^2\sin^4 2\theta_W[(\hat{t}-M_Z^2)^2+\Gamma_Z^2 M_Z^2]} \tag{3.8}$$

As we consider the strong interactions, D quarks couple to gluons in exactly the same way as ordinary quarks providing the (W, Z, γ)-gluon fusions.
iii) The amplitude of the single production of exotic down quark via W-gluon fusion, $W(p_1)+g(p_2) \to \bar{u}(p_3)+D(p_4)$, in Fig. 3.1.(c) is given by

$$\mathcal{M} = \bar{u}(4)[(ig_s\gamma^\mu T_{ij}^a)\epsilon_2^\mu \frac{(\not{p}_1 - \not{p}_3)}{\hat{t}}\epsilon_1^\nu(-i\frac{g\cos\theta}{2\sqrt{2}}\gamma^\nu(1-\gamma^5))]u(3) \tag{3.9}$$

The result for spin and color average of $< |\mathcal{M}|^2 >$ is

$$\begin{aligned} < |\mathcal{M}|^2 > &= \frac{1}{4}\frac{g_s^2 g^2 \cos\theta^2}{8\hat{t}^2}(\frac{1}{8}\sum_{i,j} T_{ij}^a T_{ij}^{a*})(-g^{\mu\beta})(-g^{\nu\alpha} + (q^\nu q^\alpha / M_W^2)) \quad (3.10) \\ &\times Tr[(\not{p}_4 + m)\gamma^\mu(\not{p}_1 - \not{p}_3)\gamma^\nu(1-\gamma^5)\ \not{p}_3\gamma^\alpha(1-\gamma^5)(\not{p}_1 - \not{p}_3)\gamma^\beta] \end{aligned}$$

here

$$(\frac{1}{8}\sum_{i,j} T_{ij}^a T_{ij}^{a*}) = 1/2$$

is the complete color factor in squares of matrix elements. We compute the differential cross section is

$$\begin{aligned} \frac{d\hat{\sigma}}{d\hat{t}}(Wg \to \bar{u}D) &= \frac{\pi\alpha_s\alpha\cos^2\theta}{32\sin^2\theta_W \hat{s}^2\hat{t}^2 M_W^2}[2M_W^4(m^2+\hat{t}) - 2M_W^2\hat{t}(\hat{s}+\hat{t}) \quad (3.11) \\ &- (m^2-\hat{s})\hat{t}^2] \end{aligned}$$

Similarly, we can write the amplitude of the single production of D via Z-gluon fusion, $Z(p_1) + g(p_2) \to \bar{d}(p_3) + D(p_4)$, in Fig. 3.1.(d) is given by

$$\mathcal{M} = \bar{u}(4)[(ig_s\gamma^\mu T_{ij}^a)\epsilon_2^\mu \frac{(\not{p}_1 - \not{p}_3)}{\hat{t}}\epsilon_1^\nu(-i\frac{g_z}{2}\gamma^\nu(v_d - a_d\gamma^5))]u(3) \quad (3.12)$$

and the differential cross section as follows

$$\begin{aligned} \frac{d\hat{\sigma}}{d\hat{t}}(Zg \to \bar{d}D) &= \frac{\pi\alpha_s\alpha(a_d^2+v_d^2)}{8\sin^2 2\theta_W \hat{s}^2\hat{t}^2 M_Z^2}[2M_Z^4(m^2+\hat{t}) - 2M_Z^2\hat{t}(\hat{s}+\hat{t}) \quad (3.13) \\ &- (m^2-\hat{s})\hat{t}^2] \end{aligned}$$

Finally, another mechanism of the production of D quarks is photon-gluon fusion in Fig. 3.1.(e). The amplitude of this process is written as

$$\mathcal{M} = \bar{u}(4)[(ig_s\gamma^\mu T_{ij}^a)\epsilon_2^\mu \frac{(\not{p}_1 - \not{p}_3)}{\hat{t}}\epsilon_1^\nu(-i\frac{g_z}{2}\gamma^\nu(v_d - a_d\gamma^5))]u(3) \quad (3.14)$$

and corresponding differential cross sections are written

$$\frac{d\hat{\sigma}}{d\hat{t}}(\gamma g \to \bar{d}D) = \frac{\pi\alpha_s\alpha}{24\hat{s}^2\hat{t}}[-\hat{s}-\hat{t}] \tag{3.15}$$

The total production cross section is obtained by folding the partonic cross section over the parton distributions in the proton. In numerical calculations of the total cross sections we have used the MRST parametrization [61] for the partons and the Weizsäcker-Williams distribution [75, 76] for photons in electrons. For illustrations we have assumed an upper bound of $\sin^2\theta \lesssim 0.05$ in numerical calculations which is appropriate as being at the order of CKM angle. The calculated total cross sections corresponding to five subprocesses have been displayed in Figures 3.2-3.6 as functions of D masses m for two center of mass energies. In these figures solid (dashed) lines are for $\sqrt{s}$=1.4 (1) TeV. In Tables 3.2 and 3.3, we present the total production cross sections of the five reactions for various masses at THERA and LHeC, respectively. As can be seen, for 100-300 GeV D quarks Z-gluon and γ-gluon fusions are dominant reactions but for higher mass range contributions of these fusions decrease very fast.

Table 3.2: The total cross sections in pb for the signal processes for the exotic quarks at THERA.

m(GeV)	100	200	300	400	500
$\sigma_S(eu \to \nu_e D)$	4.01	2.84	1.79	0.99	0.46
$\sigma_S(ed \to eD)$	0.27	0.18	0.11	0.053	0.022
$\sigma_S(Wg \to \bar{u}D)$	3.16	1.25	0.39	0.10	0.019
$\sigma_S(Zg \to \bar{d}D)$	23.95	9.30	2.91	0.73	0.14
$\sigma_S(\gamma g \to \bar{d}D)$	59.62	9.78	1.73	0.29	0.041

Table 3.3: The total cross sections in *pb* for the signal processes for the exotic quarks at LHeC.

m(GeV)	200	400	600	800	1000
$\sigma_S(eu \to \nu_e D)$	3.61	1.97	0.83	0.24	0.036
$\sigma_S(ed \to eD)$	0.25	0.12	0.044	0.011	0.0013
$\sigma_S(Wg \to \bar{u}D)$	2.09	0.45	0.061	0.0048	$1.79\text{x}10^{-4}$
$\sigma_S(Zg \to \bar{d}D)$	16.14	3.49	0.47	0.037	$1.42\text{x}10^{-3}$
$\sigma_S(\gamma g \to \bar{d}D)$	15.16	1.23	0.094	0.0049	$1.42\text{x}10^{-4}$

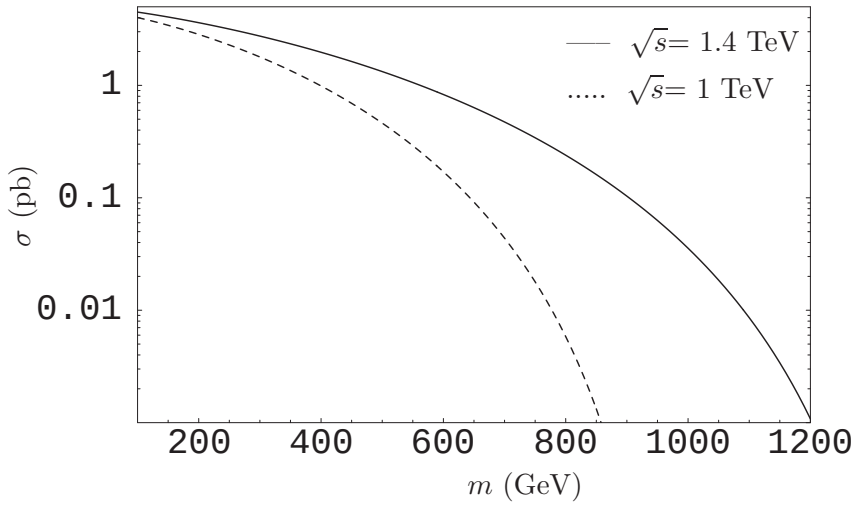

Figure 3.2: The total production cross sections for the subprocesses $eu \to \nu_e D$ as a functions of m.

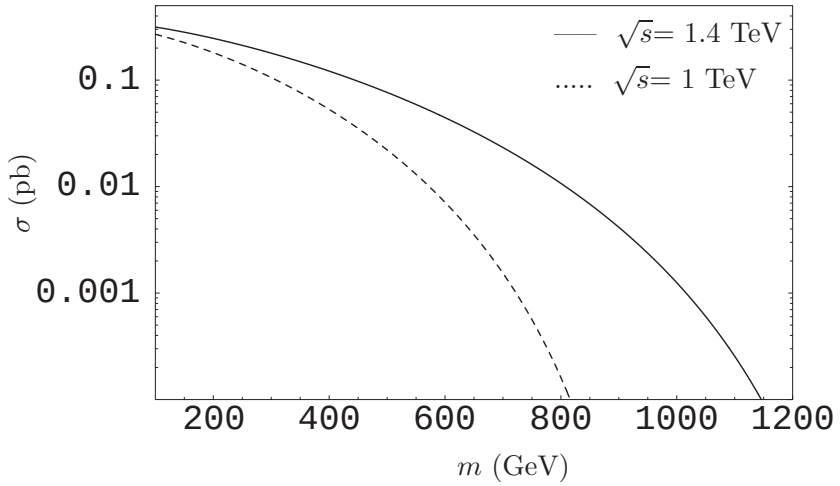

Figure 3.3: The total production cross sections for the subprocesses $ed \to eD$ as a functions of m.

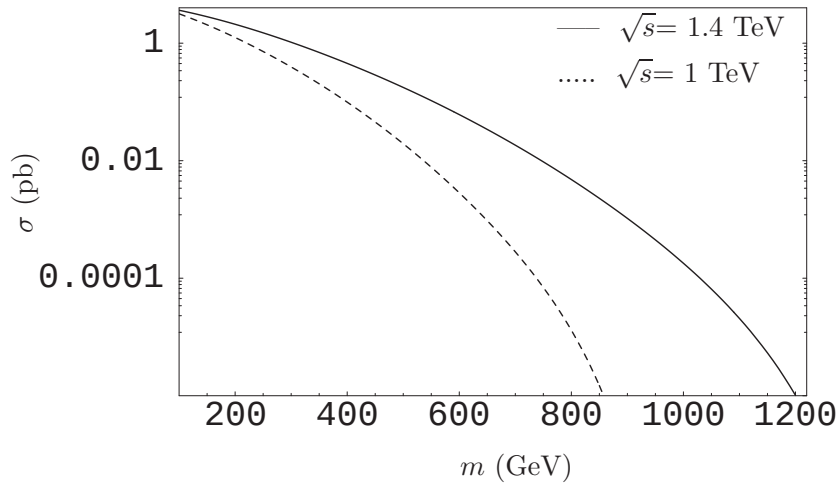

Figure 3.4: The total production cross sections for the subprocesses $Wg \to \bar{u}D$ as a functions of m.

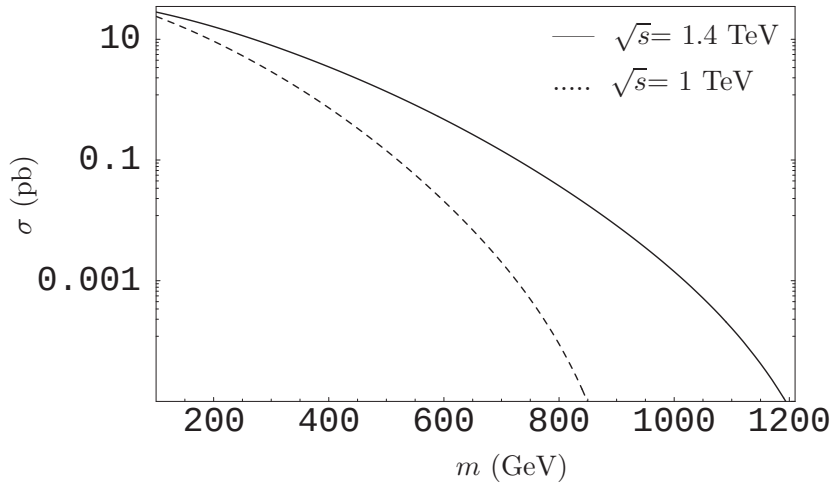

Figure 3.5: The total production cross sections for the subprocesses $Zg \to \bar{d}D$ as a function of m.

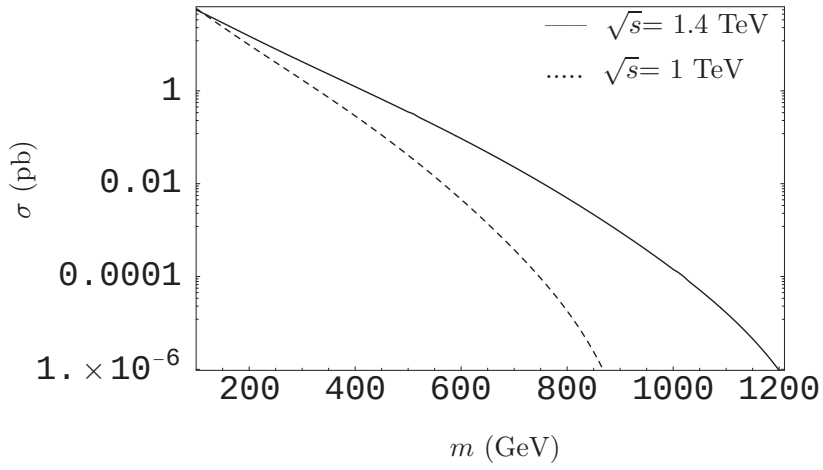

Figure 3.6: The total production cross sections for the subprocesses $\gamma g \to \bar{d}D$ as a functions of m.

3.1.2 Decays of D

Since these exotic quarks must be at a scale well above 100 GeV [77], the main decays of them would be $D \to dZ$ and $D \to uW$ and calculations of the partial decay widths as follows;

i) Calculations of $D \to dZ$ decay widths

From Eq. (3.1), the amplitude of the $D(1) \to d(2)Z(3)$ decay process can be written as

$$\mathcal{M} = \frac{g_Z}{4} \sin\theta \cos\theta \bar{u}(1)[\gamma^\nu(1-\gamma^5)]u(2)\epsilon^*_\mu \tag{3.16}$$

squaring of this amplitude and averaging over D and d quarks polarization states, we find

$$\begin{aligned} < |\mathcal{M}|^2 > \;\; &= \;\; \frac{g_Z^2}{16} \sin^2\theta \cos^2\theta Tr[\not{p}_2\gamma^\mu(1-\gamma^5)(\not{p}_1 + m)\gamma^\nu(1-\gamma^5)] \\ &\quad \times \sum_{pol} \epsilon^*_\mu \epsilon_\nu \end{aligned} \tag{3.17}$$

The sum over physical polarization states of Z boson is

$$\sum_{pol} \epsilon^*_\mu \epsilon_\nu = g_{\mu\nu} - \frac{q_\mu q_\nu}{M_Z^2} \tag{3.18}$$

and $p_1 \cdot p_2 = (m^2 - M_Z^2)/2$. Inserting these expression into Eq. (3.17), we find

$$< |\mathcal{M}|^2 >= \frac{g_z^2 \sin^2\theta \cos^2\theta}{8} [\frac{m^4 + M_Z^2 m^2 - 2M_Z^4}{M_Z^2}] \tag{3.19}$$

and plugging into Eq. (2.2) gives

$$\Gamma(D \to dZ) = \frac{g_Z^2 \sin^2\theta \cos^2\theta (m - M_Z^2)}{64\pi m^3 M_Z} [m^4 + M_Z^2 m^2 - 2M_Z^4] \tag{3.20}$$

here $g_z = \sqrt{4\pi\alpha}/\sin\theta_w \cos\theta_w$

$$\Gamma(D \to dZ) = \frac{\alpha \sin^2\theta \cos^2\theta}{16 \sin^2\theta_W \cos^2\theta_W M_Z}[m + \frac{M_Z^2}{m} - 2\frac{M_Z^4}{m^3}] \tag{3.21}$$

ii) Calculations of $D \to uW$ decay widths

Similarly, the other decay modes of D is $D(1) \to u(2)W(3)$. From Eq. (3.1), we can write amplitude of this process as

$$\mathcal{M} = \frac{g}{2\sqrt{2}} \sin\theta \bar{u}(2)[\gamma^\mu(1-\gamma^5)]u(1)\epsilon_\mu^* \tag{3.22}$$

and after squaring of this amplitude is given

$$\begin{aligned} < |\mathcal{M}|^2 > &= \frac{g^2}{8} \sin^2\theta Tr[\not{p}_2\gamma^\mu(1-\gamma^5)(\not{p}_1 + m)\gamma^\nu(1-\gamma^5)] \\ &\times \sum_{pol} \epsilon_\mu^* \epsilon_\nu \end{aligned} \tag{3.23}$$

where summation over the polarization of W boson is

$$\sum_{pol} \epsilon_\mu^* \epsilon_\nu = g_{\mu\nu} - \frac{q_\mu q_\nu}{M_W^2} \tag{3.24}$$

and $p_1 \cdot p_2 = (m^2 - M_W^2)/2$. The squared of matrix element is computed as

$$< |\mathcal{M}|^2 >= \frac{\sin^2\theta g^2}{2}(\frac{m^4}{M_W^2} + m^2 - 2M_W^2) \tag{3.25}$$

and substituting in Eq. (2.2), we get

$$\Gamma(D \to uW) = \frac{\alpha \sin^2\theta}{8 \sin^2\theta_W M_W}[m + \frac{M_W^2}{m} - 2\frac{M_W^4}{m^3}] \tag{3.26}$$

Finally, the general form of these partial decay widths can be written as

$$\Gamma(D \to qV) = \alpha C_V \frac{m}{Y^2}(1 - 3Y^4 + 2Y^6) \tag{3.27}$$

where q is up or down quark, V denotes W^- and Z bosons, α is the fine structure constant, m is mass of the exotic quark, $Y \equiv M_V/m$, $C_W = \sin^2\theta_{mix}/8x_W$, $C_Z = (\sin\theta_{mix}\cos\theta_{mix})^2/16x_W(1 - x_W)$ and $x_W \equiv \sin^2\theta_W$. Eq. (3.27) gives rise to branching ratios of BR($D \to dZ$)=30 % and BR($D \to uW$)= 70 % which do not change significantly depending on D masses, as seen from Table 3.4.

Table 3.4: The branching ratios for D decays.

m(GeV)	BR($D \to qW$)(%)	BR($D \to qZ$)(%)
150	70.2	29.2
250	68.1	31.9
350	67.8	32.1
450	67.7	32.3

Therefore, $D \to ul^-\bar{\nu}_l$ is taken as the relevant background process since the $D \to uW$ is dominant one. In Tables 3.2 and 3.8 we present the cross sections resulting the background processes (considering only the first generation of leptons) for $\sqrt{s}$=1 and 1.4 TeV, respectively. Results reported in these tables were obtained by using the high energy package CompHEP [78] along with CTEQ6L [79] which has been used in the background calculations and an optimal cut of $P_T > 10$ GeV has taken for electron, jet and missing momenta.

In Figures 3.7-3.11, we displayed the transverse momenta, P_T of secondary electrons by assigning a mass value of 350 GeV to m giving peaks around P_T^e=30-40 GeV and the invariant mass distributions of $e - \bar{\nu}_e - q$ system resulting from the decay of D quarks for the five subreactions separately. These invariant mass spectra have Jacobian peaks of around 125-200 GeV. Similarly, in Figures 3.12-

3.16 the transverse momenta and invariant mass distributions are displayed for LHeC energy which yields peaks around 20-40 GeV for P_T^e values and 125-350 GeV for invariant mass values depending on different subprocess.

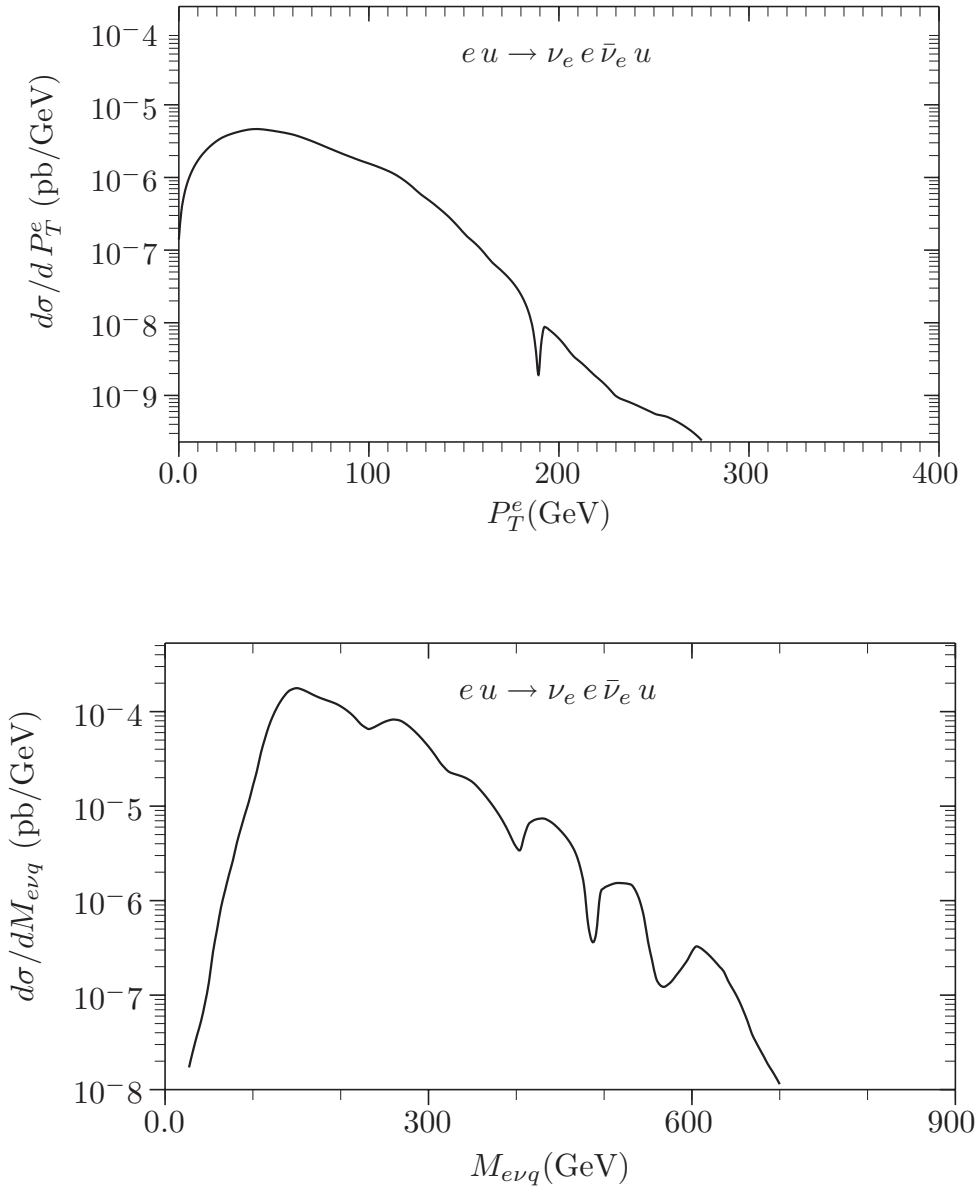

Figure 3.7: Transverse momentum P_T^e and invariant mass distributions of the backgrounds for $eu \to \nu_e\,e\,\bar{\nu}_e\,u$ process at THERA

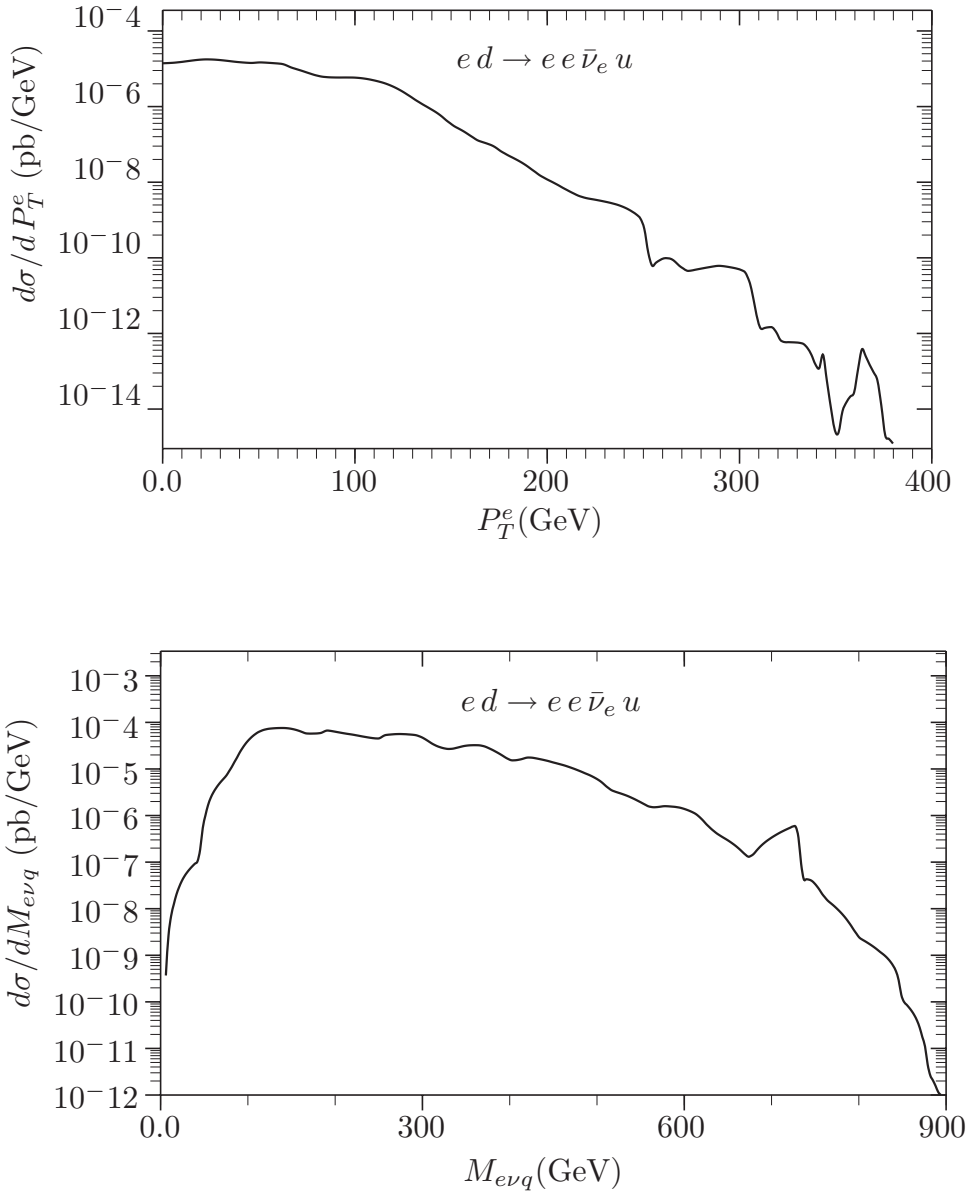

Figure 3.8: Transverse momentum P_T^e and invariant mass distributions of the backgrounds for $ed \to e\,e\,\bar{\nu}_e\,u$ process at THERA

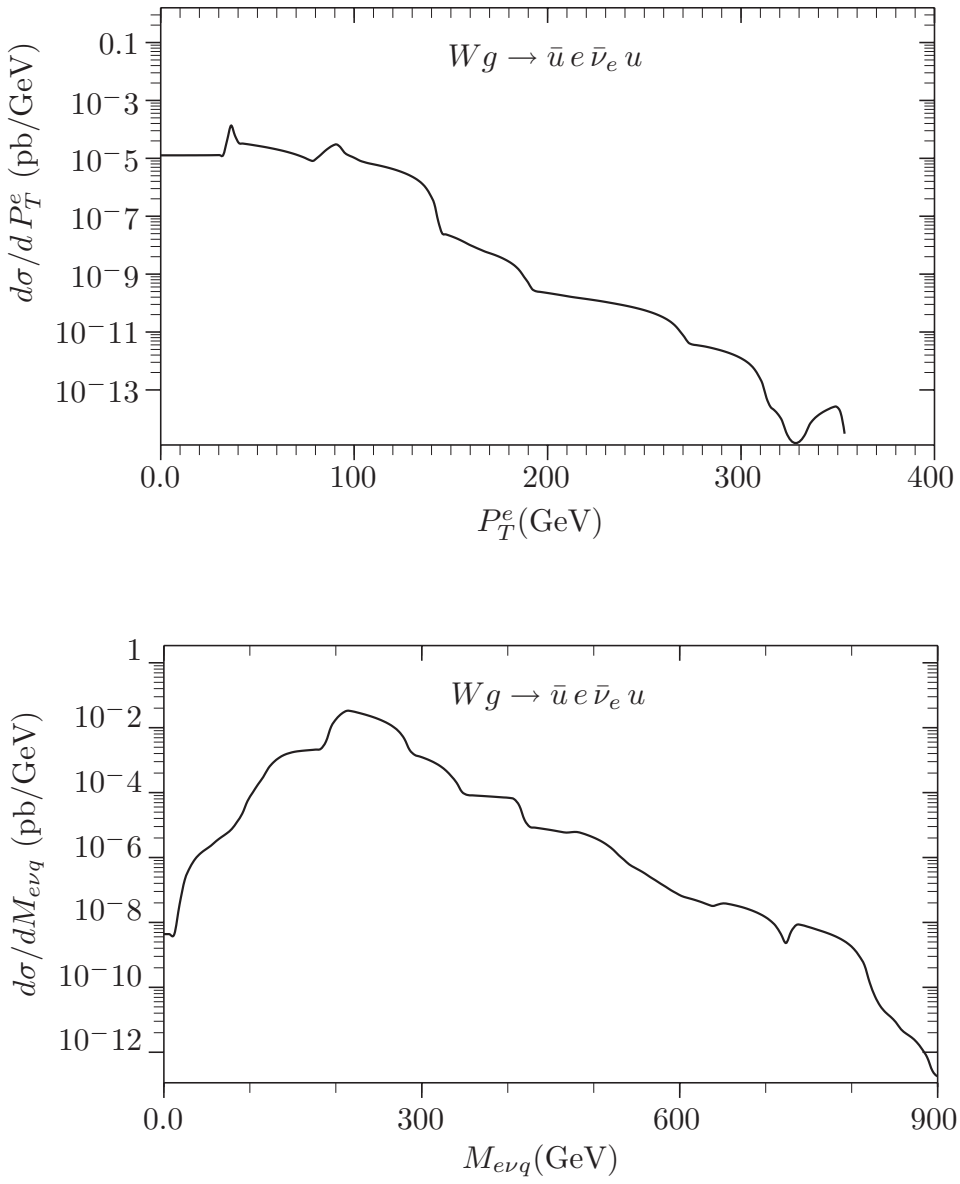

Figure 3.9: Transverse momentum P_T^e and invariant mass distributions of the backgrounds for $Wg \to \bar{u}\, e\, \bar{\nu}_e\, u$ process at THERA

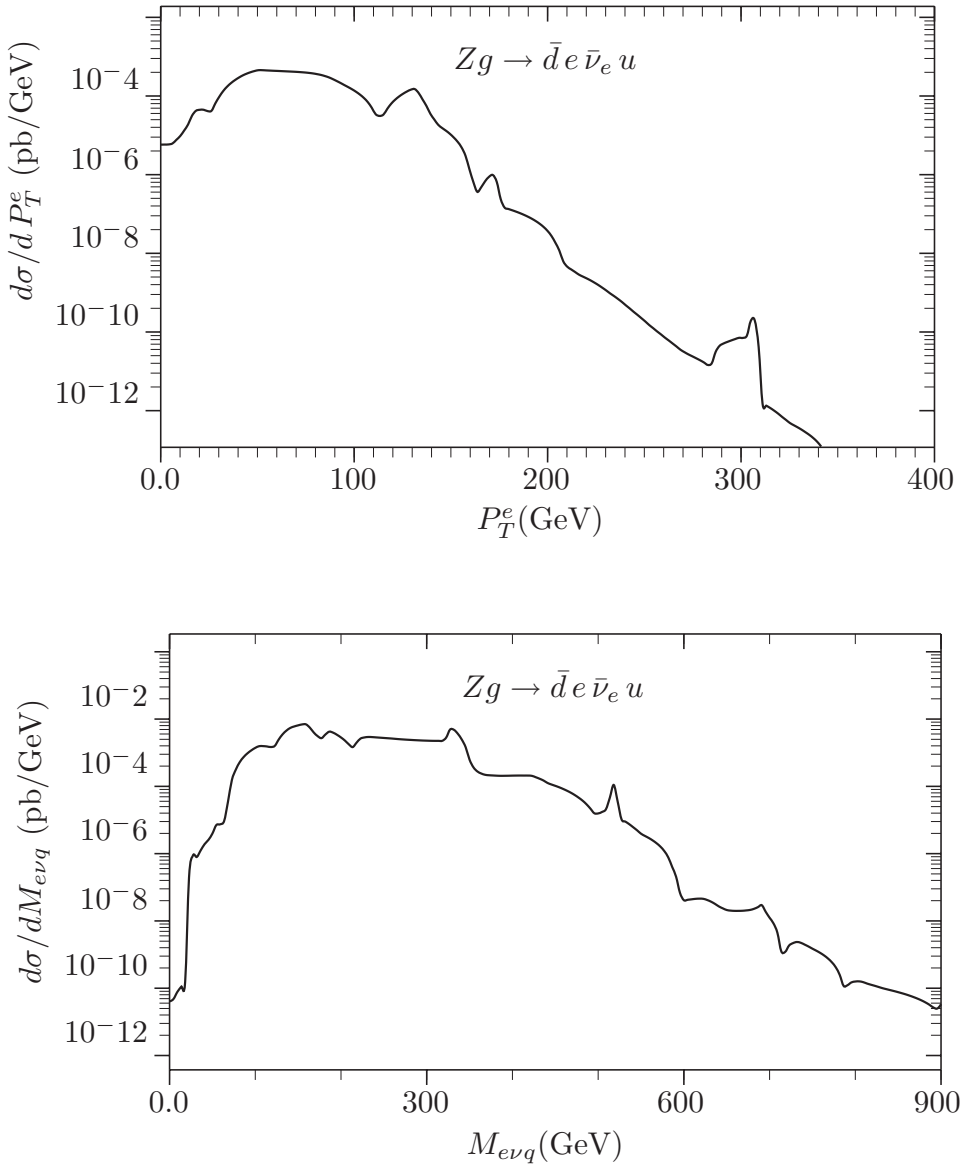

Figure 3.10: Transverse momentum P_T^e and invariant mass distributions of the backgrounds for $Zg \to \bar{d}\, e\, \bar{\nu}_e\, u$ process at THERA

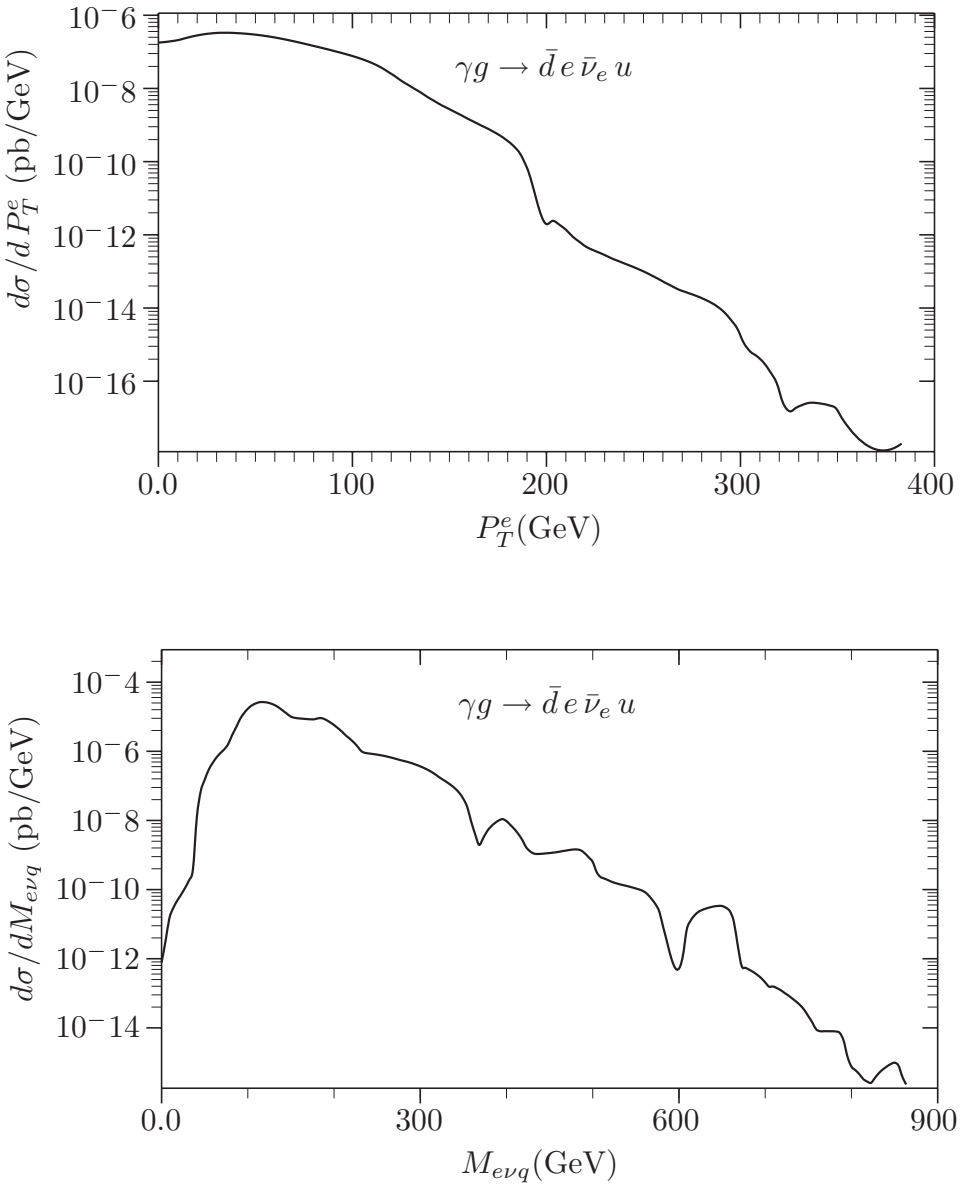

Figure 3.11: Transverse momentum P_T^e and invariant mass distributions of the backgrounds for $\gamma g \to \bar{d}\, e\, \bar{\nu}_e\, u$ process at THERA

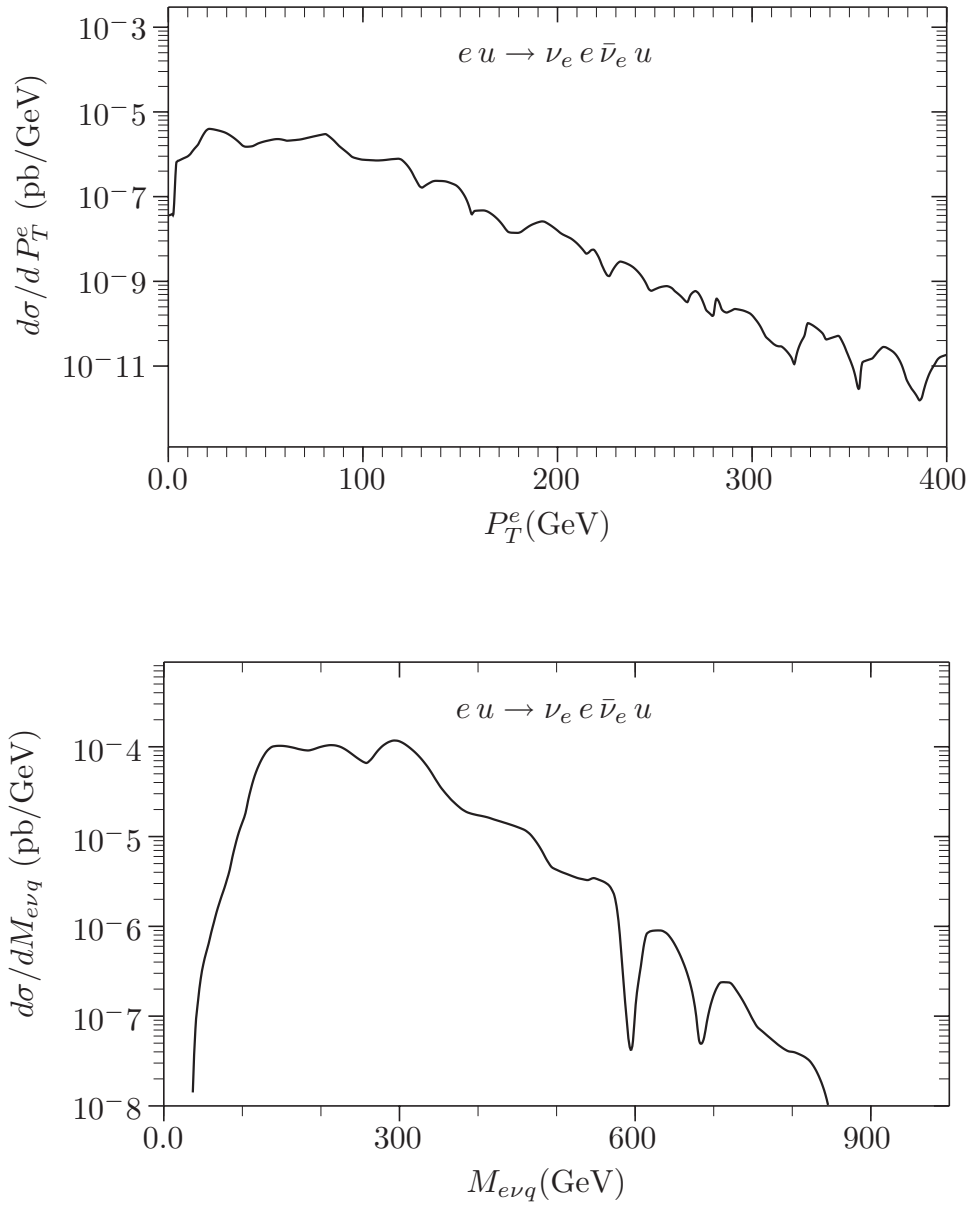

Figure 3.12: Transverse momentum P_T^e and invariant mass distributions of the backgrounds for $eu \to \nu_e\,e\,\bar{\nu}_e\,u$ process at LHeC

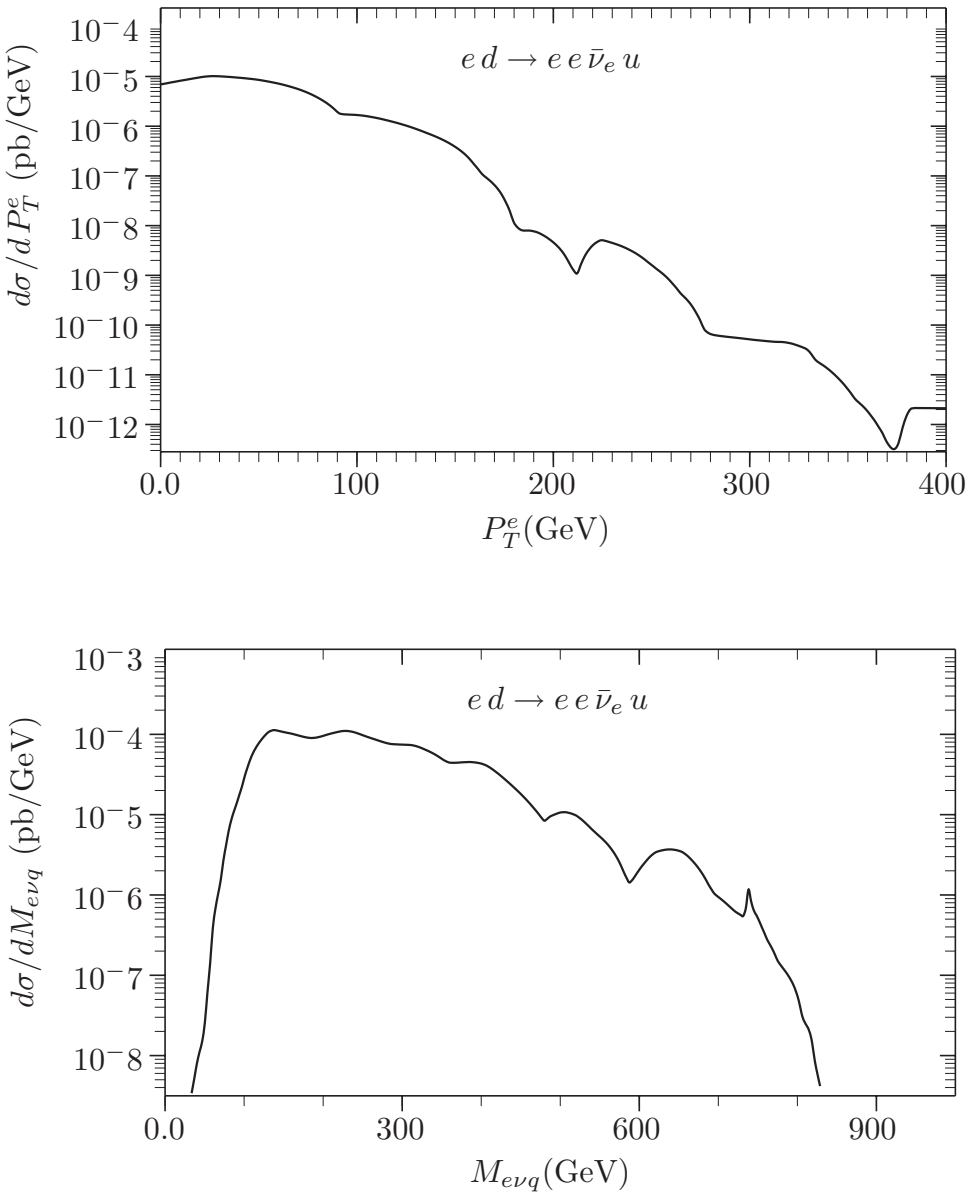

Figure 3.13: Transverse momentum P_T^e and invariant mass distributions of the backgrounds for $ed \to e\,e\,\bar{\nu}_e\,u$ process at LHeC

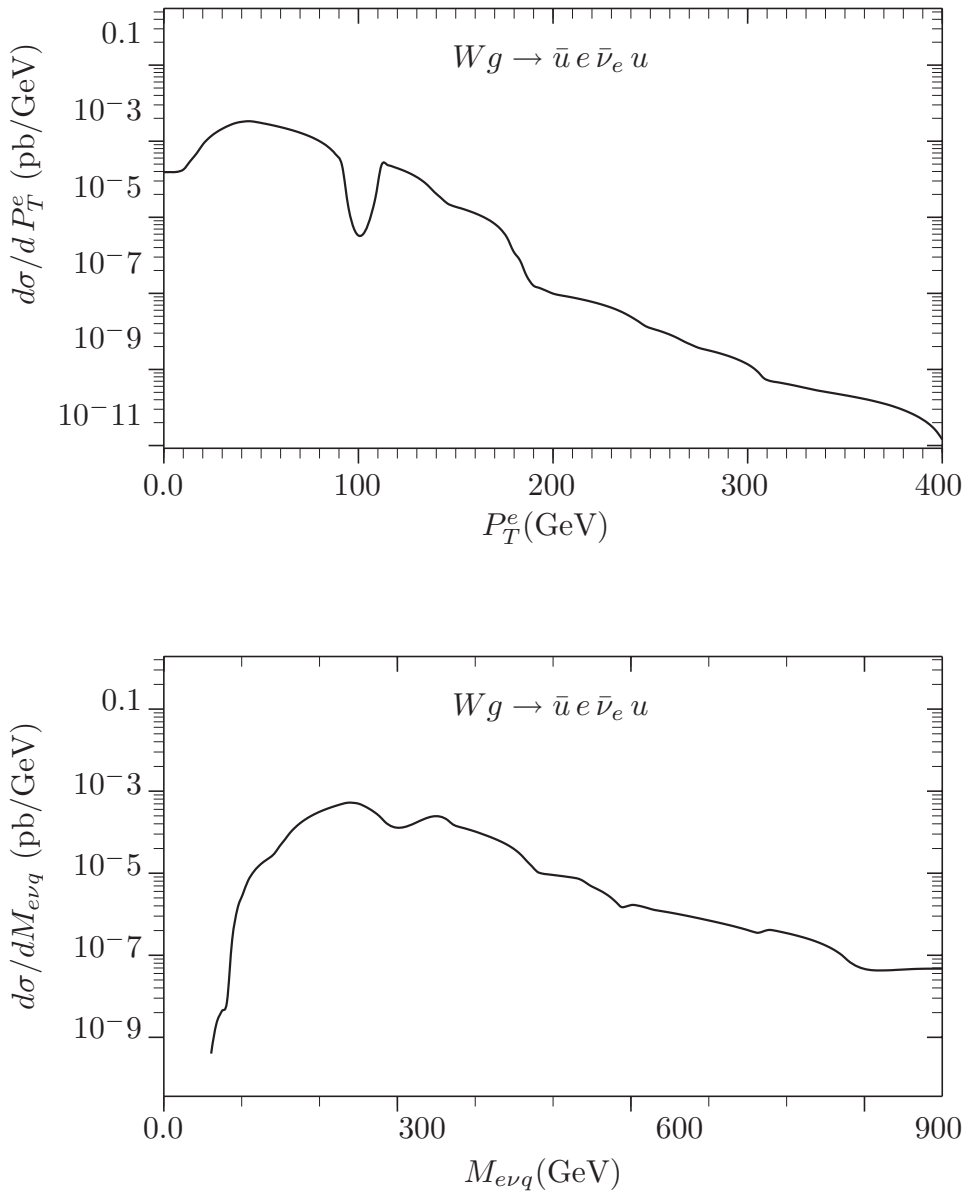

Figure 3.14: Transverse momentum P_T^e and invariant mass distributions of the backgrounds for $Wg \to \bar{u}\, e\, \bar{\nu}_e\, u$ process at LHeC

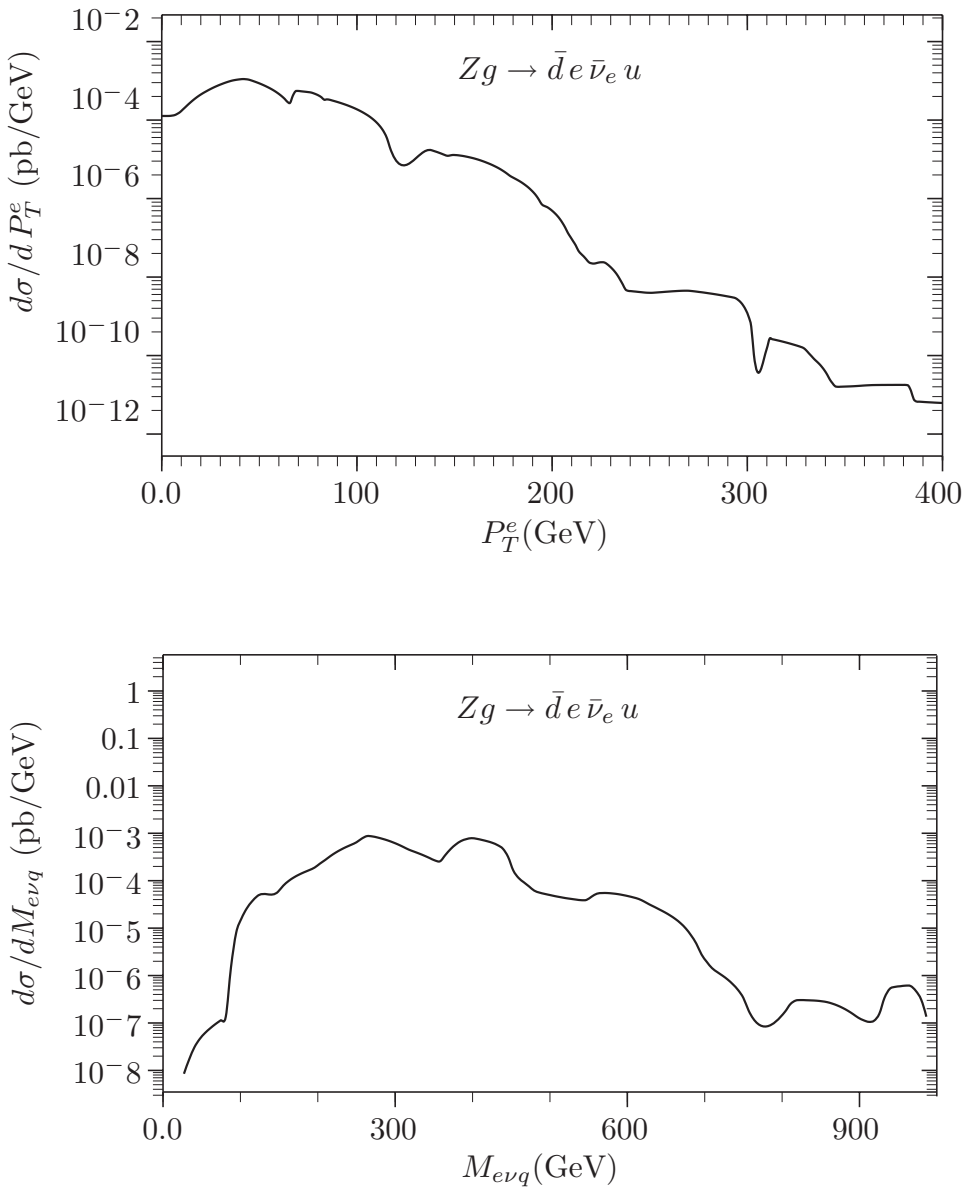

Figure 3.15: Transverse momentum P_T^e and invariant mass distributions of the backgrounds for $Zg \to \bar{d}\, e\, \bar{\nu}_e\, u$ process at LHeC

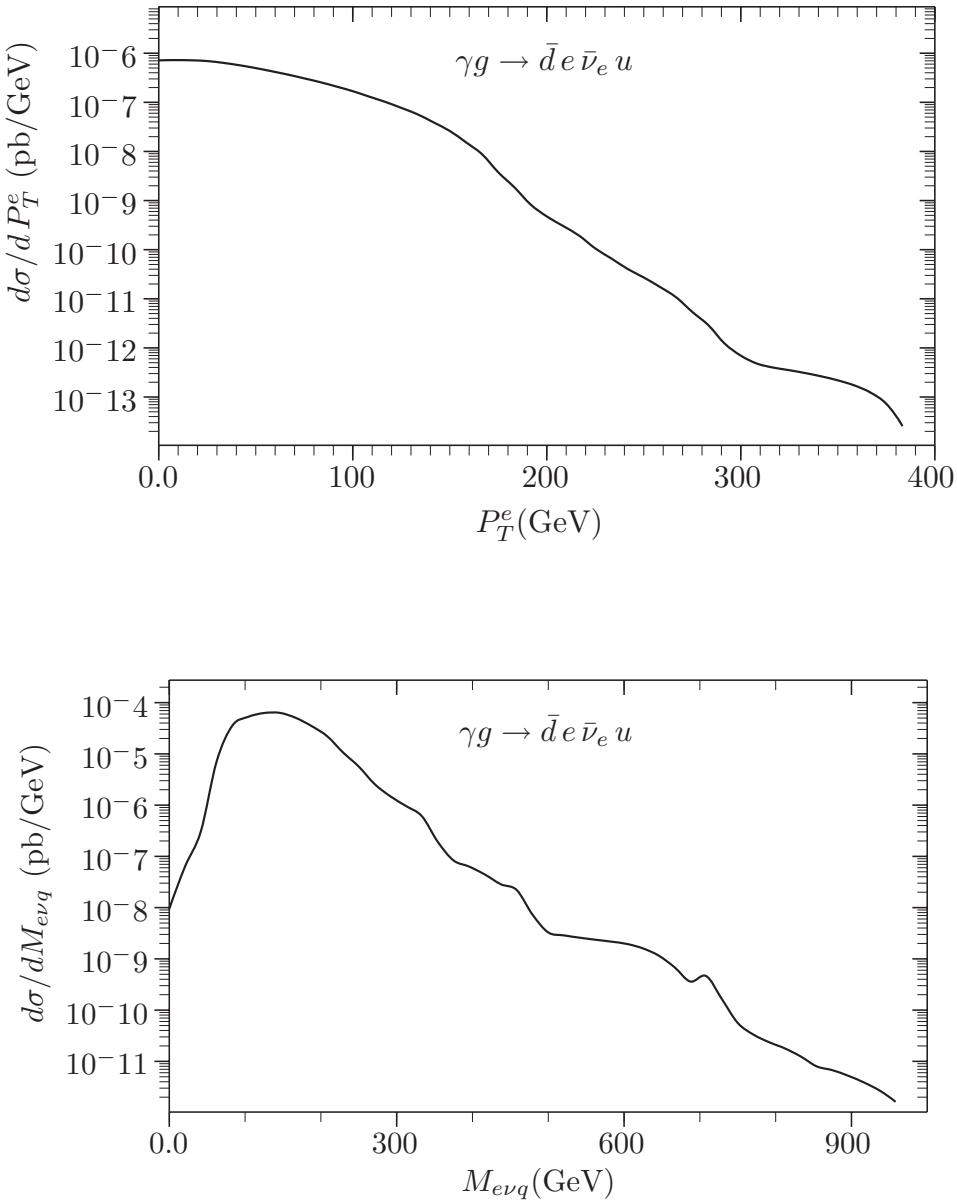

Figure 3.16: Transverse momentum P_T^e and invariant mass distributions of the backgrounds for $\gamma g \to \bar{d}\, e\, \bar{\nu}_e\, u$ process at LHeC

Table 3.5: The total cross sections for the background processes for the exotic quarks at THERA.

m(GeV)	100	200	300	400	500
$\sigma_B(eu \to \nu_e\, e\, \bar{\nu}_e\, u)$	1.122x10^{-3}	1.451x10^{-3}	4.238x10^{-4}	1.856x10^{-4}	8.976x10^{-5}
$\sigma_B(ed \to e\, e\, \bar{\nu}_e\, u)$	8.349x10^{-4}	1.095x10^{-3}	3.332x10^{-4}	8.996x10^{-4}	1.195x10^{-3}
$\sigma_B(Wg \to \bar{u}\, e\, \bar{\nu}_e\, u)$	2.011x10^{-3}	2.556x10^{-2}	7.473x10^{-2}	2.578x10^{-2}	1.425x10^{-4}
$\sigma_B(Zg \to \bar{d}\, e\, \bar{\nu}_e\, u)$	1.502x10^{-3}	7.417x10^{-3}	8.200x10^{-3}	3.843x10^{-5}	5.511x10^{-4}
$\sigma_B(\gamma g \to \bar{d}\, e\, \bar{\nu}_e\, u)$	5.071x10^{-3}	1.195x10^{-3}	3.196x10^{-4}	2.860x10^{-5}	7.210x10^{-7}

Table 3.6: The total cross sections in pb for background processes for the exotic quarks at LHeC.

m(GeV)	200	400	600	800	1000
$\sigma_B(eu \to \nu_e\, e\, \bar{\nu}_e\, u)$	1.852x10^{-3}	5.002x10^{-4}	2.157x10^{-4}	3.405x10^{-5}	7.724x10^{-6}
$\sigma_B(ed \to e\, e\, \bar{\nu}_e\, u)$	8.398x10^{-4}	5.814x10^{-5}	4.309x10^{-5}	4.619x10^{-6}	1.128x10^{-6}
$\sigma_B(Wg \to \bar{u}\, e\, \bar{\nu}_e\, u)$	5.976x10^{-3}	5.260x10^{-3}	3.330x10^{-4}	2.352x10^{-4}	2.786x10^{-5}
$\sigma_B(Zg \to \bar{d}\, e\, \bar{\nu}_e\, u)$	7.938x10^{-3}	1.399x10^{-2}	1.048x10^{-3}	9.683x10^{-6}	3.436x10^{-5}
$\sigma_B(\gamma g \to \bar{d}\, e\, \bar{\nu}_e\, u)$	1.369x10^{-3}	1.090x10^{-5}	1.239x10^{-5}	2.512x10^{-8}	1.114x10^{-9}

Table 3.7: The significance ($S/\sqrt{S+B}$) for the exotic quarks at THERA ($L = 40$ pb^{-1}).

m(GeV)	100	200	300	400	500
$eu \to \nu_e D$	12.66	10.65	8.46	6.29	4.30
$ed \to eD$	3.28	2.68	2.05	1.46	0.94
$Wg \to \bar{u}D$	11.24	7.00	3.64	1.77	0.87
$Zg \to \bar{d}D$	30.94	19.28	10.78	5.40	2.39
$\gamma g \to \bar{d}D$	48.83	19.78	8.31	3.40	1.28

Table 3.8: The significance ($S/\sqrt{S+B}$) for the exotic quarks at LHeC ($L = 10^4$ pb^{-1}).

m(GeV)	200	400	600	800	1000
$eu \to \nu_e D$	189.95	140.33	91.04	48.91	18.87
$ed \to eD$	49.58	34.85	21.67	10.35	3.54
$Wg \to \bar{u}D$	144.62	66.93	24.61	6.75	1.25
$Zg \to \bar{d}D$	401.64	186.42	68.62	19.32	3.72
$\gamma g \to \bar{d}D$	389.33	111.03	30.65	7.00	1.19

CHAPTER 4

FOURTH GENERATION NEUTRINO PRODUCTION AT FUTURE COLLIDERS

The recent observation of neutrino oscillations gives evidence that the neutrino mass is non-zero [6, 7, 8], i.e. suggesting new physics beyond the Standard Model. Searching for new massive neutrinos has thus high priority at any new collider [80, 81, 82, 83, 84, 85, 86, 87, 88, 89, 90, 91, 92, 93, 94, 95, 96, 97]. These neutrinos play also the basic role in cosmology for solving the dark matter puzzle[98, 99, 100, 101, 102, 103, 104, 106, 107, 108, 109, 110, 105].

Bounds on the possible heavy neutrino masses are obtained either from experiments at accelerators or cosmological arguments. Among the several arguments, the experimental data of D0, LEP and SLAC rule out the possibility of ν_4 with masses smaller than 45 GeV [111, 112, 113] while the cosmological limit for the upper bound is 3 TeV [114, 115, 116, 117]. Heavy neutrino searches at lepton-hadron colliders has some advantages, larger masses, for instance, are accessible compared to current e^+e^- colliders. The H1 experiments at HERA have excluded the heavy leptons with masses lower than 225 GeV [118]. We assumed a range of 200 GeV - 3 TeV for single heavy lepton masses.

The purpose of this chapter is to investigate the possible single and pair production of a heavy neutrino (ν_4) in ep, $pp(p\bar{p})$ and e^+e^- collisions in the context of a new $e\nu_4 W$ and $\nu_4\bar{\nu}_4 Z$ anomalous magnetic dipole moment type interactions and analyze the background using optimal cuts. The experimental evidence of new particles often needed access to the highest possible center of mass energy as well

as the highest possible precision of the measurements which can not be obtained within the same experimental approach. While the hadron-hadron collision technically provides highest center of mass energy, the possible highest precision of the measurements can be achieved in lepton-lepton collisions. The results of these two type collisions complement and supplement each other in many ways. This complementarity caused the hadron and lepton colliders to operate concurrently in the past and thus collaboration between the physics programmes of the two colliders is established.

The Large Hadron Collider (LHC) is presently under construction and will start operation in 2007 which will collide protons with center of mass energy of 14 TeV [119, 120]. The International Linear Colliders (ILC) is a planned to be electron-positron collider with center of mass energy range 0.5-1 TeV [121]. The THERA ($\sqrt{s}$=1 TeV) and LC$\otimes$LHC ($\sqrt{s}$=3.74 TeV) are two proposed ep machine options [55, 56]. These proposed two ep machines has a lower luminosity but it can provide the complementary information to hadron-hadron and e^+e^- colliders in TeV energy scale. For the years to come, three types of colliders will be mainly used in particle physics as far as the energy frontiers are considered. The main parameters of these future colliders are given in Table 4.1.

4.1 Possibility of Searching for Fourth Generation Neutrino at Future ep Colliders

The single production of heavy leptons ν_4 can occur via the t-channel W exchange reaction $eq \to \nu_4 q'$, by proposing the following new charged current $e\nu_4 W$ interaction

$$\mathcal{L}_{cc} = \frac{g}{\sqrt{2}}\,\bar{e}[\gamma_\mu + \frac{i}{2m_{\nu_4}}\kappa_1\sigma_{\mu\nu}q^\nu]P_L\,\nu_4\,W^\mu + h.c., \tag{4.1}$$

Table 4.1: The main parameters of future colliders

ep	E_e (TeV)	E_p (TeV)	$\sqrt{s}$ (TeV)	$L_{int}(pb^{-1})$
THERA	0.25	1	1	40
LHeC	0.7	7	1.4	10^4
LCxLHC	0.5	7	3.74	100

e^+e^-	E_{e^+} (TeV)	E_{e^-} (TeV)	$\sqrt{s}$ (TeV)	$L_{int}(pb^{-1})$
ILC	0.25	0.25	0.5	10^4
ILC	0.5	0.5	1	10^4

$p\bar{p}$	E_p (TeV)	E_p (TeV)	$\sqrt{s}$ (TeV)	$L_{int}(pb^{-1})$
LHC	7	7	14	10^5

which parallels the coupling structure for $\tau\nu W$ vertex [122]. In Eq. (4.1), κ_1 is the anomalous magnetic dipole moment factor, m_{ν_4} is the mass of the fourth generation neutrino, q is the momentum carried by the exchanged W boson, g denotes the gauge coupling relative to SU(2) symmetries, $P_L = (1-\gamma^5)/2$ is left-handed projection operator and W^μ is the field of W.

As a first step to compute the amplitude of the subprocess $eq \to \nu_4 q'$, let us write down the interaction vertices relevant for our purpose. The coupling of quarks and leptons to $W^\pm$ is a universal "V-A form; the vector factor is always [60]

$$-iU_{ij}\frac{g}{\sqrt{2}}\gamma^\mu P_L \tag{4.2}$$

here U_{ij} ($i = u, c$ and $j = d, s$ or b) is the Cabibo-Kobayashi-Maskawa (CKM) quark mixing matrix [77]:

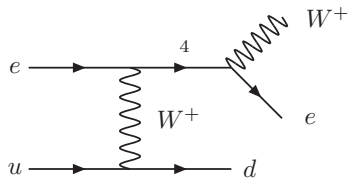

Figure 4.1: The Feynman diagram at parton level for single fourth generation neutrino production in ep collisions via charged current interaction.

$$\begin{pmatrix} d' \\ s' \\ b' \end{pmatrix} \begin{pmatrix} U_{ud} & U_{us} & U_{ub} \\ U_{cd} & U_{cs} & U_{cb} \\ U_{td} & U_{ts} & U_{tb} \end{pmatrix} \begin{pmatrix} d \\ s \\ b \end{pmatrix}$$

and the allowed range of the magnitudes of all nine CKM elements are:

$$U_{ij} = \begin{pmatrix} 0.97383 & 0.2272 & 3.96 \times 10^{-3} \\ 0.2271 & 0.97296 & 42.21 \times 10^{-3} \\ 8.14 \times 10^{-3} & 41.61x10^{-3} & 0.99100 \end{pmatrix}$$

and the vertex of $\nu_4 \to eW^-$ transition is written from Eq. (4.1) as follow

$$\gamma^\mu P_L - i\frac{\kappa_1}{2m_{\nu_4}}\sigma^{\mu\nu}q_\nu P_R \tag{4.3}$$

Using Eqs. (4.2) and (4.3), we can write the amplitude of the subprocess $e^-(p_1) + q(p_2) \to \nu_4(p_3) + q'(p_4)$ of which the Feynman diagram in Fig 4.1 as

$$\begin{aligned} \mathcal{M} &= \bar{u}(p_3)[\frac{g}{\sqrt{2}}(\gamma^\mu P_L - i\frac{\kappa_1}{2m_{\nu_4}}\sigma^{\mu\eta}q_\eta P_R)]u(p_1)(\frac{g_{\mu\nu} - q_\mu q_\nu/M_W^2}{(q^2 - M_W^2) + i\Gamma_W M_W}) \\ &\times \bar{u}(p_4)[-i\frac{g}{\sqrt{2}}\gamma^\nu P_L]u(p_2) \end{aligned} \tag{4.4}$$

and taking the Hermitian conjugate of Eq. (4.4)

$$\begin{aligned}\bar{\mathcal{M}} &= \bar{u}(p_1)[\frac{g}{\sqrt{2}}(\gamma^\alpha P_L + i\frac{\kappa_1}{2m_{\nu_4}}\sigma^{\alpha\rho}q_\rho P_R)]u(p_1)(\frac{g_{\alpha\beta} - q_\alpha q_\beta/M_W^2}{(q^2 - M_W^2) + i\Gamma_W M_W}) \\ &\times \bar{u}(p_2)[-i\frac{g}{\sqrt{2}}\gamma^\beta P_L]u(p_4) \end{aligned} \tag{4.5}$$

here Γ_W and M_W are decay widths and mass of the W boson, respectively. The squared spin-averaged invariant matrix element of these amplitude becomes

$$\begin{aligned}< |\mathcal{M}|^2 > &= \frac{g^4}{16[(q^2 - M_W^2)^2 + \Gamma_W^2 M_W^2]} \\ &\times Tr[(\not{p}_3 + m_{\nu_4})(\gamma^\mu P_L - i\frac{\kappa_1}{2m_{\nu_4}}\sigma^{\mu\eta}q_\eta P_R)\ \not{p}_1(\gamma^\alpha P_L + i\frac{\kappa_1}{2m_{\nu_4}}\sigma^{\alpha\rho}q_\rho P_L] \\ &\times Tr[\not{p}_4\gamma^\mu P_L\ \not{p}_2\gamma^\beta P_L](g_{\mu\nu} - q_\mu q_\nu/M_W^2)(g_{\alpha\beta} - q_\alpha q_\beta/M_W^2) \end{aligned} \tag{4.6}$$

We define the usual Mandelstam invariants for the process $e^-(p_1) + q(p_2) \rightarrow \nu_4(p_3) + q'(p_4)$ as $\hat{s} = (p_1 + p_2)^2, \hat{t} = (p_1 - p_3)^2$, $\hat{u} = (p_1 - p_4)^2$ and $q = (p_1 - p_3)$. We also define a variable $\hat{s} + \hat{t} + \hat{u} = m_{\nu_4}^2$ with electron and quark masses are neglected. We find the differential cross section as

$$\frac{d\hat{\sigma}}{d\hat{t}} = \frac{\pi\alpha^2[\kappa_1^2((2\hat{s} + \hat{t})m_{\nu_4}^2 - \hat{s}(\hat{t} + \hat{s}) - m_{\nu_4}^4)\hat{t} + 4m_{\nu_4}^2\hat{s}(\hat{s} - m_{\nu_4}^2)]}{16\sin^4\theta_W\hat{s}^2m_{\nu_4}^2[(\hat{t} - M_W^2)^2 + \Gamma_W^2M_W^2]} \tag{4.7}$$

here θ_W is the weak mixing angle. Using Eq. (2.24), the total production cross section is obtained by the integration over the parton distributions in the proton. For the parton distribution function $f_q(x)$ we have used the MRST parametrizations [61] and taken κ_1=0.1 for illustrative purposes. The calculated cross sections are displayed in Fig. 4.2 for the mass range from 100 to 1400 GeV at THERA and LHeC, and in Fig. 4.3 from 100 GeV to 3 TeV at LC⊗LHC.

For the mass values larger than 200 GeV, the cross sections are not sensitive to the κ_1 values at all. When the fourth generation neutrino is produced, it

Table 4.2: Total cross sections of signal and background at THERA for κ_1=0.1.

m_{ν_4}(GeV)	σ_S(pb)	σ_B (pb)
100	80.41	0.045
200	56.80	0.062
300	35.77	0.031
400	19.77	0.013
500	9.23	0.0052
600	3.41	0.0017
700	0.88	4.20×10^{-4}
800	0.12	5.77×10^{-5}
900	0.003	1.75×10^{-6}

will decay via charged current interaction $\nu_4 \to l\,W$ where $l = e,\ \mu,\ \tau$. In this work we concentrate only on $\nu_4 \to e\,W$ decay channel and consider the relevant background from the semileptonic reaction $eu \to e\,W\,d$. We present background and signal cross sections with respect to invariant mass of eW in Tables 4.2, 4.3 and 4.4 for THERA, LHeC and LC⊗LHC options, respectively. To extract the fourth generation neutrino signal and to suppress the Standard Model background one has to impose a cut on the eW invariant mass. Thus in the presentation of these tables we introduced the cuts $|m_{eW} - m_{\nu_4}|$ <25 GeV for the mass range of m_{ν_4}=100-1000 GeV and $|m_{eW} - m_{\nu_4}|$ <50 GeV for the mass range of 1-3.4 TeV which are reasonable for the mass resolution of detectors of the purposed ep machines [55, 56]. All calculations for the background were done using the high energy package CompHEP [78] with CTEQ6L [79] distribution function.

We present the distribution of invariant mass m_{We} with cuts $p_T^{e^-,j} > 10$ GeV for the background process $eu \to e^- W^+ d$ for THERA in Fig. 4.4, for LHeC in Fig. 4.5, for LC⊗LHC in Fig. 4.6. Finally, in Fig. 4.7, Fig. 4.8 and Fig. 4.9 we show the p_T distributions due to the ν_4 production at these collider options.

Table 4.3: Total cross sections of signal and background at LHeC for κ_1=0.1.

m_{ν_4}(GeV)	σ_S(pb)	σ_B (pb)
300	54.89	0.023
600	16.58	0.0037
700	9.45	1.8×10^{-3}
800	4.79	8.34×10^{-4}
900	2.07	3.42×10^{-4}
1000	0.71	1.17×10^{-4}
1100	0.17	2.94×10^{-5}
1200	0.022	4.08×10^{-5}
1300	5.55×10^{-5}	1.15×10^{-7}

Table 4.4: Total cross sections of signal and background at LC $\otimes$LHC for κ_1=0.1.

m_{ν_4}(GeV)	σ_S(pb)	σ_B (pb)
200	98.23	0.21
600	69.78	0.048
1000	44.16	0.012
1400	24.40	0.020
1800	11.31	0.0045
2200	4.09	0.0014
2600	1.00	3.60×10^{-4}
3000	0.12	4.90×10^{-5}
3400	0.0022	1.42×10^{-6}

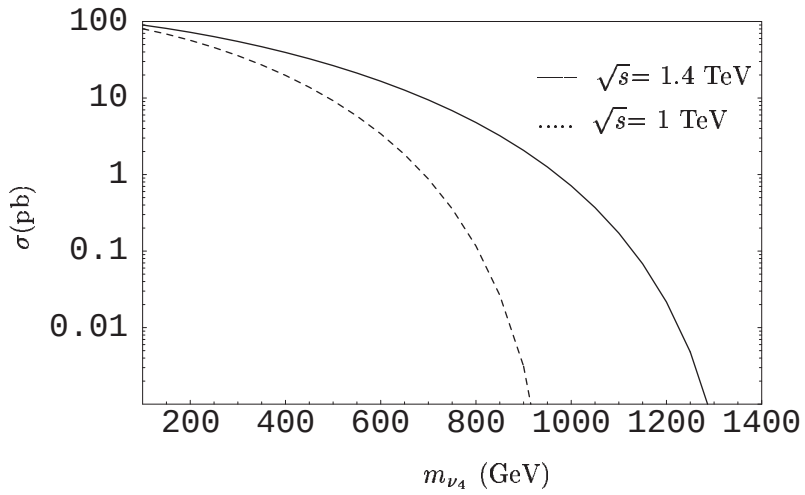

Figure 4.2: The total production cross sections of the subprocess $eu \to \nu_4 d$ as a function of m_{ν_4} at THERA and LHeC.

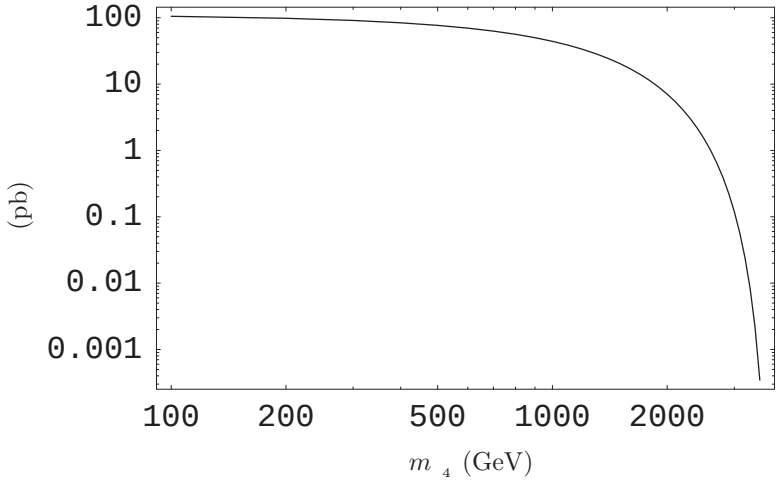

Figure 4.3: The total production cross section of the subprocess $eu \to \nu_4 d$ as a function of m_{ν_4} at LC⊗LHC.

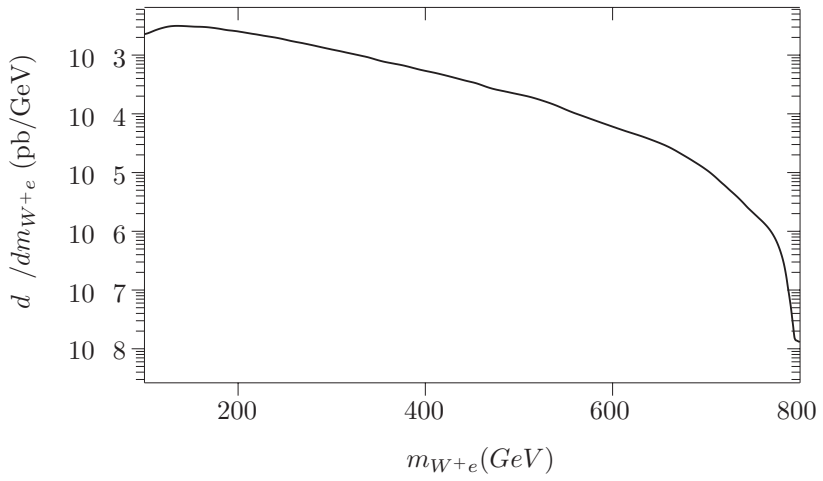

Figure 4.4: The invariant mass m_{We} distribution of the background at THERA.

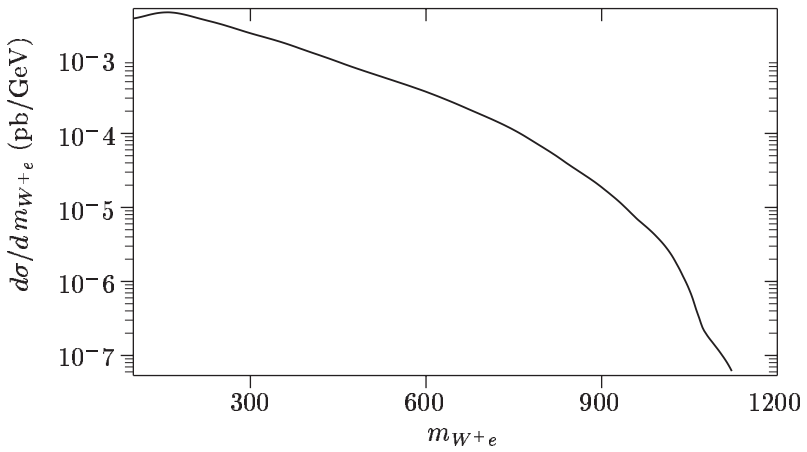

Figure 4.5: The invariant mass m_{We} distribution of the background at LHeC.

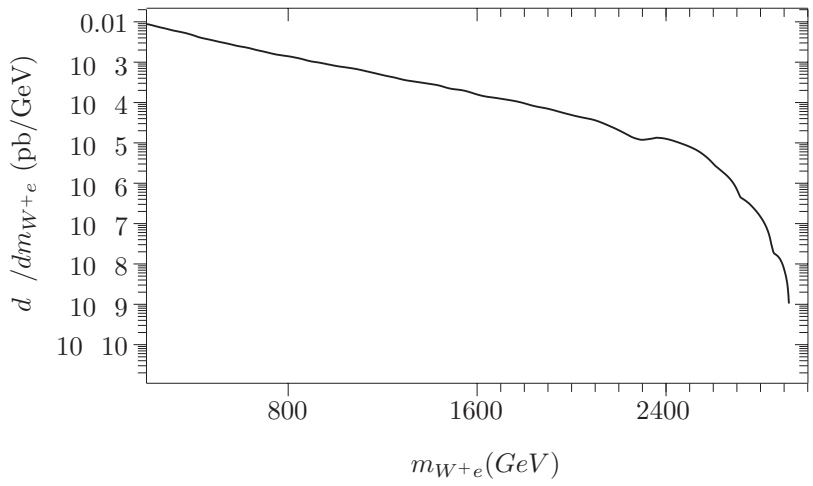

Figure 4.6: The invariant mass m_{We} distribution of the background at LC⊗LHC .

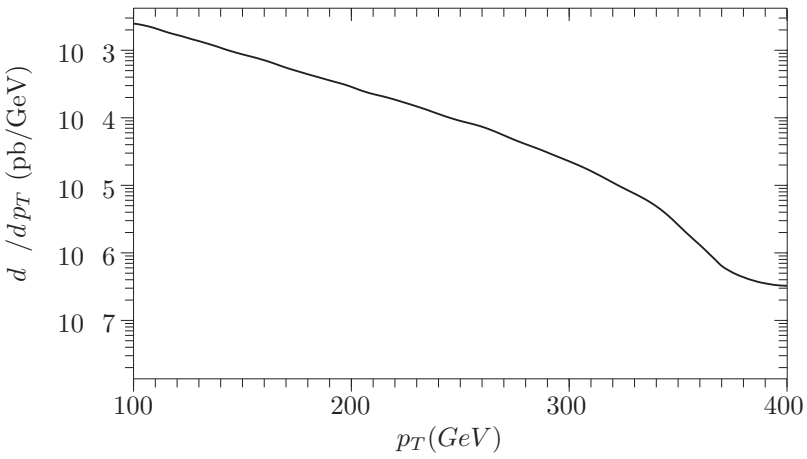

Figure 4.7: p_T distribution of the background at THERA.

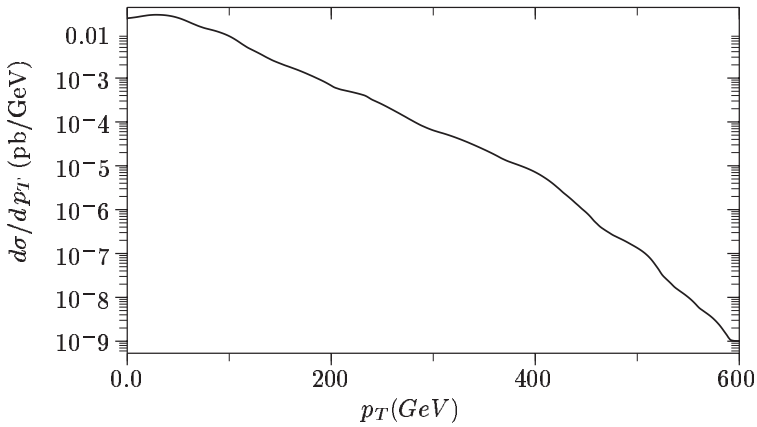

Figure 4.8: p_T distribution of the background at LHeC.

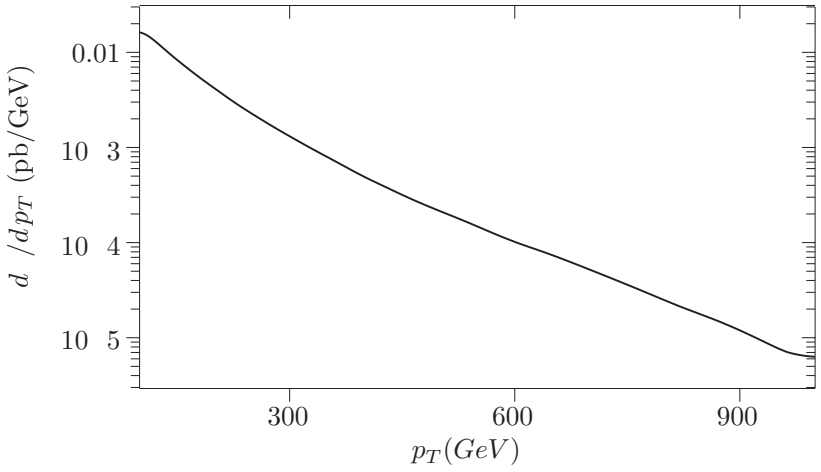

Figure 4.9: p_T distribution of the background at LC⊗LHC.

4.2 Fourth Generation Neutrino Searches using pp Colliders

The fourth generation neutrinos may be produced either in singly or pairs. In this section, we calculate the squared scattering amplitude of the processes $pp(p\bar{p}) \rightarrow e^+\nu_4 + X$ (single production) and $pp(p\bar{p}) \rightarrow \nu_4\bar{\nu}_4 + X$ (pair production)

4.2.1 Single Production

The single production of fourth generation neutrinos takes place through the subprocess $q_i(p_1) + \bar{q}'_j(p_2) \rightarrow \nu_4(p_3) + e^+(p_4)$ at hadron colliders.

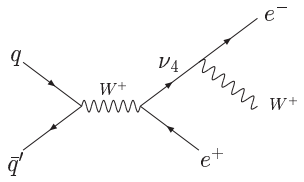

Figure 4.10: The Feynman diagram for single fourth generation neutrino production in pp or $p\bar{p}$ collisions via charged current interaction.

The amplitude of this reaction $\mathcal{M}$ corresponding to the diagram of Fig. 4.10 is

$$\begin{aligned} \mathcal{M} &= \bar{v}(p_2)[-iU_{ij}\frac{g}{\sqrt{2}}\gamma^\mu P_L]u(p_1)(\frac{g_{\mu\nu} - q_\mu q_\nu/M_W^2}{(q^2 - M_W^2) + i\Gamma_W M_W}) \\ &\times \bar{u}(p_3)[\frac{g}{\sqrt{2}}(\gamma^\nu P_L - i\frac{\kappa_1}{2m_{\nu_4}}\sigma^{\nu\rho}q^\rho P_R)]v(p_4) \end{aligned} \tag{4.8}$$

where $-iU_{ij}\frac{g}{\sqrt{2}}\gamma^\mu P_L$ is standard $q' \rightarrow q + W^-$ vertex and complex conjugate of $\mathcal{M}$ is

$$\bar{\mathcal{M}} = \bar{u}(p_1)[iU_{ij}\frac{g}{\sqrt{2}}\gamma^\alpha P_L]v(p_2)(\frac{g_{\alpha\beta} - q_\alpha q_\beta/M_W^2}{(q^2 - M_W^2) - i\Gamma_W M_W})$$

$$\times \quad \bar{v}(p_4)[\frac{g}{\sqrt{2}}(\gamma^\beta P_L + i\frac{\kappa_1}{2m_{\nu_4}}\sigma^{\beta\eta}q^\eta P_L)]u(p_3) \tag{4.9}$$

the calculation then reduces to that of product of traces

$$\begin{aligned} < |\mathcal{M}|^2 > \quad &= \frac{g^4}{16[(q^2 - M_W^2)^2 + \Gamma_W^2 M_W^2]} \\ &\times Tr[\not{p}_2\gamma^\mu P_L \ \not{p}_1\gamma^\alpha P_L](g_{\mu\nu} - q_\mu q_\nu/M_W^2)(g_{\alpha\beta} - q_\alpha q_\beta/M_W^2) \\ &\times Tr[(\not{p}_3 + m_{\nu_4})(\gamma^\nu P_L - i\frac{\kappa_1}{2m_{\nu_4}}\sigma^{\nu\rho}q_\rho P_R) \ \not{p}_4(\gamma^\beta P_L + i\frac{\kappa_1}{2m_{\nu_4}}\sigma^{\beta\eta}q_\eta P_L)] \end{aligned} \tag{4.10}$$

The usual Mandelstam variables are $\hat{s} = (p_1 + p_2)^2, \hat{t} = (p_1 - p_3)^2$, $\hat{u} = (p_1 - p_4)^2$ and satisfying $\hat{s} + \hat{t} + \hat{u} = m_{\nu_4}^2$ and also $q = p_1 + p_2$.

The differential cross section for the subprocess $q\bar{q'} \to \nu_4 e^+$ is

$$\frac{d\hat{\sigma}}{d\hat{t}}(q_i\bar{q}'_j \to e^+\nu_4) \quad = \quad \frac{\pi\alpha^2 U_{ij}^2(\hat{s} + \hat{t})[\hat{s}(4m_{\nu_4}^2 - \kappa_1^2\hat{t}) + 4m_{\nu_4}^2\hat{t} - 4m_{\nu_4}^4]}{16\sin^4\theta_W \hat{s}^2 m_{\nu_4}^2[(\hat{s} - M_W^2)^2 + \Gamma_W^2 M_W^2]} \tag{4.11}$$

The total hadronic cross sections are obtained by integrating the parton cross sections in the usual way over the parton distributions $f_i(x, Q^2)$ in proton or antiproton:

$$\sigma = \int_{m_{\nu_4}^2/s}^1 d\tau \int_\tau^1 \frac{dx}{x}[f_q(x, Q^2)f_{\bar{q'}}(\frac{\tau}{x}, Q^2) + f_{\bar{q'}}(\frac{\tau}{x}, Q^2)f_q(x, Q^2)]\hat{\sigma}(\hat{s}, m_{\nu_4}) \tag{4.12}$$

where s is the hadron-hadron center of mass energy squared which is related to $\hat{s}$, the parton-parton center of mass energy squared via $\hat{s} = xs$ and we have used CTEQ5L parametrization with $Q^2 = m_{\nu_4}^2$. The dependence of the expected cross sections on the mass of the ν_4 at the LHC ($\sqrt{s}$=14 TeV) and Tevatron ($\sqrt{s}$=1.8 TeV) are shown in Fig. 4.11.

When the fourth generation neutrino is produced, it will decay via charged current interaction $\nu_4 \to e\,W$. If the W boson is reconstructed different final

states are obtained. The first state consist of three charged leptons and a neutrino. The three charged leptons and the missing transverse energy associated with the neutrino is a identifying signature among the all SM backgrounds.

The second final state has a high branching ratio and is a hadronic channel consisting of two leptons and two jets. The signal cross section (σ_S), hadronic (σ_B^h) and leptonic (σ_B^l) background cross sections and statistical significance ($S/\sqrt{S+B}$) where S is the number of the signal events and B is the number of background events as a function of mass ν_4 are given in Table 4.5 at the LHC and in Table 4.6 at Tevatron. We analyzed invariant mass distribution which is one of the main characteristic of final state identifications. Especially, the LHC will be constructed with high resolution leptonic and hadronic detectors as well as a wide rapidity coverage [123].

We show the invariant mass distribution of hadronic and leptonic final states with $P_T^{e,j} > 10$ GeV at LHC and Tevatron in Figures 4.12. As can be seen in these figures, the SM background decreases for larger M_{ejj} and $M_{ee\nu_e}$ and the hadronic final states more pronounced than the leptonic final states for both hadron colliders. Moreover, the invariant mass distribution of the hadronic channel has a Jacobian peak peak around 250 GeV while the leptonic channel has a peak 200 GeV at the LHC. At the Tevatron, both peaks appear around 100 GeV.

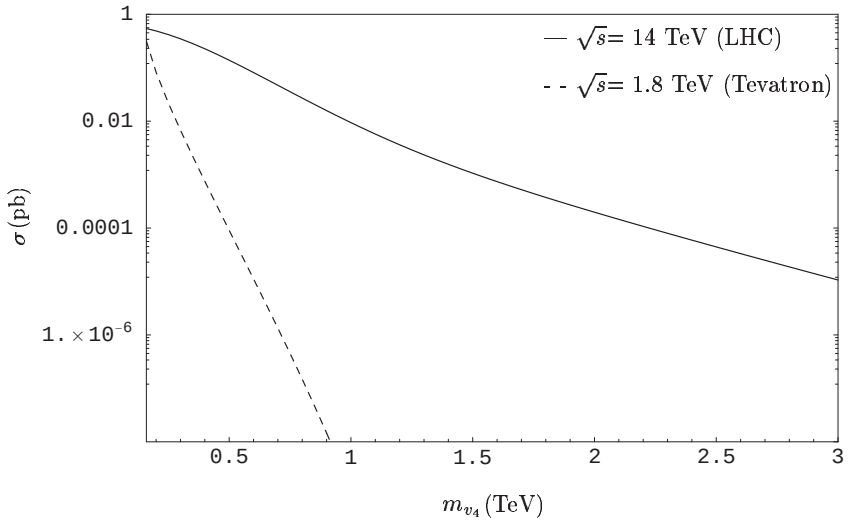

Figure 4.11: The total production cross sections for the subprocess $q\bar{q}' \to e^+\nu_4$ as a function of m_{ν_4} at the LHC and Tevatron.

Table 4.5: The total cross sections for the signal and background process and the significance for the single production of fourth generation neutrinos at LHC.

m_{ν_4}(GeV)	σ_S(pb)	σ_B^h(pb)	σ_B^l(pb)	$S/\sqrt{S+B}$
250	$4.141\text{x}10^{-1}$	$2.110\text{x}10^{-4}$	$4.904\text{x}10^{-7}$	203.43
500	$1.373\text{x}10^{-1}$	$6.800\text{x}10^{-5}$	$2.215\text{x}10^{-7}$	117.16
750	$3.532\text{x}10^{-2}$	$2.650\text{x}10^{-4}$	$5.890\text{x}10^{-7}$	59.21
1000	$9.320\text{x}10^{-3}$	$1.761\text{x}10^{-5}$	$2.058\text{x}10^{-7}$	30.50
1250	$2.877\text{x}10^{-3}$	$6.634\text{x}10^{-5}$	$1.816\text{x}10^{-8}$	16.77
1500	$1.054\text{x}10^{-3}$	$5.632\text{x}10^{-5}$	$5.088\text{x}10^{-9}$	10.00
2000	$1.964\text{x}10^{-4}$	$3.098\text{x}10^{-6}$	$4.925\text{x}10^{-9}$	4.40

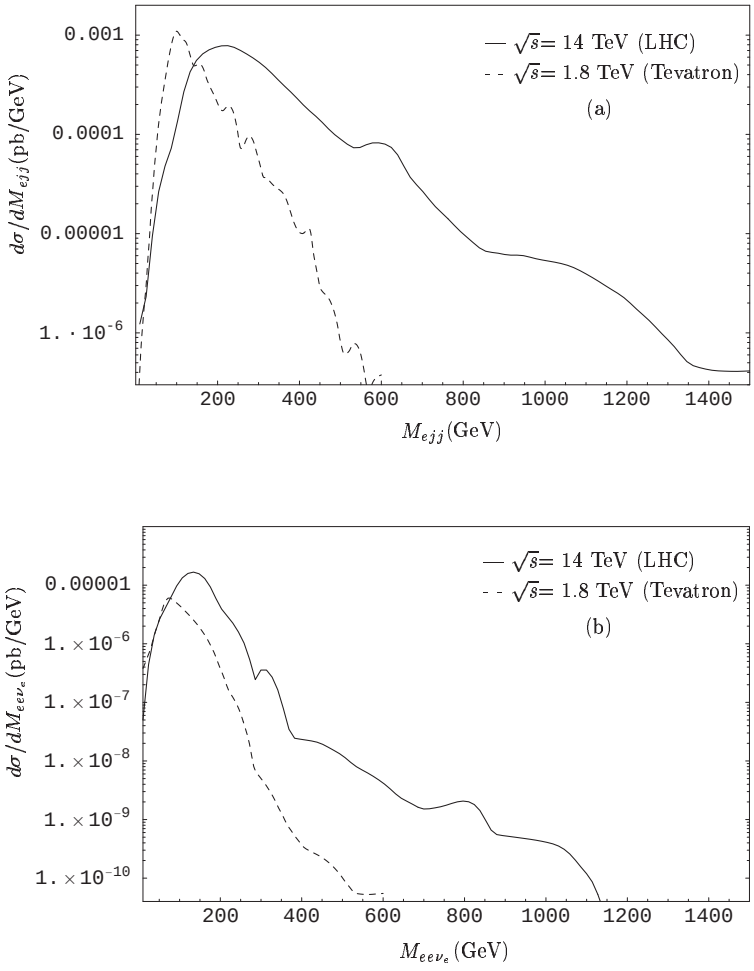

Figure 4.12: The invariant mass distributions of a) M_{ejj} b) $M_{ee\nu_e}$ for the single production of ν_4 at LHC and Tevatron

Table 4.6: The total cross sections for the signal and background process and the significance for the single production of fourth generation neutrinos at Tevatron.

m_{ν_4}(GeV)	σ_S(pb)	σ_B^h(pb)	σ_B^l(pb)	$S/\sqrt{S+B}$
150	$4.422\text{x}10^{-1}$	$1.119\text{x}10^{-3}$	$3.399\text{x}10^{-5}$	29.70
200	$8.262\text{x}10^{-1}$	$1.261\text{x}10^{-3}$	$1.500\text{x}10^{-5}$	12.76
250	$2.202\text{x}10^{-2}$	$1.031\text{x}10^{-3}$	$6.026\text{x}10^{-6}$	6.62
300	$6.781\text{x}10^{-3}$	$2.313\text{x}10^{-4}$	$1.054\text{x}10^{-6}$	3.62
350	$2.221\text{x}10^{-3}$	$2.413\text{x}10^{-4}$	$6.585\text{x}10^{-7}$	2.00
400	$7.519\text{x}10^{-4}$	$1.250\text{x}10^{-4}$	$4.306\text{x}10^{-8}$	1.14
450	$2.597\text{x}10^{-4}$	$1.498\text{x}10^{-5}$	$7.205\text{x}10^{-8}$	0.70
500	$9.081\text{x}10^{-5}$	$2.833\text{x}10^{-5}$	$4.149\text{x}10^{-9}$	0.37

4.2.2 Pair Production

The other production mechanism of the fourth generation neutrinos at hadron colliders is the pair production. We need to define the generalized form of the interaction of the fourth generation neutrino with Z. The neutral current anomalous magnetic moment type interactions for fourth generation neutrinos are described by the Lagrangian:

$$\mathcal{L}_{nc} = \frac{g}{2c_W}\,\bar{\nu}_4[\gamma_\mu(v_{\nu_4} - a_{\nu_4}\gamma^5) + \frac{i}{2m_{\nu_4}}\kappa_2\sigma_{\mu\nu}q^\nu]\nu_4\,Z^\mu + h.c., \tag{4.13}$$

where g is the standard weak coupling, $c_W = \cos\theta_W$, v_{ν_4} and a_{ν_4} are the axial-vector and vector neutral couplings of the fourth generation neutrino, κ_2 is the anomalous magnetic dipole moment form factor and m_{ν_4} is the fourth generation neutrino mass.

Pair production of ν_4 at hadron colliders is achieved through the anomalous magnetic moment type interactions via parton level process $q_i + \bar{q}_i \to \nu_4 + \bar{\nu}_4$. The Feynman diagram which contribute to this subprocess is displayed in Fig.4.13

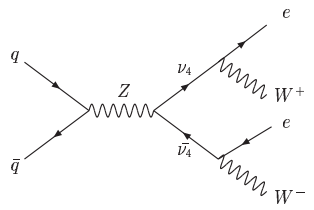

Figure 4.13: The Feynman diagram for pair production of fourth generation neutrino in pp or $p\bar{p}$ collisions

. The starting point is the effective lagrangian ,Eq. (4.13), to write s-channel subprocess $q_i(p_1) + \bar{q}_i(p_2) \to \nu_4(p_3) + \bar{\nu}_4(p_4)$ the amplitude is given as

$$\begin{aligned} \mathcal{M} &= \bar{v}(p_2)[-i\frac{g_z}{2}\gamma^\mu(v_q - a_q\gamma^5)]u(p_1)(\frac{g_{\mu\nu} - q_\mu q_\nu/M_Z^2}{(q^2 - M_Z^2) + i\Gamma_Z M_Z}) \\ &\times \bar{u}(p_3)[\frac{g_z}{2}(\gamma^\nu(v_{\nu_4} - a_{\nu_4}\gamma^5) + i\frac{\kappa_2}{2m_{\nu_4}}\sigma^{\nu\rho}q^\rho)]v(p_4) \end{aligned} \tag{4.14}$$

and Hermitian conjugate of this amplitude:

$$\begin{aligned} \bar{\mathcal{M}} &= \bar{u}(p_1)[i\frac{g_z}{2}\gamma^\alpha(v_q - a_q\gamma^5)]v(p_2)(\frac{g_{\alpha\beta} - q_\alpha q_\beta/M_Z^2}{(q^2 - M_Z^2) - i\Gamma_Z M_Z}) \\ &\times \bar{v}(p_4)[\frac{g_z}{2}(\gamma^\beta(v_{\nu_4} - a_{\nu_4}\gamma^5) - i\frac{\kappa_2}{2m_{\nu_4}}\sigma^{\beta\eta}q^\eta)]u(p_3) \end{aligned} \tag{4.15}$$

after summing over the initial-state spin average, the amplitude squared is given by

$$\begin{aligned} < |\mathcal{M}|^2 > &= \frac{g_z^4}{64[(q^2 - M_W^2)^2 + \Gamma_W^2 M_W^2]}(g_{\mu\nu} - q_\mu q_\nu/M_Z^2)(g_{\alpha\beta} - q_\alpha q_\beta/M_Z^2) \\ &\times Tr[\not{p}_2\gamma^\mu(v_q - a_q\gamma^5)\ \not{p}_1\gamma^\alpha(v_q - a_q\gamma^5)] \\ &\times Tr[(\not{p}_3 + m_{\nu_4})(\gamma^\nu(v_{\nu_4} - a_{\nu_4}\gamma^5) + i\frac{\kappa_2}{2m_{\nu_4}}\sigma^{\nu\rho}q_\rho) \\ &(\not{p}_4 - m_{\nu_4})(\gamma^\beta(v_{\nu_4} - a_{\nu_4}\gamma^5) - i\frac{\kappa_2}{2m_{\nu_4}}\sigma^{\beta\eta}q_\eta)] \end{aligned} \tag{4.16}$$

The partonic differential cross section for the $q_i + \bar{q}_i \to \nu_4 + \bar{\nu}_4$ process through

Z s-channel exchange can be written as

$$\begin{aligned}\frac{d\hat{\sigma}}{d\hat{t}}(q\bar{q}\to\nu_4\bar{\nu}_4) &= \frac{\pi\alpha^2}{16\hat{s}^2 m_{\nu_4}^2\sin^4\theta_W\cos^4\theta_W[(\hat{s}-M_Z^2)^2+\Gamma_Z^2M_Z^2]}\\ &\times \Big\{(a_q^2+v_q^2)\Big[2m_{\nu_4}^2(a_{\nu_4}^2+v_{\nu_4}^2)((\hat{s}+\hat{t})^2+\hat{t}^2-2m_{\nu_4}^2(2\hat{t}-m_{\nu_4}^2))\\ &- 4m_{\nu_4}^2\hat{s}(2a_{\nu_4}^2m_{\nu_4}^2-\hat{s}v_{\nu_4}\kappa_2)+\hat{s}\kappa_2^2((\hat{s}+\hat{t})(2m_{\nu_4}^2-\hat{t})-m_{\nu_4}^4)\Big]\\ &- 8a_{\nu_4}a_qv_qv_{\nu_4}+\kappa_2)m_{\nu_4}^2\hat{s}(2m_{\nu_4}^2-\hat{s}-2\hat{t})\Big\} \qquad (4.17)\end{aligned}$$

The hadronic cross section $pp(p\bar{p})\to\nu_4\bar{\nu}_4+X$ is calculated as a function of center

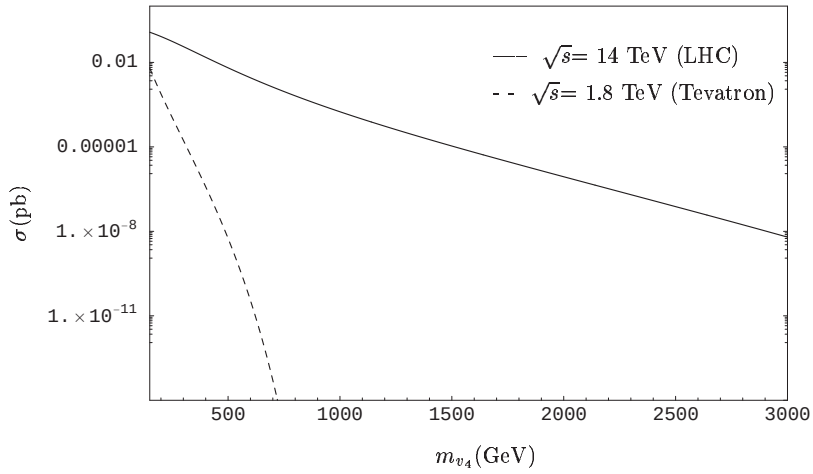

Figure 4.14: The total production cross sections for the subprocess $q\bar{q}\to\nu_4\bar{\nu_4}$ as a function of m_{ν_4} at the LHC and Tevatron.

of mass energy s, κ_2 and m_{ν_4}, from Eq. (4.12). We present the total hadronic cross section as a function of mass of the fourth generation neutrino at the LHC (solid line) and Tevatron (dashed line) in Fig. 4.14. In Fig. 4.15 we depict the leptonic (a) and hadronic (b) invariant mass distributions coming from decay of ν_4 at the LHC and Tevatron. As shown in these figures, the invariant mass distribution of the hadronic and leptonic final states have a Jacobian peak around 200 GeV at the LHC and 100 GeV at the Tevatron. The total signal cross section

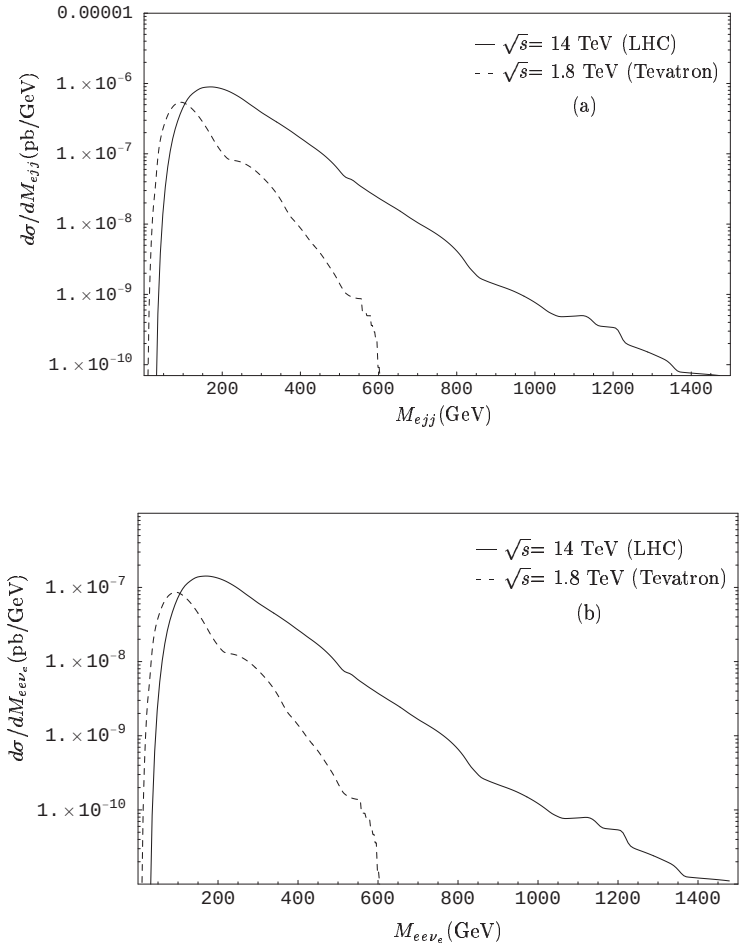

Figure 4.15: The invariant mass distributions of a) M_{ejj} b) $M_{ee\nu_e}$ for the pair production of ν_4 at LHC and Tevatron

(σ_S), hadronic (σ_B^h) and leptonic (σ_B^l) background cross sections and statistical significance are given in Table 4.7 at the LHC and in Table 4.8 at Tevatron.

Table 4.7: The total cross sections for the signal and background process and the significance for the pair production of fourth generation neutrino at LHC.

m_{ν_4}(GeV)	σ_S(pb)	σ_B^h(pb)	σ_B^l(pb)	$S/\sqrt{S+B}$
200	$8.318\text{x}10^{-2}$	$6.846\text{x}10^{-5}$	$1.087\text{x}10^{-5}$	91.16
400	$1.518\text{x}10^{-2}$	$1.300\text{x}10^{-6}$	$2.067\text{x}10^{-7}$	38.96
600	$2.845\text{x}10^{-3}$	$1.515\text{x}10^{-6}$	$2.410\text{x}10^{-7}$	16.86
800	$6.502\text{x}10^{-4}$	$8.018\text{x}10^{-8}$	$1.275\text{x}10^{-8}$	8.06
1000	$1.768\text{x}10^{-4}$	$5.625\text{x}10^{-8}$	$8.945\text{x}10^{-9}$	4.20
1200	$5.437\text{x}10^{-5}$	$1.235\text{x}10^{-8}$	$1.964\text{x}10^{-9}$	2.33
1400	$1.816\text{x}10^{-5}$	$1.426\text{x}10^{-8}$	$2.267\text{x}10^{-9}$	1.35

Table 4.8: The total cross sections for the signal and background process and the significance for the pair production of fourth generation neutrinos at Tevatron.

m_{ν_4}(GeV)	σ_S(pb)	σ_B^h(pb)	σ_B^l(pb)	$S/\sqrt{S+B}$
200	$7.684\text{x}10^{-4}$	$3.298\text{x}10^{-6}$	$5.244\text{x}10^{-7}$	8.74
300	$1.722\text{x}10^{-5}$	$1.221\text{x}10^{-6}$	$1.941\text{x}10^{-7}$	1.26
400	$3.380\text{x}10^{-7}$	$1.849\text{x}10^{-7}$	$2.940\text{x}10^{-8}$	0.16
500	$5.629\text{x}10^{-9}$	$7.249\text{x}10^{-8}$	$1.153\text{x}10^{-8}$	$5.9\text{x}10^{-3}$

4.3 Fourth Generation Neutrino Searches using future e^+e^- Colliders

4.3.1 Single Production

We begin with the t-channel process, $e^+(p_1)e^-(p_2) \to \nu_e(p_3) + \nu_4(p_4)$, represented in Fig. 4.16 at Born level. There is only one diagram with W exchange in the

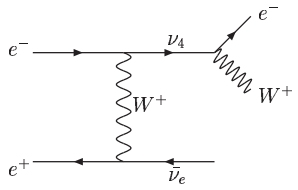

Figure 4.16: The Feynman diagram for single fourth generation neutrino production in e^+e^- collisions via charged current interaction.

t-channel. The corresponding scattering amplitude is

$$\begin{aligned}\mathcal{M} &= \bar{v}(p_1)[-i\frac{g}{\sqrt{2}}\gamma^\mu P_L]v(p_3)(\frac{g_{\mu\nu} - q_\mu q_\nu/M_W^2}{(q^2 - M_W^2) + i\Gamma_W M_W}) \\ &\times \bar{u}(p_4)[\frac{g}{\sqrt{2}}(\gamma^\nu P_L - i\frac{\kappa_1}{2m_{\nu_4}}\sigma^{\nu\rho}q^\rho P_R)]u(p_2) \end{aligned} \tag{4.18}$$

and $\bar{\mathcal{M}}$ is:

$$\begin{aligned}\bar{\mathcal{M}} &= \bar{v}(p_3)[i\frac{g}{\sqrt{2}}\gamma^\alpha P_L]v(p_1)(\frac{g_{\alpha\lambda} - q_\alpha q_\lambda/M_W^2}{(q^2 - M_W^2) - i\Gamma_W M_W}) \\ &\times \bar{u}(p_2)[\frac{g}{\sqrt{2}}(\gamma^\lambda P_L + i\frac{\kappa_1}{2m_{\nu_4}}\sigma^{\lambda\eta}q^\eta P_R)]u(p_4) \end{aligned} \tag{4.19}$$

and the spin averaged squaring matrix element is

$$\begin{aligned}< |\mathcal{M}|^2 > &= \frac{g^4}{16[(q^2 - M_W^2)^2 + \Gamma_W^2 M_W^2]} \\ &\times Tr[\not{p}_1\gamma^\mu P_L \not{p}_3\gamma^\alpha P_L](g_{\mu\nu} - q_\mu q_\nu/M_W^2)(g_{\alpha\beta} - q_\alpha q_\beta/M_W^2) \end{aligned} \tag{4.20}$$

$$\times Tr[(\not{p}_4 + m_{\nu_4})(\gamma^\nu P_L - i\frac{\kappa_1}{2m_{\nu_4}}\sigma^{\nu\rho}q_\rho P_R)\ \not{p}_2(\gamma^\beta P_L + i\frac{\kappa_1}{2m_{\nu_4}}\sigma^{\beta\eta}q_\eta P_L)]$$

We obtain following result for the differential cross section for the $e^+e^- \to \bar{\nu}_e\nu_4$ process:

$$\frac{d\sigma}{dt}(e^+e^- \to \bar{\nu}_e\nu_4) = \frac{\pi\alpha^2(s+t)[s(4m_{\nu_4}^2 - \kappa_1^2 t) + 4m_{\nu_4}^2 t - 4m_{\nu_4}^4]}{16\sin^4\theta_W s^2 m_{\nu_4}^2[(t-M_W^2)^2 + \Gamma_W^2 M_W^2]} \quad (4.21)$$

Integrating over the t, we obtain the total cross section for $e^+e^- \to \bar{\nu}_e\nu_4$. In Fig.4.17, we show the cross section for $e^+e^- \to \bar{\nu}_e\nu_4$ at $\sqrt{s}$= 500 GeV (dashed curve) and $\sqrt{s}$= 1 TeV (solid line) as a function of m_{ν_4}. The invariant mass distribution of the leptonic and hadronic final states of the final W from ν_4 decay are shown in Fig.4.18. These graphs indicate that the leptonic and hadronic final states have similar magnitudes. In Tables 4.9 and 4.10, the signal cross section (σ_S), hadronic (σ_B^h) and leptonic (σ_B^l) background cross sections and statistical significance ($S/\sqrt{S+B}$) are listed as a function of mass ν_4 at $\sqrt{s}$=500 GeV and $\sqrt{s}$=1 TeV ILC options, respectively.

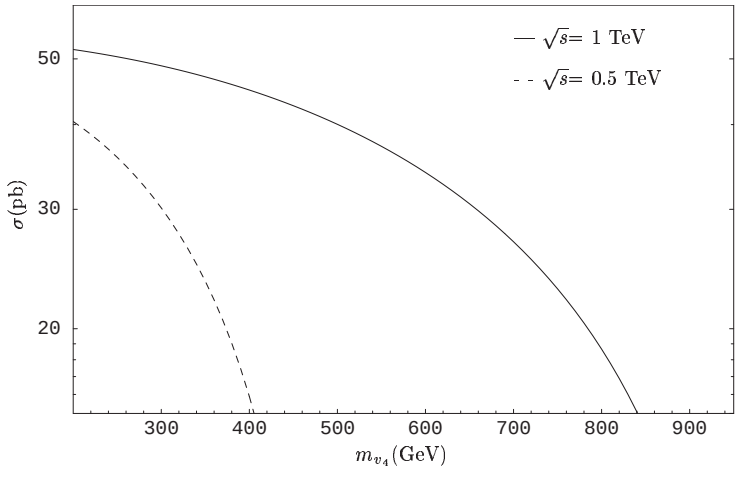

Figure 4.17: The total production cross sections for the process $e^+e^- \to \bar{\nu}_e\nu_4$ as a function of m_{ν_4} for ILC.

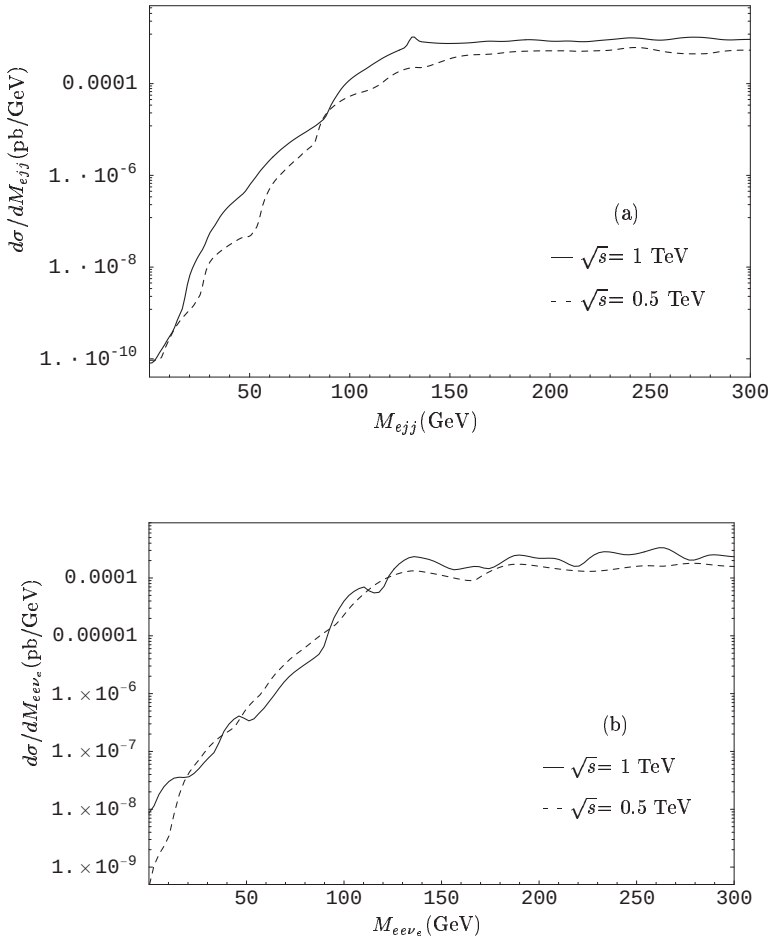

Figure 4.18: The invariant mass distributions of a) M_{ejj} b) $M_{ee\nu_e}$ for the single production of ν_4 at ILC($\sqrt{s}$= 0.5 TeV and 1 TeV)

Table 4.9: The total cross sections for the signal and background process and the significance for the single fourth generation neutrinos at ILC ($\sqrt{s}$= 0.5 TeV).

m_{ν_4}(GeV)	σ_S(pb)	σ_B^h(pb)	σ_B^l(pb)	$S/\sqrt{S+B}$
150	43.973	8.584x10^{-3}	3.622x10^{-3}	2096.77
200	40.422	8.873x10^{-3}	3.740x10^{-3}	2009.25
250	35.790	7.482x10^{-3}	3.286x10^{-3}	1890.91
300	30.145	7.507x10^{-3}	3.554x10^{-3}	1735.50
350	23.499	7.257x10^{-3}	3.148x10^{-3}	1532.30
400	15.892	6.406x10^{-3}	5.377x10^{-3}	1260.02
450	7.476	1.469x10^{-2}	8.955x10^{-3}	863.50

Table 4.10: The total cross sections for the signal and background process and the significance for the single fourth generation neutrinos at ILC ($\sqrt{s} = 1$ TeV).

m_{ν_4}(GeV)	σ_S(pb)	σ_B^h(pb)	σ_B^l(pb)	$S/\sqrt{S+B}$
200	51.573	1.120x10^{-2}	4.384x10^{-3}	2270.71
300	48.824	9.570x10^{-3}	3.520x10^{-3}	2209.40
400	44.977	7.140x10^{-3}	2.491x10^{-3}	2120.62
500	40.033	5.464x10^{-3}	1.653x10^{-3}	2000.70
600	33.995	4.020x10^{-3}	1.196x10^{-3}	1843.66
700	26.866	3.162x10^{-3}	8.233x10^{-4}	1638.97
800	18.657	2.622x10^{-3}	2.286x10^{-3}	1365.82
900	9.413	3.177x10^{-3}	5.274x10^{-3}	970.06

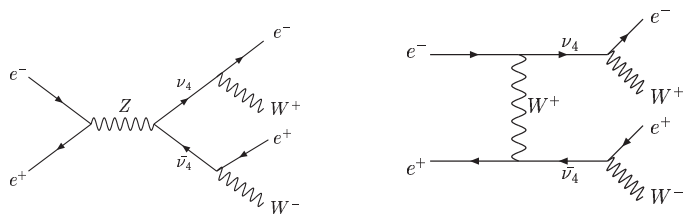

Figure 4.19: The Feynman diagram for pair production of fourth generation neutrino in pp or $p\bar{p}$ collisions

4.3.2 Pair Production

The matrix element for the reaction $e^-(p_1) + e^+(p_2) \rightarrow \nu_4(p_3) + \bar{\nu}_4(p_4)$ can be written as the sum of the two subamplitudes corresponding to the above diagrams :

$$\mathcal{M}(e^- + e^+ \rightarrow \nu_4 + \bar{\nu}_4) = \mathcal{M}_s + \mathcal{M}_t$$

where $\mathcal{M}_s$ and $\mathcal{M}_t$ contain the exchange of a particle in the channels corresponding to the Mandelstam variables s and t.

By using the effective Lagrangian Eqs. (4.1) and (4.13), it is easy to write the

invariant amplitude $\mathcal{M}_s$ is given as

$$\begin{aligned}\mathcal{M}_s &= \bar{v}(p_2)[-i\frac{g_z}{2}\gamma^\mu(v_e - a_e\gamma^5)]u(p_1)(\frac{g_{\mu\nu} - q_\mu q_\nu/M_Z^2}{(q^2 - M_Z^2) + i\Gamma_Z M_Z}) \\ &\times \bar{u}(p_3)[\frac{g_z}{2}(\gamma^\nu(v_{\nu_4} - a_{\nu_4}\gamma^5) + i\frac{\kappa_2}{2m_3}\sigma^{\nu\rho}q^\rho)]v(p_4) \qquad (4.22)\end{aligned}$$

and we evaluate the complex conjugate of $\mathcal{M}_s$:

$$\begin{aligned}\bar{\mathcal{M}}_s &= \bar{u}(p_1)[-i\frac{g_z}{2}\gamma^\mu(v^e - a^e\gamma^5)]v(p_2)(\frac{g_{\mu\nu} - q_\mu q_\nu/M_Z^2}{(q^2 - M_Z^2) - i\Gamma_Z M_Z}) \\ &\times \bar{v}(p_4)[\frac{g_z}{2}(\gamma^\nu(v^{\nu_4} - a^{\nu_4}\gamma^5) + i\frac{\kappa_2}{2m_3}\sigma^{\nu\rho}q^\rho)]u(p_3) \qquad (4.23)\end{aligned}$$

the spin average squared of the corresponding matrix element is written as follows:

$$\begin{aligned}< |\mathcal{M}_s|^2 > &= \frac{g_z^4}{64[(q^2 - M_W^2)^2 + \Gamma_W^2 M_W^2]}(g_{\mu\nu} - q_\mu q_\nu/M_Z^2)(g_{\alpha\beta} - q_\alpha q_\beta/M_Z^2) \\ &\times Tr[\not{p}_2\gamma^\mu(v_e - a_e\gamma^5)\ \not{p}_1\gamma^\alpha(v_e - a_e\gamma^5)] \qquad (4.24) \\ &\times Tr[(\not{p}_3 + m_3)(\gamma^\nu(v_{\nu_4} - a_{\nu_4}\gamma^5) + i\frac{\kappa_2}{2m_3}\sigma^{\nu\rho}q_\rho) \\ &(\not{p}_4 - m_4)(\gamma^\beta(v_{\nu_4} - a_{\nu_4}\gamma^5) - i\frac{\kappa_2}{2m_4}\sigma^{\beta\eta}q_\eta)]\end{aligned}$$

The invariant amplitude for $\mathcal{M}_t$ can be written as

$$\begin{aligned}\mathcal{M}_t &= \bar{u}(p_3)[\frac{g}{\sqrt{2}}(\gamma^\mu P_L - i\frac{\kappa_1}{2m_3}\sigma^{\mu\beta}q^\beta P_R)]u(p_1)(\frac{g_{\mu\nu} - q_\mu q_\nu/M_W^2}{(q^2 - M_W^2) + i\Gamma_W M_W}) \\ &\times \bar{v}(p_2)[\frac{g}{\sqrt{2}}(\gamma^\nu P_L + i\frac{\kappa_1}{2m_3}\sigma^{\nu\rho}q^\rho P_L)]v(p_4) \qquad (4.25)\end{aligned}$$

similarly, we write the hermitian conjugate of the $\mathcal{M}_t$:

$$\begin{aligned}\bar{\mathcal{M}}_t &= \bar{u}(p_1)[\frac{g}{\sqrt{2}}(\gamma^\alpha P_L + i\frac{\kappa_1}{2m_3}\sigma^{\alpha\lambda}q^\lambda P_L)]u(p_3)(\frac{g_{\alpha\eta} - q_\alpha q_\eta/M_W^2}{(q^2 - M_W^2) - i\Gamma_W M_W}) \\ &\times \bar{v}(p_4)[\frac{g}{\sqrt{2}}(\gamma^\eta P_L - i\frac{\kappa_1}{2m_3}\sigma^{\eta\tau}q^\tau P_R)]v(p_2) \qquad (4.26)\end{aligned}$$

The spinor part of this amplitude squared can be converted to a trace:

$$
\begin{aligned}
< |\mathcal{M}_t|^2 > &= \frac{g^4}{16[(q^2-M_W^2)^2+\Gamma_W^2 M_W^2]}(g_{\mu\nu}-q_\mu q_\nu/M_W^2)(g_{\alpha\eta}-q_\alpha q_\eta/M_W^2) \\
&\times Tr[(\not{p}_3+m_3)(\gamma^\mu P_L - i\frac{\kappa_1}{2m_3}\sigma^{\mu\beta}q^\beta P_R)\ \not{p}_1(\gamma^\alpha P_L + i\frac{\kappa_1}{2m_3}\sigma^{\alpha\lambda}q^\lambda P_L)] \\
&\times Tr[\not{p}_2((\gamma^\nu P_L + i\frac{\kappa_1}{2m_3}\sigma^{\nu\rho}q^\rho P_L)) \\
&(\not{p}_4-m_4)((\gamma^\eta P_L - i\frac{\kappa_1}{2m_3}\sigma^{\eta\tau}q^\tau P_R))]
\end{aligned} \tag{4.27}
$$

The interference term of the two diagrams can be written as follows

$$
\begin{aligned}
\mathcal{M}_s\bar{\mathcal{M}}_t &= \frac{-ig_z^2 g^2(g_{\mu\nu}-q_\mu q_\nu/M_Z^2)(g_{\alpha\eta}-q_\alpha q_\eta/M_W^2)}{32[(\hat{s}-M_Z^2)+i\Gamma_Z M_Z][(\hat{t}-M_W^2)-i\Gamma_W M_W]} \\
&\times\bar{v}(p_2)[\gamma^\mu(v_e-a_e\gamma^5)]u(p_1)\bar{u}(p_3)[(\gamma^\nu(v_{\nu_4}-a_{\nu_4}\gamma^5)+i\frac{\kappa_2}{2m_3}\sigma^{\nu\rho}q^\rho)]v(p_4) \\
&\bar{u}(p_1)[\gamma^\alpha(1-\gamma^5)+i\frac{\kappa_1}{2m_3}\sigma^{\alpha\lambda}q^\lambda(1-\gamma^5)]u(p_3) \\
&\bar{v}(p_4)[(\gamma^\eta(1-\gamma^5)-i\frac{\kappa_1}{2m_3}\sigma^{\eta\tau}q^\tau(1+\gamma^5))]v(p_2)
\end{aligned} \tag{4.28}
$$

Using standard tricks of the matrix algebra we can write the sum as a trace:

$$
\begin{aligned}
< \mathcal{M}_s\bar{\mathcal{M}}_t > &= \frac{-ig_z^2 g^2(g_{\mu\nu}-q_\mu q_\nu/M_Z^2)(g_{\alpha\eta}-q_\alpha q_\eta/M_W^2)}{32[(\hat{s}-M_Z^2)+i\Gamma_Z M_Z][(\hat{t}-M_W^2)-i\Gamma_W M_W]} \\
&Tr[\gamma^\mu(v_e-a_e\gamma^5)\ \not{p}_1(\gamma^\alpha(1-\gamma^5)+i\frac{\kappa_1}{2m_3}\sigma^{\alpha\lambda}q^\lambda(1-\gamma^5)) \\
&(\not{p}_3+m_3)(\gamma^\nu(v_{\nu_4}-a_{\nu_4}\gamma^5)+i\frac{\kappa_2}{2m_3}\sigma^{\nu\rho}q^\rho) \\
&(\not{p}_4-m_4)(\gamma^\eta(1-\gamma^5)-i\frac{\kappa_1}{2m_3}\sigma^{\eta\tau}q^\tau(1+\gamma^5))\ \not{p}_2]
\end{aligned} \tag{4.29}
$$

Proceeding in the same way, in order to obtain $< \bar{\mathcal{M}}_s\mathcal{M}_t >$ we take the product of Eq. (4.23) and Eq. (4.25). Finally, total differential cross section for the process $e^+e^- \to \nu_4\bar{\nu}_4$ is in the following form:

$$
\frac{d\sigma}{dt}(e^+e^- \to \nu_4\bar{\nu}_4) = \frac{1}{16\pi s^2}[< |\mathcal{M}_t|^2 > + < |\mathcal{M}_s|^2 >
$$

$$+ < \mathcal{M}_s \bar{\mathcal{M}}_t > + < \bar{\mathcal{M}}_s \mathcal{M}_t > \qquad (4.30)$$

and

$$\begin{aligned}
\frac{d\sigma}{dt}(e^+e^- \to \nu_4\bar{\nu}_4) &= \frac{\pi\alpha^2}{s^2 \sin^4\theta_W}\Big\{\frac{1}{m_{\nu_4}^2 \cos^4\theta_W[(s-M_Z^2)^2+\Gamma_Z^2 M_Z^2]} \qquad (4.31)\\
&\times \Big\{(a_e^2+v_e^2)\Big[2m_{\nu_4}^2(a_{\nu_4}^2+v_{\nu_4}^2)((s+t)^2+t^2-2m_{\nu_4}^2(2t-m_{\nu_4}^2))\\
&- 4m_{\nu_4}^2 s(2a_{\nu_4}^2 m_{\nu_4}^2 - s v_{\nu_4}\kappa_2) + s\kappa_2^2((\hat{s}+t)(2m_{\nu_4}^2-t)-m_{\nu_4}^4)\Big]\\
&- 8a_{\nu_4}a_e v_e(v_{\nu_4}+\kappa_2)m_{\nu_4}^2 s(2m_{\nu_4}^2-s-2t)\Big\}\\
&+ \frac{1}{256M_W^4 m_{\nu_4}^4[(t-M_W^2)^2+\Gamma_W^2 M_W^2]}\\
&\times \Big\{4(m_{\nu_4}^2-t)^2(4m_{\nu_4}^4-2m_{\nu_4}^2 t\kappa_1^2-t^2\kappa_1^2)m_{\nu_4}^4\\
&+ (4(\kappa_1^2+16)m_{\nu_4}^8 - 4(4s(\kappa_1^2+8)+t(\kappa_1^4+4\kappa_1^2+32))m_{\nu_4}^6\\
&+ (64s^2+8st(\kappa_1^4+10\kappa_1^2+16)+t^2 m_{\nu_4}^4(9\kappa_1^4+20\kappa_1^2+64))m_{\nu_4}^4\\
&- 2t\kappa_1^2(24s^2+8ts(\kappa_1^2+3)+t^2(3\kappa_1^2+4))m_{\nu_4}^2\\
&+ t^2(8s^2+8ts+t^2)\kappa_1^4)M_W^4 + 8((t\kappa_1^2+8s)m_{\nu_4}^8\\
&- 2tm_{\nu_4}^6(2s+\hat{t})\kappa_1^2+t^3\kappa_1^2 m_{\nu_4}^4)M_W^2\Big\}\\
&+ \frac{\sin^2\theta_W[(s-M_Z^2)\Gamma_W M_W-(t-M_W^2)\Gamma_Z M_Z]}{32\cos^2\theta_W M_W^2 m_{\nu_4}^2[(s-M_Z^2)^2+\Gamma_Z^2 M_Z^2][(t-M_W^2)^2+\Gamma_W^2 M_W^2]}\\
&\times \Big\{4m_{\nu_4}^4(a_e+v_e)(a_{\nu_4}(m_{\nu_4}^2-(s+2t)m_{\nu_4}^2+t^2)\\
&- (m_{\nu_4}^2+(s-2t)m_{\nu_4}^2+t^2)v_{\nu_4}+s(t-m_{\nu_4}^2)\kappa_2)\\
&- \Big\{v_e\Big\{v_{\nu_4}\{2(\kappa_{\nu_4}^2+4)m_{\nu_4}^6-8s+t(3\kappa_1^2+16)m_{\nu_4}^4\\
&+ (8s^2+ts(\kappa_1^2+16)+8t^2)m_\nu^2+t^2(2s+t)\kappa_1^2\}\\
&+ a_{\nu_4}\{-2(\kappa_1^2-4)m_{\nu_4}^6+(t(5\kappa_1^2-16)-24s)m_{\nu_4}^4\\
&+ (8s^2-t\hat{s}(\kappa_1^2-16)-4t^2(\kappa_1^2-2))m_{\nu_4}^2+t^2(2s+t)\kappa_1^2\}\\
&+ s(-8m_{\nu_4}^4+(-t\kappa_1^2+8(s+t))m_{\nu_4}^2+t^2\kappa_1^2)\kappa_2\Big\}\\
&+ a_e\Big\{-v_{\nu_4}\{2(\kappa_1^2-4)m_{\nu_4}^6+(8s+t(16-3\kappa_1^2))m_{\nu_4}^4
\end{aligned}$$

$$
\begin{aligned}
&+ \quad (-8s^2 + ts(\kappa_1^2 - 16) - 8t^2)m_{\nu_4}^2 + t^2(2s+t)\kappa_1^2\} \\
&+ \quad a_{\nu_4}\{2(\kappa_1^2+4)m_{\nu_4}^6 - (24s + t(5\kappa_1^2+16))m_{\nu_4}^4 \\
&+ \quad (8s^2 + t\hat{s}(\kappa_1^2+16) + 4t^2(\kappa_1^2+2))m_{\nu_4}^2 - t^2(2s+t)\kappa_1^2\} \\
&+ \quad s(-8m_{\nu_4}^4 + (8s + t(\kappa_1^2+8))m_{\nu_4}^2 - t^2\kappa_1^2)\kappa_2\Big\}\Big\}M_W^2\Big\}\Big\} \qquad (4.32)
\end{aligned}
$$

We display total cross sections for the pair production of ν_4 as a function of m_{ν_4} in Fig 4.20 for the two ILC options. Similarly, we presented σ_S, σ_B^h, σ_B^l and $(S/\sqrt{S+B})$ as a function of mass at the two options of the ILC ($\sqrt{s}$=0.5-1 TeV) in Table 4.11 and Table 4.12. The invariant mass distributions of leptonic and hadronic final states are shown in Figs. 4.21 for two ILC options.

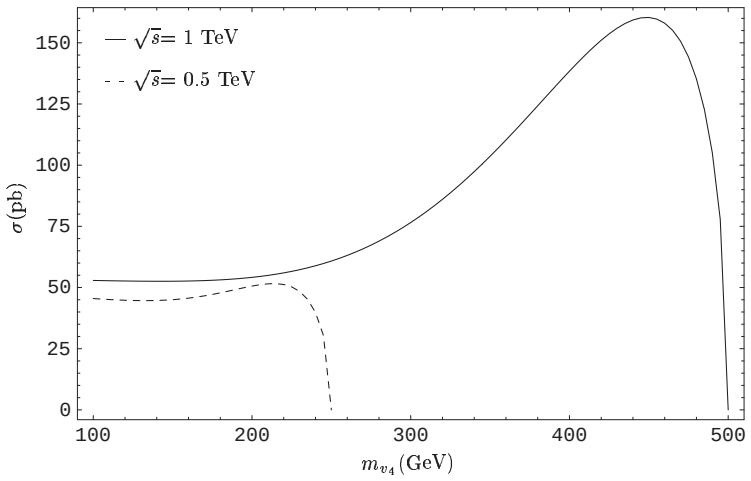

Figure 4.20: The total production cross sections for the process $e^+e^- \to \nu_4\bar{\nu_4}$ as a function of m_{ν_4} for ILC.

Table 4.11: The total cross sections for the signal and background process and the significance for the pair production of fourth generation neutrinos at ILC ($\sqrt{s}$= 0.5 TeV.)

m_{ν_4}(GeV)	σ_S(pb)	σ_B^h(pb)	σ_B^l(pb)	$S/\sqrt{S+B}$
100	45.373	$4.345\text{x}10^{-4}$	$6.909\text{x}10^{-5}$	2130.08
150	44.930	$3.613\text{x}10^{-4}$	$5.745\text{x}10^{-5}$	2119.66
200	50.523	$3.155\text{x}10^{-4}$	$5.017\text{x}10^{-5}$	2247.72
250	14.445	$2.762\text{x}10^{-4}$	$4.393\text{x}10^{-5}$	1201.86

Table 4.12: The total cross sections for the signal and background process and the significance for the pair production of fourth generation neutrinos at ILC ($\sqrt{s}$= 1 TeV.)

m_{ν_4}(GeV)	σ_S(pb)	σ_B^h(pb)	σ_B^l(pb)	$S/\sqrt{S+B}$
200	54.125	$1.045\text{x}10^{-3}$	$1.662\text{x}10^{-4}$	2326.45
300	76.536	$6.090\text{x}10^{-4}$	$9.686\text{x}10^{-5}$	2766.50
400	138.391	$4.402\text{x}10^{-4}$	$7.000\text{x}10^{-5}$	3720.09
500	36.122	$3.104\text{x}10^{-4}$	$4.935\text{x}10^{-5}$	1900.57

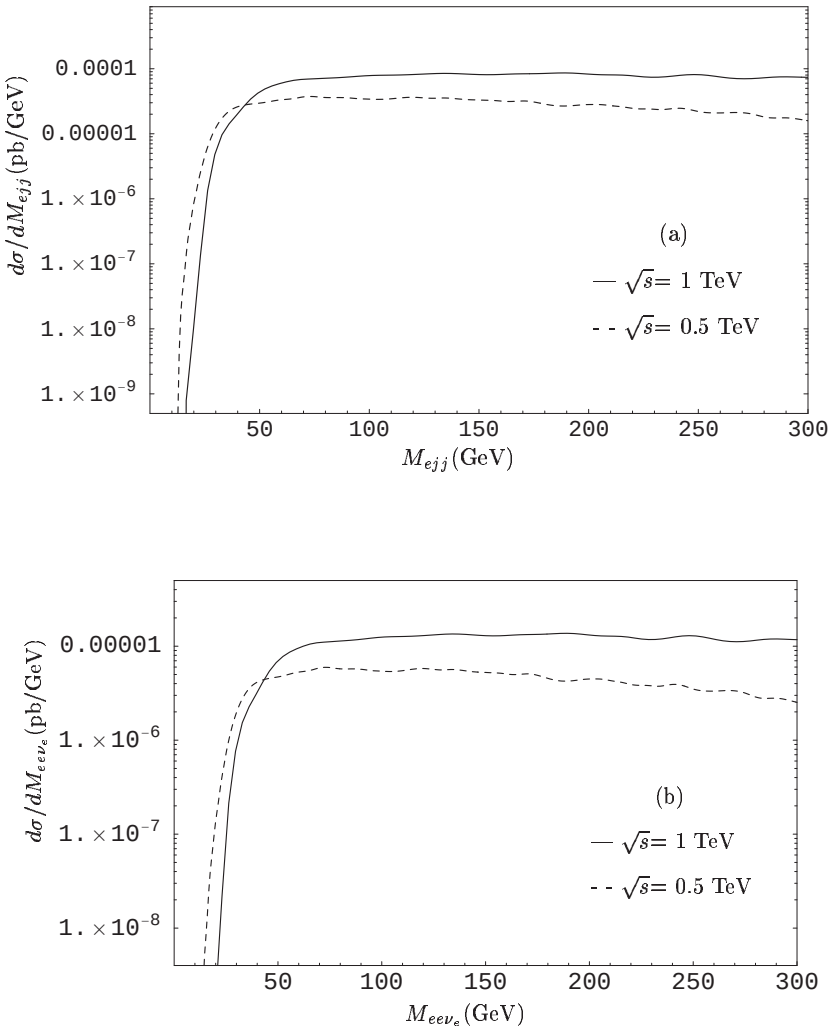

Figure 4.21: The invariant mass distributions of a) M_{ejj} b) $M_{ee\nu_e}$ for the pair production of ν_4 at ILC($\sqrt{s}$= 0.5 TeV and 1 TeV)

CHAPTER 5

CONCLUSIONS

Because of some shortcomings inherent in the SM, a new approach beyond the SM necessitated for the solution of these. As well as, the forthcoming collider experiments might discover new physics which could hold the answer to these questions. In this framework, we focused on three problems and the results of these studies are as follows:

In chapter 2, we have considered the anomalous single production of fourth family up-quarks via the FCNC couplings at future ep colliders. We have shown that the reaction $eq \to eu_4$ can take place at an observable rate at these colliders. Hence, the fourth family up-quark will manifest itself at THERA and Linac $\otimes$ LHC with masses below 500 GeV and 1 TeV, respectively. Thus the future lepton-hadron colliders have promising potential in searching for manifestations of non-standard physics.

In chapter 3, we have investigated charge -1/3 weak isosinglet vectorlike quarks predicted by E_6 theories. We found that a very clear signature for the semileptonic $e\nu_e u$ final state at two high energy electron-proton colliders options THERA and LHeC is possible. As presented in Tables 3.5 and 3.6 the background cross sections varies in the range of the order of $10^{-3} - 10^{-7}$ pb at THERA for 500 GeV quarks and $10^{-5} - 10^{-9}$ pb at LHeC for 1000 GeV quarks. As seen from Tables 3.7 and 3.8, exotic quark masses can be as high as 450 GeV and 1.2 TeV at the center of mass energies of $\sqrt{s} = 1$ and 1.4 TeV, respectively, taking $S/\sqrt{S+B} > 5$, S is the number of signals and B is that of background events, as an observation limit of

signal. In obtaining these numerical values, we have taken an appropriate mixing angle value of $\sin^2\theta$=0.05 which is at the order of the angle in the CKM matrix.

In chapter 4, we have studied the present and future colliders potential for the discovery of the fourth generation neutrino. We use the significance formula $S/\sqrt{S+B} \geq 5$ (5σ) which is the discovery potential of the events with ν_4, where "S" and B are the number of signal and background events, respectively. Then it is seen from Table 4.2 that, neutrino masses up to 700 GeV can be reached at the $\sqrt{s}$=1 TeV THERA option with an integrated luminosity of 40 pb^{-1}. These masses could be as high as 1.2 TeV at LHeC ($\sqrt{s}$=1.4 TeV) with an integrated luminosity of 10^4 pb^{-1} in Table 4.3 and 2.8 TeV at the $\sqrt{s}$=3.74 TeV LC$\otimes$LHC option with an integrated luminosity of 100 pb^{-1} according to Table 4.4. The number of events corresponding to these mass upper bounds are about 35 at THERA, 200 at LHeC and 40 at LC$\otimes$LHC.

According to the 5σ criteria, single neutrino with masses up to around 2 TeV and 250 GeV for the LHC in Table 4.5 and Tevatron in Table 4.6, respectively is found possible while the pair neutrinos mass limits can be obtained as 1 TeV at the LHC and 250 GeV at the Tevatron according to Tables 4.7 and 4.8, respectively. As you can see from Tables 4.9,4.10, 4.11 and 4.12, the future e^+e^- collider options have a large signal cross section and statistical significance higher than four times up to center of mass energy of these colliders. Thus, these e^+e^- colliders provide the best limits on fourth generation neutrinos masses.

REFERENCES

[1] S. L. Glashow, "Partial Symmetries Of Weak Interactions," Nucl. Phys. **22**, 579 (1961).

[2] S. Weinberg, "A Model Of Leptons," Phys. Rev. Lett. **19**, 1264 (1967).

[3] P. W. Higgs, "Broken Symmetries and The Masses of Gauge Bosons," Phys. Rev. Lett. **13**, 508 (1964).

[4] P. W. Higgs, "Broken symmetries, massless particles and gauge fields," Phys. Lett. **12**, 132 (1964).

[5] P. W. Higgs, "Spontaneous Symmetry Breakdown Without Massless Bosons," Phys. Rev. **145**, 1156 (1966).

[6] Y. Fukuda *et al.* [Super-Kamiokande Collaboration], "Evidence for oscillation of atmospheric neutrinos," Phys. Rev. Lett. **81**, 1562 (1998).

[7] Q. R. Ahmad *et al.* [SNO Collaboration], "Direct evidence for neutrino flavor transformation from neutral-current interactions in the Sudbury Neutrino Observatory," Phys. Rev. Lett. **89**, 011301 (2002).

[8] K. Eguchi *et al.* [KamLAND Collaboration], "First results from KamLAND: Evidence for reactor anti-neutrino disappearance," Phys. Rev. Lett. **90**, 021802 (2003).

[9] A. Aguilar *et al.* [LSND Collaboration], "Evidence for neutrino oscillations from the observation of anti-nu/e appearance in a anti-nu/mu beam," Phys. Rev. D **64**, 112007 (2001) [arXiv:hep-ex/0104049].

[10] W. Pauli, letter to radioactive ladies and gentlemen at the Tübingen conference, 4 dec. 1930.

[11] E. Fermi, "Trends to a theory of beta radiation. (in italian)," Nuovo Cim. **11**, 1 (1934).

[12] F. Reines and C. L. Cowan, "Detection Of The Free Neutrino," Phys. Rev. **92**, 830 (1953).

[13] G. Danby, J. M. Gaillard, K. Goulianos, L. M. Lederman, N. Mistry, M. Schwartz and J. Steinberger, "Observation Of High-Energy Neutrino Reactions And The Existence Of Two Kinds Of Neutrinos," Phys. Rev. Lett. **9**, 36 (1962).

[14] K. Kodama *et al.* [DONUT Collaboration], "Observation of tau-neutrino interactions," Phys. Lett. B **504**, 218 (2001) [arXiv:hep-ex/0012035].

[15] B. Pontecorvo, "Neutrino Experiments And The Question Of Leptonic-Charge Conservation," Sov. Phys. JETP **26**, 984 (1968) [Zh. Eksp. Teor. Fiz. **53**, 1717 (1967)].

[16] Z. Maki, M. Nakagawa and S. Sakata, "Remarks On The Unified Model Of Elementary Particles," Prog. Theor. Phys. **28**, 870 (1962).

[17] M. H. Ahn *et al.* [K2K Collaboration], "Indications of neutrino oscillation in a 250-km long-baseline experiment," Phys. Rev. Lett. **90** (2003) 041801 [arXiv:hep-ex/0212007].

[18] M. F. Sohnius, "Introducing Supersymmetry," Phys. Rept. **128**, 39 (1985).

[19] H. E. Haber and G. L. Kane, "The Search For Supersymmetry: Probing Physics Beyond The Standard Model," Phys. Rept. **117**, 75 (1985).

[20] E. Farhi and L. Susskind, "Technicolor," Phys. Rept. **74**, 277 (1981).

[21] N. Arkani-Hamed, S. Dimopoulos and G. R. Dvali, "The hierarchy problem and new dimensions at a millimeter," Phys. Lett. B **429**, 263 (1998) [arXiv:hep-ph/9803315].

[22] I. Antoniadis, N. Arkani-Hamed, S. Dimopoulos and G. R. Dvali, "New dimensions at a millimeter to a Fermi and superstrings at a TeV," Phys. Lett. B **436**, 257 (1998) [arXiv:hep-ph/9804398].

[23] N. Arkani-Hamed, S. Dimopoulos and G. R. Dvali, "Phenomenology, astrophysics and cosmology of theories with sub-millimeter dimensions and TeV scale quantum gravity," Phys. Rev. D **59**, 086004 (1999) [arXiv:hep-ph/9807344].

[24] T. Appelquist, H. C. Cheng and B. A. Dobrescu, "Bounds on universal extra dimensions," Phys. Rev. D **64**, 035002 (2001) [arXiv:hep-ph/0012100].

[25] D. Atwood, L. Reina and A. Soni, "Phenomenology of two Higgs doublet models with flavor changing neutral currents," Phys. Rev. D **55**, 3156 (1997) [arXiv:hep-ph/9609279].

[26] T. G. Rizzo, "Phenomenology Of Exotic Particles In E(6) Theories," Phys. Rev. D **34**, 1438 (1986).

[27] J. L. Hewett and T. G. Rizzo, "Low-Energy Phenomenology Of Superstring Inspired E(6) Models," Phys. Rept. **183**, 193 (1989).

[28] F. Zwirner, "Phenomenological Aspects Of E(6) Superstring Inspired Models," Int. J. Mod. Phys. A **3**, 49 (1988).

[29] R. N. Mohapatra and J. C. Pati, "A Natural Left-Right Symmetry," Phys. Rev. D **11**, 2558 (1975).

[30] G. Senjanovic and R. N. Mohapatra, "Exact Left-Right Symmetry And Spontaneous Violation Of Parity," Phys. Rev. D **12**, 1502 (1975).

[31] J. C. Pati and A. Salam, "Lepton Number As The Fourth Color," Phys. Rev. D **10**, 275 (1974) [Erratum-ibid. D **11**, 703 (1975)].

[32] A. Zee, "A Theory Of Lepton Number Violation, Neutrino Majorana Mass, And Oscillation," Phys. Lett. B **93**, 389 (1980) [Erratum-ibid. B **95**, 461 (1980)].

[33] A. Ghosal, Y. Koide and H. Fusaoka, "Lepton flavor violating Z decays in the Zee model," Phys. Rev. D **64**, 053012 (2001) [arXiv:hep-ph/0104104].

[34] L. Randall and R. Sundrum, "A large mass hierarchy from a small extra dimension," Phys. Rev. Lett. **83**, 3370 (1999) [arXiv:hep-ph/9905221].

[35] [LEP Collaborations], "A combination of preliminary electroweak measurements and constraints on the standard model," arXiv:hep-ex/0412015.

[36] G. Bhattacharyya and R. N. Mohapatra, "A non-supersymmetric interpretation of the CDF e+ e- gamma gamma + missing E(T) event," Phys. Rev. D **54**, 4204 (1996) [arXiv:hep-ph/9606408].

[37] J. F. Gunion, D. W. McKay and H. Pois, "A Minimal four family supergravity model," Phys. Rev. D **53**, 1616 (1996) [arXiv:hep-ph/9507323].

[38] M. Carena, H. E. Haber and C. E. M. Wagner, "Four-Generation Low Energy Supersymmetry with a Light Top Quark," Nucl. Phys. B **472**, 55 (1996) [arXiv:hep-ph/9512446].

[39] Z. Berezhiani and E. Nardi, "Realistic SUSY model with four Fermion families, natural R parity and tau-neutrino in the eV range," Phys. Lett. B **355**, 199 (1995) [arXiv:hep-ph/9503367].

[40] N. J. Evans, "Additional fermion families and precision electroweak data," Phys. Lett. B **340**, 81 (1994) [arXiv:hep-ph/9408308].

[41] F. Potter, "Geometrical basis for the standard model," Int. J. Theor. Phys. **33**, 279 (1994).

[42] P. H. Frampton, P. Q. Hung and M. Sher, "Quarks and leptons beyond the third generation," Phys. Rept. **330**, 263 (2000) [arXiv:hep-ph/9903387].

[43] H. J. He, N. Polonsky and S. f. Su, "Extra families, Higgs spectrum and oblique corrections," Phys. Rev. D **64**, 053004 (2001) [arXiv:hep-ph/0102144].

[44] K. M. Belotsky, T. Damour and M. Y. Khlopov, "Implications of a solar-system population of massive 4th generation neutrinos for underground searches of monochromatic neutrino annihilation signals," Phys. Lett. B **529**, 10 (2002) [arXiv:astro-ph/0201314].

[45] K. Abe *et al.* [VENUS Collaboration], "Search For Isolated Photons From Flavor Changing Neutral Current Decay Of A New Quark At The Kek E+ E- Collider Tristan," Phys. Rev. Lett. **63**, 1776 (1989).

[46] M. Z. Akrawy *et al.* [OPAL Collaboration], "Evidence For Final State Photons In Multi - Hadronic Decays Of The Z0," Phys. Lett. B **246**, 285 (1990).

[47] S. Eno *et al.* [AMY Collaboration], "Search For A Fourth Generation Charge -1/3 Quark," Phys. Rev. Lett. **63**, 1910 (1989).

[48] M. Maltoni, V. A. Novikov, L. B. Okun, A. N. Rozanov and M. I. Vysotsky, "Extra quark-lepton generations and precision measurements," Phys. Lett. B **476**, 107 (2000) [arXiv:hep-ph/9911535].

[49] V. A. Novikov, L. B. Okun, A. N. Rozanov and M. I. Vysotsky, "Extra generations and discrepancies of electroweak precision data," Phys. Lett. B **529** (2002) 111 [arXiv:hep-ph/0111028].

[50] B. Mukhopadhyaya and D. P. Roy, "Tevatron mass limits for heavy quarks decaying via flavor changing neutral current," Phys. Rev. D **48**, 2105 (1993) [arXiv:hep-ph/9210279].

[51] B. Holdom, "The discovery of the fourth family at the LHC: What if?," JHEP **0608**, 076 (2006) [arXiv:hep-ph/0606146].

[52] B. Holdom, "t' at the LHC: The physics of discovery," JHEP **0703**, 063 (2007) [arXiv:hep-ph/0702037].

[53] G. D. Kribs, T. Plehn, M. Spannowsky and T. M. P. Tait, "Four Generations and Higgs Physics," Phys. Rev. D **76**, 075016 (2007) [arXiv:0706.3718 [hep-ph]].

[54] P. Q. Hung and M. Sher, "Experimental constraints on fourth generation quark masses," arXiv:0711.4353 [hep-ph].

[55] H. Abramowicz *et al.* [TESLA-N Study Group], "TESLA: The superconducting electron positron linear collider with an integrated X-ray laser laboratory. Technical design report. Pt. 6: Appendices. Chapter 2: THERA: Electron proton scattering at s**(1/2) approx. 1-TeV," DESY-01-011.

[56] S. Sultansoy, "Linac-ring type colliders: Second way to TeV scale," Eur. Phys. J. C **33**, S1064 (2004) [arXiv:hep-ex/0306034].

[57] T. Han, K. Whisnant, B. L. Young and X. Zhang, "Top-Quark Decay Via the Anomalous Coupling $\bar{t}c\gamma$ at Hadron Phys. Rev. D **55**, 7241 (1997) [arXiv:hep-ph/9603247].

[58] T. Han and J. L. Hewett, "Top charm associated production in high energy e+ e- collisions," Phys. Rev. D **60**, 074015 (1999) [arXiv:hep-ph/9811237].

[59] A. Aktas *et al.* [H1 Collaboration], "Search for single top quark production in e p collisions at HERA," Eur. Phys. J. C **33**, 9 (2004) [arXiv:hep-ex/0310032].

[60] D. J. Griffiths, "Introduction To Elementary Particles," *New York, USA: Wiley (1987) 392p.*

[61] A. D. Martin, R. G. Roberts, W. J. Stirling and R. S. Thorne, "Parton distributions: A new global analysis," Eur. Phys. J. C **4**, 463 (1998) [arXiv:hep-ph/9803445].

[62] J. F. Gunion and R. Vogt, "Intrinsic charm at high-Q**2 and HERA data," arXiv:hep-ph/9706252.

[63] S. Atag, A. Celikel, A. K. Ciftci, S. Sultansoy and U. O. Yilmaz, "The Fourth SM family, breaking of mass democracy and the CKM mixings," Phys. Rev. D **54**, 5745 (1996).

[64] E. Arik, O. Cakir and S. Sultansoy, "Anomalous single production of the fourth SM family quarks at Tevatron," Phys. Rev. D **67**, 035002 (2003) [arXiv:hep-ph/0208033].

[65] V. D. Barger, N. Deshpande, R. J. N. Phillips and K. Whisnant, "Extra Fermions In E_6 Superstring Theories," Phys. Rev. D **33**, 1912 (1986) [Erratum-ibid. D **35**, 1741 (1987)].

[66] J. L. Hewett, "E(6) Exotic Quark Production In E P Collisions," Phys. Lett. B **196**, 223 (1987).

[67] F. M. L. Almeida, J. A. Martins Simoes, C. M. Porto, P. P. Queiroz and A. J. Ramalho, "Exotic quark production at DESY HERA energies," Phys. Rev. D **50** (1994) 5627.

[68] T. G. Rizzo, "Exotic Quark Production At e+ e- Colliders," Phys. Rev. D **40**, 754 (1989).

[69] F. del Aguila, E. Laermann and P. M. Zerwas, "Exotic E_6 Particles in e+ e- Annihilation," Nucl. Phys. B **297**, 1 (1988).

[70] T. C. Andre and J. L. Rosner, "Exotic Q = -1/3 quark signatures at high-energy hadron colliders," Phys. Rev. D **69**, 035009 (2004) [arXiv:hep-ph/0309254].

[71] T. G. Rizzo, "Signals for exotic quark production at hadron colliders," Phys. Lett. B **181**, 385 (1986).

[72] J. Kang, P. Langacker and B. D. Nelson, "Theory and Phenomenology of Exotic Isosinglet Quarks and Squarks," arXiv:0708.2701 [hep-ph].

[73] G. A. Schuler, "Heavy Flavor Production At Hera," Nucl. Phys. B **299**, 21 (1988).

[74] J. B. Dainton, M. Klein, P. Newman, E. Perez and F. Willeke, "Deep inelastic electron nucleon scattering at the LHC," arXiv:hep-ex/0603016.

[75] C. F. von Weizsacker, "Radiation Emitted In Collisions Of Very Fast Electrons," Z. Phys. **88**, 612 (1934).

[76] E. J. Williams, "Nature Of The High-Energy Particles Of Penetrating Radiation And Status Of Ionization And Radiation Formulae," Phys. Rev. **45**, 729 (1934).

[77] W. M. Yao *et al.* [Particle Data Group], "Review of particle physics," J. Phys. G **33**, 1 (2006).

[78] A. Pukhov *et al.*, "CompHEP: A package for evaluation of Feynman diagrams and integration over multi-particle phase space. User's manual for version 33," arXiv:hep-ph/9908288.

[79] H. L. Lai *et al.*, "Global QCD analysis and the CTEQ parton distributions," Phys. Rev. D **51**, 4763 (1995).

[80] H. E. Haber and M. H. Reno, "Signatures of Heavy Neutrino Production at the CERN Collider," Phys. Rev. D **34**, 2732 (1986).

[81] C. T. Hill and E. A. Paschos, "A Naturally Heavy Fourth Generation Neutrino," Phys. Lett. B **241**, 96 (1990).

[82] E. Ma and J. T. Pantaleone, "Heavy Majorana Neutrino Production," Phys. Rev. D **40**, 2172 (1989).

[83] J. Gluza and M. Zralek, "Heavy neutrinos production and decay in future e+ e- colliders," Phys. Rev. D **55**, 7030 (1997) [arXiv:hep-ph/9612227].

[84] G. Bhattacharyya and D. Choudhury, "Fourth-Generation Leptons at LEP2," Nucl. Phys. B **468**, 59 (1996) [arXiv:hep-ph/9512317].

[85] K. Zuber, "On the physics of massive neutrinos," Phys. Rept. **305**, 295 (1998) [arXiv:hep-ph/9811267].

[86] G. Cvetic, C. S. Kim and C. W. Kim, "Heavy Majorana neutrinos at e+ e- colliders," Phys. Rev. Lett. **82**, 4761 (1999) [arXiv:hep-ph/9812525].

[87] G. Cvetic and C. S. Kim, "Heavy Majorana neutrino production at electron muon colliders," Phys. Lett. B **461**, 248 (1999) [arXiv:hep-ph/9906253].

[88] F. M. L. Almeida, Y. D. A. Coutinho, J. A. Martins Simoes and M. A. B. do Vale, "On a signature for heavy Majorana neutrinos in hadronic collisions," Phys. Rev. D **62**, 075004 (2000) [arXiv:hep-ph/0002024].

[89] F. M. L. Almeida, Y. D. A. Coutinho, J. A. Martins Simoes and M. A. B. do Vale, "Dirac and Majorana heavy neutrinos at LEP II," Eur. Phys. J. C **22**, 277 (2001) [arXiv:hep-ph/0101077].

[90] O. Panella, M. Cannoni, C. Carimalo and Y. N. Srivastava, "Signals of heavy Majorana neutrinos at hadron colliders," Phys. Rev. D **65**, 035005 (2002) [arXiv:hep-ph/0107308].

[91] F. M. L. de Almeida, Y. D. A. Coutinho, J. A. Martins Simoes and M. A. B. do Vale, "Heavy Majorana neutrinos at a very large electron-proton collider," Phys. Rev. D **65**, 115010 (2002).

[92] J. Peressutti and O. A. Sampayo, "Signals for Majorana neutrinos in a gamma gamma collider," Phys. Rev. D **67**, 017302 (2003) [arXiv:hep-ph/0211355].

[93] S. Bray, J. S. Lee and A. Pilaftsis, "Heavy Majorana neutrino production at e- gamma colliders," Phys. Lett. B **628**, 250 (2005) [arXiv:hep-ph/0508077].

[94] A. Ali, A. V. Borisov and D. V. Zhuridov, "Heavy Majorana neutrinos in dilepton production in deep-inelastic lepton-proton scattering," Phys. Atom. Nucl. **68**, 2061 (2005) [Yad. Fiz. **68**, 2123 (2005)].

[95] D. Atwood, S. Bar-Shalom and A. Soni, "Signature of heavy Majorana neutrinos at a linear collider: Enhanced charged Higgs pair production," Phys. Rev. D **76**, 033004 (2007) [arXiv:hep-ph/0701005].

[96] J. Kersten and A. Y. Smirnov, "Right-Handed Neutrinos at LHC and the Mechanism of Neutrino Mass Generation," Phys. Rev. D **76**, 073005 (2007) [arXiv:0705.3221 [hep-ph]].

[97] F. del Aguila, J. A. Aguilar-Saavedra and R. Pittau, "Heavy neutrino signals at large hadron colliders," JHEP **0710**, 047 (2007) [arXiv:hep-ph/0703261].

[98] S. Raby and G. B. West, "A Fourth Generation Neutrino With A Standard Higgs Scalar Solves Both The Solar Neutrino And Dark Matter Problems," Phys. Lett. B **202**, 47 (1988).

[99] E. Roulet, "Ultrahigh-Energy Neutrino Absorption By Neutrino Dark Matter," Phys. Rev. D **47**, 5247 (1993).

[100] X. D. Shi and G. M. Fuller, "A new dark matter candidate: Non-thermal sterile neutrinos," Phys. Rev. Lett. **82**, 2832 (1999) [arXiv:astro-ph/9810076].

[101] I. F. M. Albuquerque, L. Hui and E. W. Kolb, "High energy neutrinos from superheavy dark matter annihilation," Phys. Rev. D **64**, 083504 (2001) [arXiv:hep-ph/0009017].

[102] Y. Uehara, "Right-handed neutrinos as superheavy dark matter," JHEP **0112**, 034 (2001) [arXiv:hep-ph/0107297].

[103] A. Masiero and S. Pascoli, "Neutrinos as dark matter candidates," Int. J. Mod. Phys. A **17**, 1723 (2002).

[104] K. Cheung and O. Seto, "Phenomenology of TeV right-handed neutrino and the dark matter model," Phys. Rev. D **69**, 113009 (2004) [arXiv:hep-ph/0403003].

[105] K. M. Belotsky, M. Y. Khlopov, K. I. Shibaev, D. Fargion and R. V. Konoplich, "Heavy neutrinos of 4th generation in searches for dark matter," Grav. Cosmol. **11** (2005) 16.

[106] A. Boyarsky, A. Neronov, O. Ruchayskiy, M. Shaposhnikov and I. Tkachev, "How to find a dark matter sterile neutrino?," Phys. Rev. Lett. **97**, 261302 (2006) [arXiv:astro-ph/0603660].

[107] R. Allahverdi, B. Dutta and A. Mazumdar, "Unifying inflation and dark matter with neutrino masses," Phys. Rev. Lett. **99**, 261301 (2007) [arXiv:0708.3983 [hep-ph]].

[108] R. N. Mohapatra *et al.*, "Theory of neutrinos: A white paper," Rept. Prog. Phys. **70**, 1757 (2007) [arXiv:hep-ph/0510213].

[109] G. Belanger, A. Pukhov and G. Servant, "Dirac Neutrino Dark Matter," arXiv:0706.0526 [hep-ph].

[110] G. M. Kremer, "Dark energy interacting with neutrinos and dark matter: a phenomenological theory," Gen. Rel. Grav. **39**, 965 (2007) [arXiv:0704.0371 [gr-qc]].

[111] S. Abachi *et al.* [D0 Collaboration], "Search for fourth generation neutral heavy leptons," FERMILAB-CONF-95-254-E.

[112] [LEP Collaborations], "Electroweak parameters of the Z0 resonance and the Standard Model: the LEP Collaborations," Phys. Lett. B **276**, 247 (1992).

[113] [LEP Collaborations], "A combination of preliminary electroweak measurements and constraints on the standard model," arXiv:hep-ex/0412015.

[114] D. Fargion, M. Y. Khlopov, R. V. Konoplich and R. Mignani, "On the possibility of searching for heavy neutrinos at accelerators," Phys. Rev. D **54**, 4684 (1996).

[115] B. W. Lee and S. Weinberg, "Cosmological Lower Bound On Heavy-Neutrino Masses," Phys. Rev. Lett. **39**, 165 (1977).

[116] M. I. Vysotsky, A. D. Dolgov and Y. B. Zeldovich, "Cosmological Limits On The Masses Of Neutral Leptons," JETP Lett. **26**, 188 (1977).

[117] Ya. B. Zeldovich, Adv. Astron. Astrophys. **3**, 241 (1965).

[118] T. Ahmed *et al.* [H1 Collaboration], "A Search for heavy leptons at HERA," Phys. Lett. B **340**, 205 (1994).

[119] D. Boussard *et al.* [LHC Study Group], "The Large Hadron Collider: Conceptual Design," CERN-AC-95-05-LHC.

[120] J. G. Branson, D. Denegri, I. Hinchliffe, F. Gianotti, F. E. Paige and P. Sphicas [ATLAS and CMS Collaborations], "High transverse momentum physics at the Large Hadron Collider: The ATLAS and CMS Collaborations," Eur. Phys. J. direct C **4**, N1 (2002).

[121] J. A. Aguilar-Saavedra *et al.* [ECFA/DESY LC Physics Working Group], "TESLA Technical Design Report Part III: Physics at an e+e- Linear Collider," arXiv:hep-ph/0106315.

[122] T. G. Rizzo, "Searching for anomalous tau nu W couplings," Phys. Rev. D **56**, 3074 (1997).

[123] W. W. Armstrong *et al.* [ATLAS Collaboration], "ATLAS: Technical proposal for a general-purpose p p experiment at the Large Hadron Collider at CERN," CERN-LHCC-94-43.

[124] M. E. Peskin and D. V. Schroeder, "An Introduction To Quantum Field Theory," *Reading, USA: Addison-Wesley (1995) 842 p*

[125] J. D. Bjorken and S. D. Drell, "Relativistic Quantum Mechanics," *Newyork, USA: McGraw-Hill (1964), 300 p.*

[126] I. J. R. Aitchison and A. J. G. Hey, "Gauge theories in particle physics: A practical introduction. Vol. 1: From relativistic quantum mechanics to QED," *Bristol, UK: IOP (2003) 406 p.*

[127] I. J. R. Aitchison and A. J. G. Hey, "Gauge theories in particle physics: A practical introduction. Vol. 2: Non-Abelian gauge theories: QCD and the electroweak theory," *Bristol, UK: IOP (2004) 454 p.*

APPENDIX A

PAULI AND DIRAC MATRICES AND TRACE THEOREMS

In this appendix, we follow conventions used in the textbook by D. Griffiths [60], M.E. Peskin and D. V. Schroeder [124], J. D. Bjorken and S. D. Drell [125] and I. J. R. Aitchison and A. J. G. Hey [126, 127]

A.1 Pauli Matrices

Pauli matrices are three Hermitian, unitary, traceless 2×2 matrices:

$$\sigma_1 = \begin{pmatrix} 0 & 1 \\ 1 & 0 \end{pmatrix} \; \sigma_2 = \begin{pmatrix} 0 & -i \\ i & 0 \end{pmatrix} \; \sigma_3 = \begin{pmatrix} 1 & 0 \\ 0 & -1 \end{pmatrix}$$

and we record some properties of pauli matrices as follows

$$\sigma_i \sigma_j = \delta_{ij} + \epsilon_{ijk}\sigma_k; \quad [\sigma_i, \sigma_j] = 2\epsilon_{ijk}\sigma_k \quad ; \{\sigma_i, \sigma_j\} = 2\delta_{ij}$$

$$(a \cdot \sigma)(b \cdot \sigma) = a \cdot b + i\sigma \cdot (a \times b); \quad e^{i\theta \cdot \sigma} = \cos\theta + i\theta \cdot \sigma \sin\theta$$

A.2 Dirac Matrices

We first prove some useful properties of Dirac matrices. We start with the definitions of the γ matrices:

$$\gamma^0 = \begin{pmatrix} I & 0 \\ 0 & -I \end{pmatrix} \qquad \gamma^i = \begin{pmatrix} 0 & \sigma^i \\ -\sigma^i & 0 \end{pmatrix} i = 1, 2, 3. \tag{A.1}$$

These matrices satisfy the Clifford -Algebra

$$\{\gamma^\mu, \gamma^\nu\} = 2g^{\mu\nu}, \tag{A.2}$$

that is in Minkowski space $(\gamma^0)^2 = I$ and $(\gamma^i)^2 = -I$. The Minkowski space has the metric

$$g^{\mu\nu} = \begin{pmatrix} 1 & 0 & 0 & 0 \\ 0 & -1 & 0 & 0 \\ 0 & 0 & -1 & 0 \\ 0 & 0 & 0 & -1 \end{pmatrix}$$

with $g^{\mu\nu}g_{\mu\nu} = 4$ and $g_{\mu\nu}g^{\nu\rho} = \delta^\rho_\mu$. The following relations hold:

$$\begin{aligned} &\gamma_\mu\gamma^\mu = 4 \\ &\gamma_\mu\gamma^\nu\gamma^\mu = -2\gamma^\nu \\ &\gamma_\mu\gamma^\nu\gamma^\lambda\gamma^\mu = 4g^{\nu\lambda} \\ &\gamma_\mu\gamma^\nu\gamma^\lambda\gamma^\sigma\gamma^\mu = -2\gamma^\sigma\gamma^\lambda\gamma^\nu \\ &\sigma_{\mu\nu} = (i/2)[\gamma^\mu, \gamma^\nu] \\ &\sigma_{\mu\nu} = -\sigma_{\nu\mu}. \end{aligned} \tag{A.3}$$

Furthermore the matrix γ^5 (chirality operator) is defined as

$$\gamma^5 = i\gamma^0\gamma^1\gamma^2\gamma^3 \tag{A.4}$$

and properties of γ^5 so that the following relations are satisfied:

$$\begin{aligned} (\gamma^5)^2 &= I \\ \{\gamma^\mu, \gamma^5\} &= 0. \end{aligned} \tag{A.5}$$

In taking traces we form hermitian conjugates of matrix elements for which

$$[\bar{u}(p', s')\Gamma u(p, s)]^\dagger = \bar{u}(p, s)\bar{\Gamma}u(p', s')$$

with

$$\bar{\Gamma} \equiv \gamma^0\Gamma^\dagger\gamma^0$$

for example

$$\begin{aligned} \bar{\gamma}^\mu &= \gamma^0\gamma^{\mu\dagger}\gamma^0 = \gamma^\mu \\ \bar{\sigma}^{\mu\nu} &= \gamma^0\sigma^{\mu\nu\dagger}\gamma^0 = \sigma^{\mu\nu} \\ \overline{i\gamma^5} &= \gamma^0(i\gamma^5)^\dagger\gamma^0 = i\gamma^5 \\ \overline{\gamma^\mu\gamma^5} &= \gamma^0(\gamma^\mu\gamma^5)^\dagger\gamma^0 = -\gamma^5\gamma^\mu \\ \overline{\sigma^{\mu\nu}\gamma^5} &= \gamma^0(\sigma^{\mu\nu}\gamma^5)^\dagger\gamma^0 = -\gamma^5\sigma^{\mu\nu}. \end{aligned} \tag{A.6}$$

While calculating Feynman diagrams traces of γ-matrices occur. To calculate them the following relations have been used :

$$
\begin{aligned}
&Tr[1] = 4 \\
&Tr[\gamma^{\mu_1} ... \gamma^{\mu_{2n+1}}] = 0 \\
&Tr[\gamma^{\mu}\gamma^{\nu}] = g^{\mu\nu} \\
&Tr[\not{a}\ \not{b}] = 4a \cdot b \\
&Tr[\not{a}\ \not{b}\ \not{c}\ \not{d}] = 4[(a \cdot b)(c \cdot d) - (a \cdot c)(b \cdot d) + (a \cdot d)(b \cdot c)] \\
&Tr[\gamma_5] = 0 \\
&Tr[\gamma_5\ \not{a}\ \not{b}] = 0 \\
&Tr[\gamma_5\ \not{a}\ \not{b}\ \not{c}\ \not{d}] = 4i\epsilon_{\mu\nu\lambda\sigma} a^{\mu} b^{\nu} c^{\lambda} d^{\sigma},
\end{aligned}
\tag{A.7}
$$

where $\epsilon_{\mu\nu\lambda\sigma}$ is the total antisymmetric Levi-Civita-Tensor defined by

$$
\epsilon_{\mu\nu\lambda\sigma} = \begin{cases} -1 & \text{, if } \mu\nu\lambda\sigma \text{ is an even permutation of } 0123, \\ +1 & \text{, if } \mu\nu\lambda\sigma \text{ is an odd permutation,} \\ 0 & \text{, if any two indices are the same.} \end{cases}
\tag{A.8}
$$

and the contraction of a four-vector with γ-matrix has the conventional abbreviation

$$\not{a} = \gamma_{\mu} a^{\mu}$$

and the relations $\not{a}\ \not{a} = a^2$ and $\not{a}\ \not{k} = 2(pk) - \not{k}\ \not{p}$ holds.

CURRICULUM VITAE

Abdulkadir Şenol

Adres:

Department of Physics,

Abant İzzet Baysal University

14280 Bolu, Turkey

Phone: +90 374 2541000

Fax: +90 374 2534642

Email: abdulkadirsenol@gmail.com

Personal Details:

Gender: Male

Date of birth: 04th of December, 1976

Place of birth: Istanbul, Turkey

Education:

1993-1998 Undergraduate Studies in Physics at the Ankara University

1999-2002 MSc in Physics at the Abant İzzet Baysal University

Thesis: Search For New Physics Via FCNC Processes at Lepton-Hadron Colliders.

2002-2008 PhD in Physics at the Abant İzzet Baysal University

Thesis: Search For Physics Beyond The Standard Model with Additional Non-standard particles at Future Colliders.

Specialization: High Energy Physics.

Publications:

1.A. T. Alan, A. Senol and N. Karagoz. "Exotic quark production in e p collisions" Phys. Lett. B **639**, 266 (2006) [arXiv:hep-ph/0511199].

2. A. Senol and A. T. Alan. "Possibility of searching for fourth generation neutrino at future e p colliders" Phys. Lett. B **632**, 357 (2006) [arXiv:hep-ph/0508171].

3. A. T. Alan, A. Senol and O. Cakir "Anomalous production of fourth family up quarks at future lepton hadron colliders" Europhys. Lett. **66**, 657 (2004) [arXiv:hep-ph/0312021].

4. A. T. Alan, A. Senol and A. T. Tasci "CP violating asymmetries in the flavor changing single top quark production" J. Phys. G **29**, 279 (2003) [arXiv:hep-ph/0205195].

5. A. T. Alan and A. Senol. "Single top production at HERA and THERA" Europhys. Lett. **59**, 669 (2002) [arXiv:hep-ph/0202119]

6. A. T. Alan and A. Senol. "Lepton flavor changing neutral current processes at lepton hadron colliders" Acta Phys. Polon. B **33**, 1343 (2002) [arXiv:hep-ph/0110294].

Presentations:

1. "Anomalous production of fourth family up quarks at future lepton hadron colliders" A. T. Alan, A. Senol and O. Cakir, Workshop on Recent Developments at High Energy Physics , University of Abant Izzet Baysal, Bolu, 23-25 June 2004.

2. "Single Fourth Family Up Quark Production At Future Lepton Hadron Collid-

ers", A.T. Alan and A.Senol, Fifth General Conference on Balkan Physics Union, BPU-5, August 25-29, 2003, Vrnjacka Banja, Serbia and Montenegro.

3. "Lepton flavor changing neutral current processes at lepton hadron colliders", A.T. Alan and A.Senol,Ankara High Energy Physics Workshop, Middle East Technical University, May 2002.

Conference and Summer School Attended:

1."Central European School in Particle Physics, Institute of Particle and Nuclear and Summer Schools Attended Physics, Faculty of Mathematics and Physics Charles University, Prague-Czech Republic, 12-20 September 2007.

2. "International Summer School on High Energy Physics: Standard Model and Beyond", Akyaka, Mugla-Turkey, 25-30 September 2006.

3. "International Workshop on Physics Beyond the Standard Model", Mugla, Turkey, 22-26 September 2005.

4. "Summer School on Particle Physics" 13-24 June 2005, ICTP, Trieste, Italy.

5."23rd International Physics Conference", Mugla, Turkey, 13-16 September 2005.

6."Quantization, Dualities and Integrable Systems IV" University of Abant Izzet Baysal, Bolu, 1-4 February 2005.

7."Workshop on Recent Developments at High Energy Physics" , University of Abant Izzet Baysal, Bolu, 23-25 June 2004.

8."Fifth General Conference of the Balkan Physical Union", BPU-5, Vrnjacka Banja, Serbia and Montenegro, August 25-29, 2003.

9."1st Hellenic Turkish International Physics Conference", Bodrum-Turkey and Kos- Greece, 10-15 September 2001.

10."CP Violation and B Physics Workshop", University of Ankara, Turkey, 18-21

September 2000.

Projects:

1. "Models extending the Standard Model and Searching for New particles at this Models " AIBU Research Fund, Grant No.2005.03.02.216 (Researcher).

2. "Flavor Changing Reactions at Lepton-Hadron Colliders" AIBU Research Fund, Grant No.2001.03.02.93 (Researcher)

Working Experience:

1999-2008 Working in Abant İzzet Baysal University, Physics Department as a Research Assistant.